Molecular counting in Moloney murine leukemia virus assembly

by

Silas Frederick Johnson

A dissertation submitted in partial fulfillment
of the requirements for the degree of
Doctor of philosophy
(Microbiology and Immunology)
in the University of Michigan
2012

Dissertation committee:

Professor Alice Telesnitsky, Chair
Professor Kathy Spindler
Associate Professor Akira Ono
Assistant Professor Aaron Goldstrohm

2012

To Rachael

Acknowledgments

I am deeply grateful to those who have guided and accompanied me on my PhD journey. First, I would like to thank Alice Telesnitsky for her mentorship over the three years I spent in her lab. Alice welcomed me into her lab with open arms and subsequently invested considerable time and effort into my training as a graduate student. In addition to her encouragment and support, I appreciated her toughness and willingness to challenge me. Thank you Alice.

Science is not a solitary endevour! I could not have performed the research described in this dissertation without the assistance of my labmates in the Telesnitsky lab. I would like to extend special thanks to Sergei Kharytonchyk, Sarra Keene, and Eric Garcia for their help and support. In addition, Steve King and Vicki Larson were very patient with me and taught me alot when I was starting in the lab. Thank you all for making my time in the lab an enjoyable one.

I would like to thank the members of my thesis committee for their insight, advice, and for keeping me on track. Thank you Kathy Spindler, Akira Ono, and Aaron Goldstrohm. I would like to especially thank Kathy for critically reading and editing my manuscript and dissertation.

Finally, I would like to thank my family. My parents (Marge and Fred), my older sister and her family (Molly, Paul, and Luka), my brother and his wife (Sam and Liz), my younger sister (Annie), and my parents-in-law (Bob and Sarah). You are all a great source of joy and inspiration. Thank you for your unconditional love and support. Most importantly, I would like to thank my wife Rachael. I could

not have done this without you. Thank you for believing in me and having my back no matter what. I love you very much!

The work described in Chapter II was previously published in:

Johnson, S. F., E. L. Garcia, M. F. Summers, and A. Telesnitsky. 2012. Moloney murine leukemia virus genomic RNA packaged in the absence of a full complement of wild type nucleocapsid protein. Virology 430:100-109.

The microscopy experiments described in Chapter IV (Fig IV-2) were performed by Nicholas Llewellyn.

Table of Contents

List of Figures

Abstract

The Moloney murine leukemia virus (MoMLV) particle is composed of roughly 2,500 Gag polyproteins, 125 Gag-Pol polyproteins, and precisely two copies of genomic RNA (gRNA) in the form of a dimer. The Gag polyprotein is responsible for directing MoMLV assembly and for recruiting both Gag-Pol and the gRNA dimer for incorporation during assembly. Each of the thousands of Gag molecules in a MoMLV particle contains the domains required to bind both Gag-Pol and gRNA. The mechanisms that account for the conserved asymmetrical numerical proportions of these molecules are unknown. The goal of this dissertation was to examine the parameters that define the molecular proportions of Gag, Gag-Pol, and the gRNA dimer in the MoMLV particle.

In order to test the hypothesis that only a small number of Gag molecules within the MoMLV particle are required to recruit gRNA for incorporation during MoMLV assembly, MoMLV particles were produced that contained variable proportions of two types of Gag molecules: one that was able to participate in high-affinity gRNA packaging interactions and one that was not. Utilizing these mixed particles, results showed that MoMLV gRNA was packaged in the absence of a full complement of packaging competent Gag.

To test the hypothesis that the molecular counting mechanism responsible for incorporating MoMLV Gag-Pol and the gRNA dimer are distinct, an

experimental system was constructed that allowed the proportion of Gag to Gag-Pol and Gag to gRNA to be manipulated. Using this system, our results showed that the incorporation of Gag-Pol into MoMLV is a stochastic process that is dependent on intracellular expression ratios. In contrast, incorporation of gRNA was shown to be a non-random and saturable, thus not strictly dependent of intracellular expression ratios. These results support a model whereby the proportions of Gag and Gag-Pol co-assembled are determined by a distinct mechanism from that which defines Gag and gRNA ratios.

Chapter I

Introduction

Moloney murine leukemia virus

Retroviruses are defined by a remarkable replication cycle. The retrograde flow of genetic information from genomic RNA to DNA during reverse transcription and the integration of the proviral DNA product into the host cell chromosomal DNA are the major defining characteristics of the retrovirus family Retroviridae (23, 42).

Classification and nomenclature

The family Retroviridae is divided into seven genera based on genetic structure and morphology: alpharetrovirus, betaretrovirus, gammaretrovirus, deltaretrovirus, epsilonretrovirus, lentivirus, and spumavirus. Moloney murine leukemia virus is a representative member of the gammaretrovirus genus, whereas human immunodeficiency virus type-1 (HIV-1), the well-studied human pathogen, is a representative member of the lentivirus genus (129).

Murine leukemia viruses are further classified by their cell tropism. Ecotropic viruses infect only cells of their characteristic host species. For example, the ecotropic MoMLV infects cells of mouse or rat origin. Xenotropic murine leukemia viruses infect cells of non-rodent origin, and amphotropic or polytropic viruses infect both rodent cells and cells of other species (23).

Based on its genetic structure, MoMLV is part of a group of retroviruses commonly known as “simple” retroviruses. MoMLV’s relatively simple RNA genome contains only three genes: *gag*, *pol*, and *env*. These three genes are conserved among all retroviruses and encode the viral structural proteins and viral enzymes. In contrast, HIV-1 is part of a group known as “complex” retroviruses because in addition to *gag*, *pol*, and *env*, a complex retrovirus’ genome contains additional accessory genes (23, 42). The work described in this dissertation utilizes MoMLV, which has been used as a model system in retrovirology for over 50 years.

Pathogenesis

MoMLV is an oncogenic retrovirus that induces tumors in its murine host (32, 77). It was first isolated from mouse sarcoma tissue in 1960 by its namesake, John Moloney (88). MoMLV induces T-cell lymphoma in infected mice by activating cellular proto-oncogenes in infected cells (reviewed in (32)). Typically, cellular proto-oncogenes, such as *prim-1*, or *c-myc* in the case of MoMLV, are activated due to the insertion of proviral DNA in close proximity to an oncogene (32). Insertional activation of proto-oncogenes by MoMLV results in the development of lymphoma in mice within months of infection at a very high rate of incidence (88).

The MoMLV RNP

Retroviruses are ribonucleoprotein (RNP) complexes comprised of RNA and protein, surrounded by a lipid envelope. The major RNA component of the MoMLV RNP is two copies of the viral RNA genome, and the major protein

component of the RNP is the viral structural polyprotein Gag. The major as well as minor components of the MoMLV RNP will be discussed in the following section.

MoMLV RNAs

The template for transcription of MoMLV RNA is the integrated proviral DNA (Fig I-1A). Structurally, the proviral DNA consists of identical 5' and 3' long terminal repeats (LTRs) flanking the internal coding sequence (124, 138). The LTRs consist of three regions termed U3 (3' unique), R (direct repeat), and U5 (5' unique). The U3 region of the 5' LTR contains the promoter and enhancer elements required for transcription initiation. Within the coding sequence, *gag* and *pol* are present in the same open reading frame, while *env* is present in a separate reading frame that overlaps slightly with the *gag/pol* reading frame at its 5' end.

Transcription of the full-length viral RNA is mediated by the host cell RNA polymerase II and is defined by a start site at the first base of the 5' R region and the cleavage and polyadenylation site immediately downstream the 3' R region (Fig I-1A). Like most cellular mRNAs, the viral transcript is subject to post-transcriptional processing events including 5' capping and 3' poly(A) tail addition. The resulting sense-stranded transcript is ~8.3kb in length and is flanked by 5' and 3' untranslated regions (UTRs). The full-length transcript serves two functions: (i) to serve as mRNA from which *gag* and *gag-pol* are expressed and (ii) to be packaged by MoMLV as the viral genome (Fig I-1A).

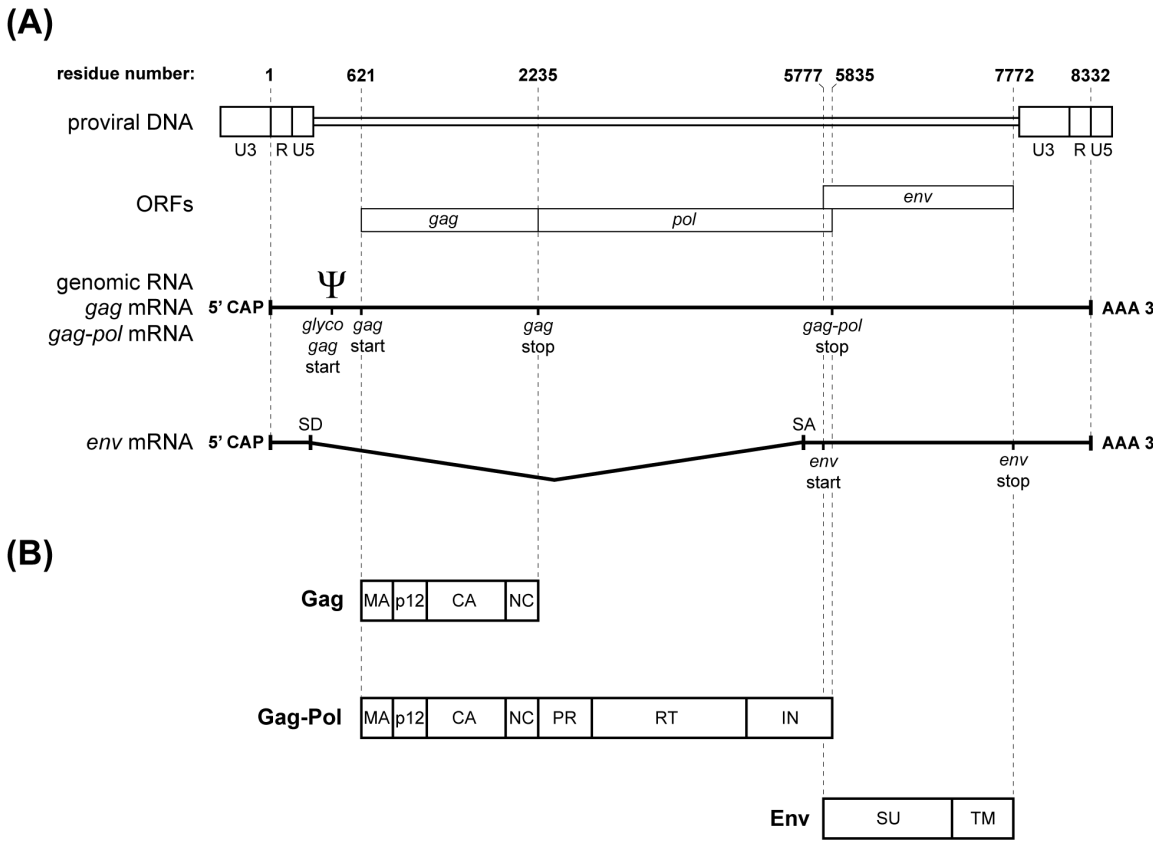

Figure I-1: MoMLV RNAs and polyproteins. (A) Schematic diagram of both the MoMLV full-length RNA and the spliced *env* mRNA, which are derived from the proviral DNA. Abbreviations include: 3' unique sequence (U3), direct repeat sequence (R), 5' unique sequence (U5), "Psi" or Packaging Signal (Ψ), splice donor site (SD), and splice acceptor site (SA). (B) Polyprotein products of MoMLV RNAs. The Gag (group specific antigen) polyprotein consists of the following domains: matrix (MA), p12 late domain, capsid (CA), and nucleocapsid (NC). Gag-Pol consists of the Gag domains as well as the Pol (polymerase) domains, including: protease (PR), reverse transcriptase (RT), and integrase (IN). The Env (envelope) polyprotein consists of the surface (SU) and transmembrane (TM) domains.

Alternative splicing of the primary full-length viral RNA transcript yields additional sub-genomic mRNAs. The sub-genomic *env* mRNA is produced via removal of the sequence between the splice donor (SD) and splice acceptor (SA) sites by the host-cell splicing machinery (Fig I-1A). Furthermore, removal of the sequence between an alternative SD site (SD') and SA produces a 4.4kb sized sub-genomic mRNA that may be important for MoMLV replication (28, 55).

Downstream of the SD site, within the 5' UTR of the full-length transcript, is a sequence termed psi (Ψ) for "packaging signal" (80) (Fig I-1A). Ψ functions as a *cis*-acting packaging signal during recruitment and incorporation of gRNA into assembling virions (34, 80, 93). Due to Ψ's position downstream of SD but upstream of SD', RNA splicing removes it from the *env* mRNA. However, Ψ is maintained in the 4.4kb sub-genomic transcript, which therefore may be incorporated into assembling virions (28, 55, 81). The role of Ψ in RNA packaging and virus assembly are discussed in greater detail in a dedicated section later in this chapter.

MoMLV polyproteins

Retroviruses have maximized the coding capacity of their relatively compact genomes by coordinating the expression of multiple proteins from a single RNA. The full-length MoMLV transcript (Fig I-1A) serves as mRNA for the production of three polyproteins: Gag ($Pr65^{Gag}$), Gag-Pol ($Pr180^{Gag\text{-}Pol}$), and glyco-Gag ($gPr80^{Gag}$) (Fig I-1A and B). Gag-Pol is produced when the Gag stop codon is occasionally read-through via termination suppression. The resulting Gag-Pol fusion is identical to Gag in its N-terminus. Glyco-Gag is produced by

occasional transcription initiation at the atypical CUG start codon upstream of the Gag AUG start codon, and is modified by glycosylation post-translationally. The sub-genomic *env* transcript serves as mRNA for the production of the single Env polyprotein ($gPr80^{Env}$) (Fig I-1B).

The retroviral polyproteins consist of smaller proteins that are liberated by proteolytic cleavage, further adding to the coding capacity of compact retroviral genomes. For MoMLV, the structural polyprotein Gag is cleaved into four proteins: matrix (MA or p15), p12, capsid (CA or p30), and nucleocapsid (NC or p10) (Fig I-1B). MoMLV Gag-Pol polyprotein processing liberates the four Gag proteins in addition to the three Pol proteins, including: protease (PR or p14), reverse transcriptase (RT or p80), and integrase (IN or p46) (Fig I-1B). The MoMLV Env polyprotein is processed into the surface glycoprotein (SU or gp70) and the transmembrane domain (TM or p15E) protein (Fig I-1B).

Virion structure

Cryo-electron microscopy reveals that the MoMLV particle is roughly spherical, with a diameter of ~100-120nm (144), and like all retroviruses it is surrounded by an envelope derived from the host cell plasma membrane (Fig I-2). For newly assembled immature viral particles, the inner leaflet of the viral envelope is lined with a layer of hexameric Gag rings arranged in a paracrystalline lattice (144). Gag-Pol polyproteins are also present within the lattice (Fig I-2). Two copies of the MoMLV gRNA are contained within

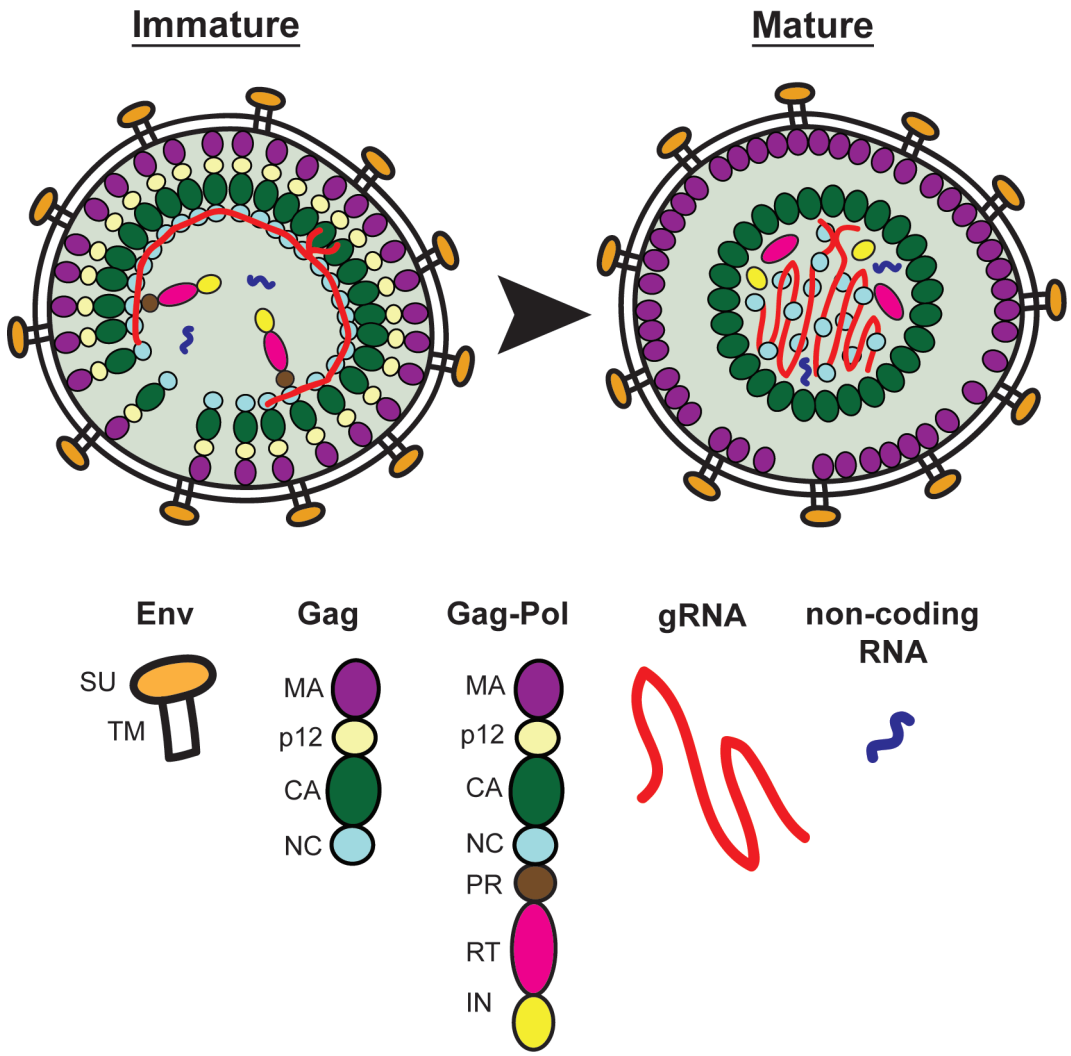

Figure I-2: MoMLV particle structure. Stylized depictions of an immature (left) and mature (right) MoMLV virion. The viral protein components depicted here include Env, Gag, and Gag-Pol. The viral RNA component depicted here includes a single gRNA dimer, consisting of two gRNAs connected in a dimer linkage toward their 5' ends. Also depicted here are host cell non-coding RNAs.

the interior of the viral particle and are associated with the Gag polyprotein lattice (Fig I-2A). Studding the viral envelope are the envelope proteins, consisting of the SU and TM domains.

Proteolytic processing of the Gag and Gag-Pol polyproteins during particle maturation by PR results in a dramatic rearrangement of the interior components of the MoMLV particle (Fig I-2). MA remains associated with the viral envelope while CA condenses to form a pleiomorphic but generally spherical protein core (144). NC is found associated with the viral gRNA inside the CA core along with the viral enzymes RT and IN.

Host Cell RNAs

Host cellular RNAs are also present within retroviral RNPs (Fig I-2). MoMLV selectively packages many host cellular non-coding RNAs, including for example: 7SL RNA, mY RNAs, U6 snRNA, and $tRNA^{pro}$ (99). 7SL RNA is the structural component of the signal recognition particle (SRP), which is responsible for targeting secretory and membrane proteins to the endoplasmic reticulum (63). mY RNAs are present in cells within RNPs called RoRNPs that have been implicated in playing a role in RNA quality control (20). U6 snRNA functions during pre-mRNA splicing as part of the cell spliceosome complex (136). With the exception of $tRNA^{pro}$, which primes the reverse transcription reaction (78), the functions of these RNAs in MoMLV replication are unknown.

MoMLV replication cycle

The retroviral replication cycle may be divided into two phases: early and late. The early events consist of: (i) attachment and entry, (ii) reverse

transcription, (iii) nuclear entry, and (iv) integration. The late events consist of: (i) transcription, (ii) RNA processing and nuclear export, (iii) translation, (iv) assembly and RNA packaging, and (v) release and maturation (Fig I-3).

Early events

The MoMLV replication cycle begins with entry of the viral RNP into the host cell. Entry is initiated by interactions between the viral envelope proteins and the host cell surface receptor, which in the case of ecotropic MoMLV is the cell surface cationic amino acid transporter mCAT-1 (1, 67). Host cell attachment, mediated by receptor interactions, is followed by fusion of the viral envelope with the host cell plasma membrane, thereby allowing the viral core and its contents access to the host cell cytoplasm.

Following internalization, the MoMLV CA core dissociates in a process known as uncoating, a mechanism which is poorly understood in retroviruses, even for the well-studied HIV-1 (2). Next, the single-stranded RNA genome is converted to double-stranded DNA (dsDNA) in the reverse transcription reaction catalyzed by the viral RT enzyme. Subsequently, the viral dsDNA is transported to the nucleus as part of a pre-integration complex (PIC) comprised of partially disassembled CA core,NC, and IN (8). Recent studies have shown that the viral p12 protein binds the viral dsDNA and is an important component of the MLV PIC (109). Interestingly, MoMLV PICs are only able to gain access to the host cell nucleus when the nuclear membrane dissociates during mitosis (74, 115). Consequently, productive MoMLV infection occurs concurrent with cell cycle progression of the host cell.

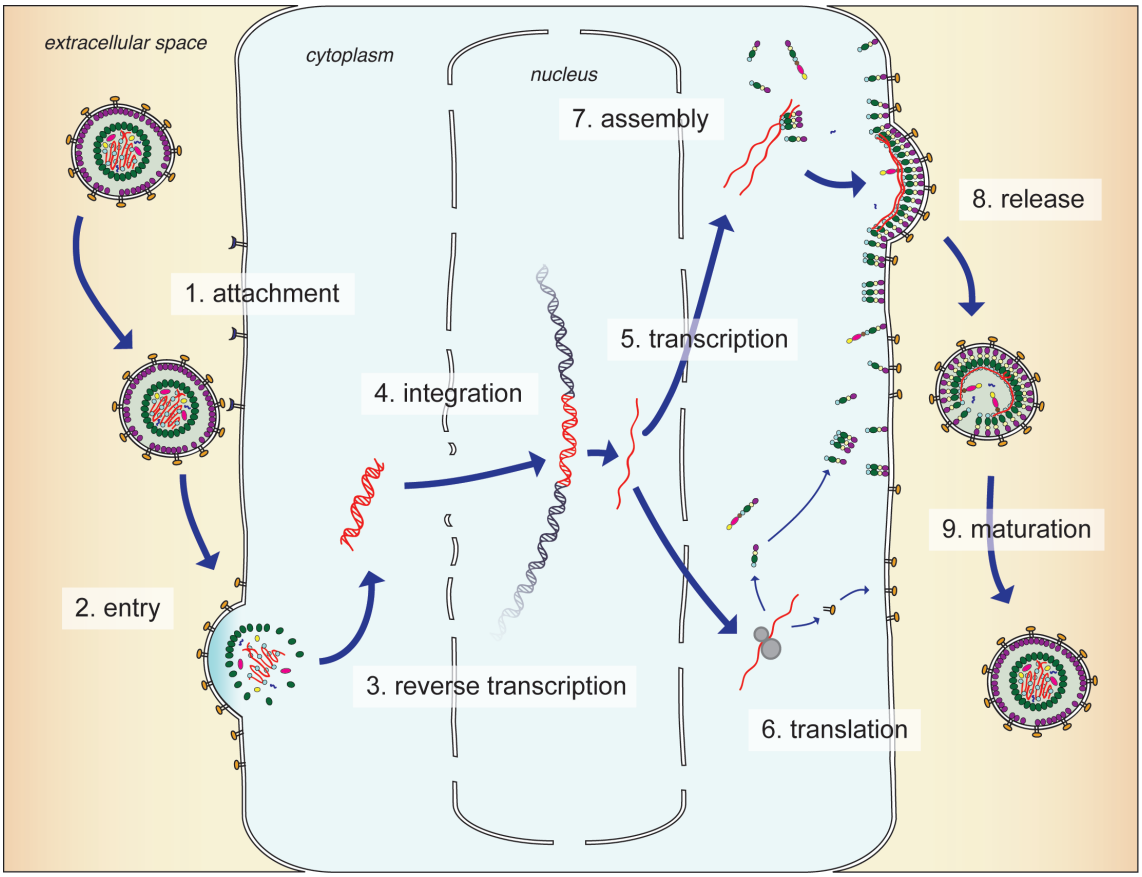

Figure I-3: MoMLV replication cycle. The MoMLV replication cycle can be separated into two major phases: early and late. The early phase steps depicted here include: (1) attachment of the MoMLV virion to the host cell, (2) entry of the viron contents into the host cell cytoplasm, (3) reverse transcription of the viral gRNA into dsDNA, and (4) integration of the viral dsDNA into the host cell genome. The late phase steps depicted here include: (5) transcription of the MoMLV RNA from the integrated provirus, (6) translation of the viral polyproteins from the viral RNAs, (7) assembly of viral proteins and gRNAs at the host cell plasma membrane, followed by (8) virion release and (9) maturation.

Once inside the nucleus, the proviral DNA is inserted into the host cell chromosomal DNA in a stepwise process known as integration (73). The viral enzyme IN catalyzes the host DNA strand cutting and viral DNA joining reactions. Genome-wide studies of retroviral integration have revealed a preference for MoMLV proviral DNA insertion within the transcriptional start sites of active genes (85, 143). Integration is an essential and defining characteristic of the retroviral replication cycle, since the late replication events are completely dependent on this step.

Late events

Late events of the MoMLV replication cycle begin with the transcription of the full-length MoMLV RNA (described above) from the proviral DNA by the host cell transcriptional machinery. In a manner similar to cellular mRNAs (65), the viral RNA must by extensively processed prior to nuclear egress. Processing includes 5'-cap addition, 3'-end cleavage, and poly(A) tail addition. In addition, RNA splicing produces the sub-genomic viral RNAs. Following processing, the viral RNAs are exported to the cytoplasm via an undefined trafficking pathway. However, some studies suggest that sequences within the 5'-UTR, including Ψ, may function in nuclear export, at least in the case of full-length viral RNA (4).

Nuclear export of viral RNAs is followed by translation of the MoMLV polyproteins Gag, Gag-Pol, and Env. For cellular mRNAs, translation typically initiates when the ribosome recognizes the 5'-cap and scans towards the 3' end until the first AUG start codon is reached. However, some evidence suggests this

ribosome scanning mechanism may not be utilized in the case of retroviral translation, due to the high degree of secondary structure present in the leader region of viral RNAs. For MoMLV, an internal ribosome entry site (IRES) within the RNA may exist that allows the ribosome to avoid sequences upstream of *gag* (7).

Next, the Gag and Gag-Pol polyproteins are targeted to sites of virus assembly at the host cell plasma membrane, along with two copies of gRNA coupled in an RNA dimer. The role of Gag in virus assembly, gRNA dimerization, and packaging will be discussed in greater detail in the following section. The Env glycoprotein is also targeted to the host cell plasma membrane. However, Env is translated by ribosomes on the ER and shuttled into the host cell secretory pathway, thereby ensuring host cell surface expression.

Finally, following assembly of the MoMLV RNP complex at the host cell plasma membrane, newly forming virions are released from the host cell into the extracellular space in an ESCRT-dependent manner (107). At this point, PR-mediated proteolytic polyprotein processing liberates the subdomains of Gag and Gag-Pol, thereby rendering the newly formed virus particle fully infectious and primed to repeat the replication cycle in a new host cell.

MoMLV Assembly

The association of Gag polyproteins induces assembly of retroviral particles. In addition to the four structural domains, MoMLV Gag contains three functional domains important for assembly: (i) MA targets Gag to sites of assembly; (ii) CA mediates Gag-Gag multimerization interactions; and (iii) NC

binds RNA, which in turn promotes additional Gag-Gag interactions. The integration of these simultaneous interactions drives particle formation.

Gag PM targeting

Retroviruses bud from the host cell plasma membrane (PM). MoMLV Gag interactions with the PM are mediated by co-translational myristylation of the N-terminus of MA (52, 113). The current model for PM binding posits that the myristyl moiety in Gag is initially inaccessible for PM interactions due to the conformation of MA. Interactions with the phospholipids PI(4,5)P2 (phosphatidylinositol 4,5-bisphosphate) and PS (phosphatidylserine) on the inner leaflet of the PM are thought to expose and stabilize the myristyl moiety, thereby allowing insertion in and docking to the PM. MA-mediated attachment of Gag to the PM is thought to be followed by lateral movement of the molecules to lipid rafts or other microdomains where budding occurs (48). In addition to the myristyl moiety, a conserved region within MA known as the highly basic region (HBR) is also predicted to play a role in membrane binding (94). Interestingly, glyco-Gag also increases the release of MoMLV at lipid rafts, suggesting a role for glyco-Gag in PM targeting (97).

Gag multimerization

During assembly, the immature MoMLV particle is stabilized by lateral interactions between Gag polyproteins within a structural lattice. These Gag-Gag interactions occur primarily within the CA domain of Gag (37). MoMLV CA contains two domains, a tapered N-terminal domain (CA-NTD) and globular C-terminal domain (CA-CTD) (90). Gag molecules are linked by contacts between

CA-NTDs within Gag hexamers, the primary unit of the structural lattice (90). The CA-CTD contains a conserved domain known as the major homology region (MHR), and mutations within this domain impair virus assembly (140). Structural data confirms that the CA-CTD joins neighboring Gag hexamers within the lattice (36).

The NC domain of Gag also promotes Gag multimerization during assembly via so-called nonspecific interactions with RNAs (110). Purified recombinant retroviral Gag proteins only assemble into virus like particles (VLPs) *in vitro* with the addition of RNA (15). Moreover, deletion of the NC domain of MoMLV Gag results in a severe defect in virus assembly in cells (92). These results implicate RNA as a key co-factor in MoMLV assembly and suggest that Gag-RNA interactions are as important to MoMLV assembly as the Gag-Gag and Gag-PM interactions described above.

Gag-Pol Incorporation

The CA domain of MoMLV Gag is thought to be important for Gag-Pol incorporation into newly forming virions, in a manner similar to that for HIV-1 (reviewed in (53)). With HIV-1, Gag-Pol incorporation is dependent on sequences within the CA regions of Gag and Gag-Pol (56, 128). Although CA-CA interactions are thought to be the primary route for incorporation of Gag-Pol, Pol proteins can be incorporated into virions outside of the context of Gag-Pol for both HIV-1 and MoMLV (14, 17). For HIV-1, Gag-Pol initially multimerizes with Gag in the cytoplasm (47, 70), and this is followed by Gag-dependent targeting to sites of assembly at membranes (21, 104, 125). Viral RNA plays an important

role in facilitating Gag/Gag-Pol interactions (66), presumably by facilitating Gag-Gag multimerization and not by direct gRNA/Gag-Pol interactions (66).

MoMLV gRNA packaging

Retroviruses selectively incorporate gRNA into assembling virions from a cellular RNA pool, where viral gRNAs are vastly outnumbered by host mRNAs. The selective enrichment of gRNA in retroviral particles is due to specific *cis*-acting packaging elements on the gRNA and *trans*-acting packaging elements on the Gag polyprotein.

Cis-acting packaging elements

As described above, the *cis*-acting gRNA packaging signal, or Ψ, is contained within the 5'-UTR from nucleotides 215-565 (Fig I-1) (80). This highly structured region of the 5'-UTR is termed the "classic Ψ" and is comprised of a series of stem loops, including: DIS-1 and DIS-2 (dimerization initiation site 1 and 2), and SL-C an SL-D (stem loop C and D). Mutations or deletions of Ψ abrogate gRNA packaging (34, 80, 93) whereas reinsertion of Ψ toward the 3' end of the genome has been shown to restore gRNA packaging (79). Nucleotides 310-374, which encompass SL-C and SL-D, are termed the core encapsidation signal (CES), and are sufficient to direct packaging of heterologous RNAs (91). However, gRNA packaging is most efficient with an intact "classic Ψ" element and additional downstream nucleotides (5). Interestingly, a 17bp element downstream of the *env* stop codon toward the 3' end of the genome has also been implicated in gRNA packaging, but its contribution is less well understood (145).

Trans-acting packaging elements

The retroviral *trans*-acting gRNA packaging element is the NC domain of Gag (reviewed in (110)). MoMLV NC contains a single RNA binding domain characterized by a conserved "zinc-knuckle" motif (C-X_2-C-X_4-H-X_4-C; C=Cys, H=His, X=variable) (51). Mutations within the "zinc-knuckle" motif of NC disrupt virus assembly, gRNA packaging, and infectivity (43, 46, 83, 92, 111). Additionally, treatment of retroviral particles with zinc-ejecting chemotherapeutic agents inhibits infectivity (114).

gRNA dimerization

Retroviruses selectively package two copies of their RNA genomes joined by a dimer linkage. Electron microscopy studies originally demonstrated that gRNAs isolated from MoMLV are linked toward their 5' ends (95). Subsequent studies confirmed that gRNA dimers are coupled by specific sequences within the 5' UTR known as the dimer linkage site (DLS). The MoMLV DLS has been defined by the stem loops DIS-1 and DIS-2 from nucleotides 204-208 and 283-298 within the 5' UTR (76). The positioning of the DLS such that it overlaps with Ψ ensures that gRNA dimerization and packaging are functionally linked (reviewed in (25)).

The MoMLV Ψ/DLS contains several high affinity NC binding sites defined by conserved Py-Py-Py-G (Py=pyrimidine, G=guanosine) sequences (26, 29). Within the gRNA monomer, the high affinity NC binding sites are sequestered by base pairing interactions. However, the stepwise process of dimerization, whereby initial intermolecular base pair "kissing interactions" between DIS loops

on separate RNAs are followed by the formation of stable extended intermolecular dimer interface interactions, results in the exposure of high-affinity NC binding sites (25, 40, 76, 86, 87). The conversion of packaging-incompetent RNA monomer to packaging-competent RNA dimer represents a molecular "switch" that ensures selective engagement of dimers for packaging by NC (25).

Sub-cellular localization

The sub-cellular site of gRNA dimerization likely differs among retroviruses (reviewed in (60)). The frequency of genetic marker reassortment between coexpressed retroviral gRNAs suggests that MoMLV gRNA dimerization occurs at or near sites of transcription in the nucleus, whereas HIV-1 gRNA dimerization occurs later in the cytoplasm (reviewed in (100)). The location of initial Gag-gRNA dimer interactions is unknown. However, in the case of HIV-1, recent studies suggest that a small number of Gag molecules engage the gRNA dimer in the cytoplasm prior to trafficking to sites of assembly at the PM (61, 69).

MoMLV RNP Stoichiometry

Recent studies with HIV-1 have allowed the stoichiometry of retroviral RNP constituents to be refined (reviewed in (10)). The following section summarizes our current knowledge regarding the copy numbers of major protein and RNA components of the retroviral RNP. Most stoichiometric studies have focused on HIV-1, and their conclusions are extended here to MoMLV by analogy.

Gag

Initial estimates of the stoichiometry of Gag were based on cryo-electron tomography and scanning transmission EM (STEM) of *in vitro*-assembled envelope-free HIV-1 Gag particles (12). For an average immature 145 nm particle, the calculated number of Gag molecules was ~5,000 per particle (12). This estimate was updated when cryo-electron tomography of *in vivo*-assembled HIV-1 particles demonstrated that membrane bound particles contain an incomplete spherical Gag lattice shell (11, 142). Presumably, gaps in the Gag lattice shell of *in vivo*-assembled HIV-1 particles permit membrane curvature during virus budding (10). Reflecting the incompleteness of the Gag shell, newer estimates place the number of Gag molecules per particle at ~2,500 for an average 130 nm particle (16).

Gag-Pol

The number of Gag-Pol molecules per HIV-1 particle was determined to be ~5% the number of Gag molecules (141). Calculations based on this number suggest that each particle would contain ~125 Gag-Pol molecules per the average ~2,500 Gag particle (16). Unlike MLV, the HIV-1 *pol* reading frame is offset from the *gag* reading frame by -1 nucleotide. This necessitates a -1 ribosomal frameshift to translate the HIV-1 Gag-Pol polyprotein (57). The translation frameshift occurs ~5% of the time at a “slippery” sequence at the end of *gag* and results in a Gag:Gag-Pol protein ratio of of 20:1 (reviewed in (9, 39, 53)).

For MLV, readthrough of the *gag* stop codon to produce Gag-Pol also occurs at a frequency of ~5% (reviewed in (50)), resulting in the same 20:1 ratio. The correlation between the number of Gag-Pol molecules per HIV-1 particle (~5% relative to Gag) and the frameshift frequency (~5%) suggests that the incorporation of HIV-1 Gag-Pol into assembling virions is stochastic.

The mechanism that regulates readthrough frequency of the MLV *gag* stop codon was recently elucidated. Downstream of the *gag* stop codon is an RNA pseudoknot structure that is responsible for directing recoding of the stop codon (reviewed in (9)). New NMR-based structural data suggest that the RNA pseudoknot can adopt either of two conformations: (i) a nonpermissive conformation where readthrough is prevented, or (ii) a conformation that is permissive for readthrough. Consistent with the protein ratios observed during virus replication, the NMR structural studies showed that at physiological pH, the readthrough-permissive conformation is present at a frequency of ~5% in the total RNA (54).

Conservation of the strict 20:1 Gag:Gag-Pol expression ratio in HIV-1 and MLV suggest that maintenance of this ratio is important for virus replication. Indeed, studies where the Gag:Gag-Pol ratio have been disrupted result in defects in virus assembly and infectivity for both HIV-1 (31, 62, 103, 121) and MLV (33).

gRNA

Although it has been known for decades that retroviruses package their gRNAs as dimers, only with advances in fluorescence microscopy that allow

single-RNA-molecule sensitivity has the precise number of dimers present within a particle been determined experimentally. Chen et al. showed that HIV-1 particles, produced in cells where two uniquely labeled viral RNAs were coexpressed, were heterozygous in proportions that suggested random RNA assortment and the packaging of precisely one dimer (19).

The precise mechanism by which the single gRNA dimer specificity is achieved is unknown. Presumably, RNA size constraints are not involved in regulating the packaging of a single dimer, since gRNAs three times the normal length may be incorporated into virions (123). However, experiments do suggest that packaged gRNAs may be "counted" by their dimer linkage. When HIV-1 Ψ/DLS is duplicated on the gRNA, monomeric RNAs appear in assembling virions (117, 118).

Dissertation Overview

This dissertation addresses the mechanisms involved in determining the stoichiometry of MoMLV RNP constituents. I sought to examine the parameters that define the molecular proportions of Gag, Gag-Pol, and the gRNA dimer in the MoMLV RNP.

In the work described in this dissertation, there is a particular focus on questions surrounding numerical asymmetries between Gag, Gag-Pol, and gRNA within the RNP. For example, in Chapter II, I tested the hypothesis that only a small numerical proportion of Gag molecules within the MoMLV RNP are required to recruit gRNA for packaging during MoMLV assembly. To test this hypothesis, I produced MoMLV particles containing variable proportions of two

types of Gag molecules: one that is able to participate in high-affinity gRNA packaging interactions and one containing mutant NC that is not. Using this experimental system, I showed that MoMLV gRNA is packaged in the absence of a full complement of packaging competent Gag.

Next, in Chapter III I sought to examine the mechanism that accounts for the asymmetric proportions of Gag and Gag-Pol as well as Gag and the gRNA dimer within the MoMLV RNP. Specifically, I wished to test the hypothesis that Gag-Pol and the gRNA dimer are incorporated into MoMLV RNPs by distinct "counting" mechanisms. To test this hypothesis, I produced MoMLV particles containing variable proportions of Gag and Gag-Pol and variable proportions of Gag and gRNAs or Ψ/DLS's. By manipulating the proportions of these molecules, I showed that Gag-Pol incorporation into MoMLV particles was stochastic, whereas incorporation of gRNAs was saturable.

In Chapter IV, I summarize the conclusions of Chapters II and III, present additional preliminary data, and discuss potential future experimental directions based on the findings presented in this dissertation. Finally, I discuss the implications of altering the molecular proportions of the retroviral RNP components as a therapeutic intervention for infection.

Chapter II

Moloney murine leukemia virus genomic RNA packaged in the absence of a full complement of wild type nucleocapsid protein

Abstract

The current model for MoMLV genomic RNA (gRNA) packaging predicts that of the thousands of Gag proteins in a budding virion, only a small number (≤1%) may be necessary to recruit gRNA. Here, we examined the threshold limits of functional Gag required to package gRNA using wild-type (WT) and packaging deficient mutant nucleocapsid (NC) phenotypically mixed virions. Although gRNA packaging was severely diminished for the NC mutant, the residual encapsidated RNA dimer displayed motility on gels, thermostability, and integrity that was indistinguishable from that of WT. In phenotypically mixed virions, gRNA encapsidation recovered to within approximately two-fold of WT levels when the amount of WT NC was 5-10% of the total. Our results demonstrate that NC's roles in gRNA dimerization and packaging are genetically separable. Additionally, MoMLV gRNA packaging does not require 100% WT NC, but the amount of functional NC required is greater than the predicted minimum.

Introduction

The retroviral Gag polyprotein is responsible for directing virus assembly and genomic RNA (gRNA) packaging (reviewed in (25, 37, 75, 110)). The full-length Moloney murine leukemia virus (MoMLV) Gag polyprotein, termed

$Pr65^{Gag}$, consists of four structural domains: matrix (p15 MA), p12, capsid (p30 CA), and nucleocapsid (p10 NC). The NC domain of $Pr65^{Gag}$ is responsible for specific recruitment and packaging of MoMLV gRNA into newly forming virions (6, 111). MoMLV NC contains a single conserved ”zinc knuckle” domain (C-X_2-C-X_4-H-X_4-C; C=Cys, H=His, X=variable) (51), which is required for NC-gRNA interactions (Fig II-1A). Mutations within this domain disrupt viral assembly, gRNA packaging, and infectivity (43, 46, 83, 92, 111).

The region of MoMLV gRNA bound by NC during packaging is contained within the 5’-untranslated region (UTR) and is known as Ψ (Psi) for “packaging signal” (80). Mutations or deletions of MoMLV Ψ result in gRNAs that are poorly packaged (34, 80, 93). MoMLV gRNAs are packaged as dimers that are coupled in a dimer linkage structure (DLS). The DLS is defined by sequences that overlap with Ψ, and studies have demonstrated that the two regions, and therefore gRNA dimerization and packaging, are intimately linked (reviewed in (25)). The Ψ/DLS region contains several conserved UCUG and related Py-Py-Py-G (Py=pyrimidine) high-affinity NC binding sites (26, 29). Within the MoMLV RNA monomer, these high-affinity binding sites are sequestered by base pairing interactions; however, upon dimerization these sites are exposed and competent for NC binding (26, 40, 86, 87). This molecular “switch” provides a mechanism for the preferential recruitment of MoMLV gRNA dimers into newly forming virions.

The MoMLV NC zinc knuckle contains a conserved tryptophan (Trp 35) that plays a direct role in mediating NC-gRNA interactions. Trp 35 coordinates the binding of NC to its conserved high-affinity UCUG binding sites on the gRNA

dimer by defining a pocket into which the guanosine residue fits and binds with high affinity (26, 29). As shown in Fig II-1B, the indole functional group of Trp 35 defines one side of the guanosine binding pocket by aligning parallel with the planar pyrimidine-imidazole ring system of guanosine 309 (which is in a UCUG motif from MoMLV nucleotides 306-309). Similar guanosine binding pockets defined by conserved Trp and Phe residues are also present on both of the HIV-1 NC zinc knuckles (89, 126, 127, 130, 131). Disruption of the MoMLV guanosine binding pocket by mutating Trp 35 to Ser or Gly results in severe packaging defects (46, 83).

The number of high-affinity NC binding sites in both the MoMLV RNA monomer and gRNA dimer has been revealed by *in vitro* binding analysis. When *in vitro* transcribed RNAs consisting of nucleotides 147-623 of the MoMLV 5'-UTR are dimerized, approximately one dozen high-affinity binding sites are available for binding of recombinant NC. In contrast, when mutations in the *in vitro* transcribed RNAs are introduced that inhibit dimerization, only one or two high-affinity binding sites are available on the MoMLV monomer for recombinant NC binding (86).This observation predicts that of the putative thousands of copies of $Pr65^{Gag}$ in an MoMLV virion (by analogy to HIV; (16)), only about a dozen (or ≤1%) may need to engage in high-affinity NC-gRNA interactions to promote packaging.

To test the hypothesis that only a small number (≤1%) of gRNA binding competent $Pr65^{Gag}$ molecules may be required for MoMLV gRNA packaging during virus assembly, a MoMLV mutant containing a single tryptophan-to-

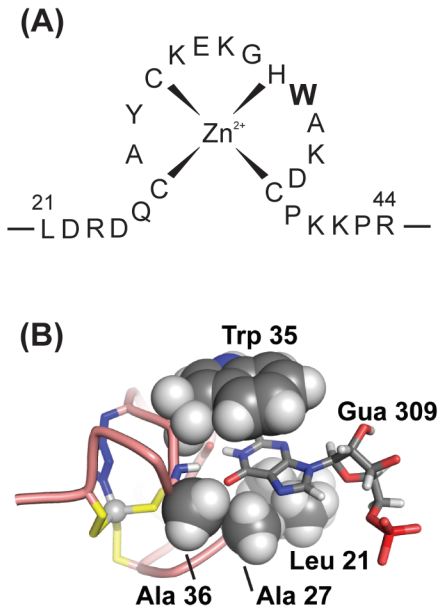

Figure II-1: Interactions between the MoMLV NC "zinc knuckle" domain and gRNA high affinity binding sites. (A) Schematic representation of the zinc knuckle of MoMLV NC from amino acids 21 to 44. Trp 35 (W) is shown in bold. (B) The guanosine binding site of the MoMLV zinc knuckle is defined on one side by the side chain of Trp 35 and the other by the side chains of Ala 36, Ala 27, and Leu 21. The zinc atom is shown coordinated by the cysteine (yellow) and histidine (blue) side chains of the conserved "CCHC" zinc knuckle. Depicted here is guanosine (Gua) 309, which is in a high affinity UCUG binding site from MoMLV nucleotides 306-309.

glycine substitution at amino acid position 35 within the zinc knuckle of NC was co-expressed with WT NC to generate phenotypically mixed virions containing both WT and W35G NCs. Single cycle replication properties and the amounts and properties of gRNA packaging for mixed virions containing limiting amounts of WT NC were examined directly.

Results

W35G NC mutant virus production

In order to determine the threshold levels of NC required for gRNA packaging, a MoMLV zinc knuckle mutant was first constructed and characterized. A single mutation of Trp 35 within the zinc knuckle of NC was selected based on (i) previous studies demonstrating that mutations of this residue do not affect MoMLV assembly but lead to significant reductions in gRNA packaging (46, 83), and (ii) *in vitro* structural and biophysical studies showing that this residue contributes to the high-affinity gRNA binding (26).

To examine the impact of the Trp 35 NC mutation on virus production, 293T-derived ET cells (106) were transfected with WT and W35G mutant proviral plasmids (pGPP(WT) and pGPP(W35G), Fig II-2A), and virus production was quantified by a reverse transcriptase (RT) assay (Fig II-2B). Media harvested from cells transfected with the W35G mutant proviral plasmid exhibited an approximate two-fold reduction in RT activity per volume compared to those transfected with the WT proviral plasmid (Fig II-2B).

To determine the cause of this decrease in RT release into the medium, viral and cell-associated proteins of the WT and W35G mutant were compared

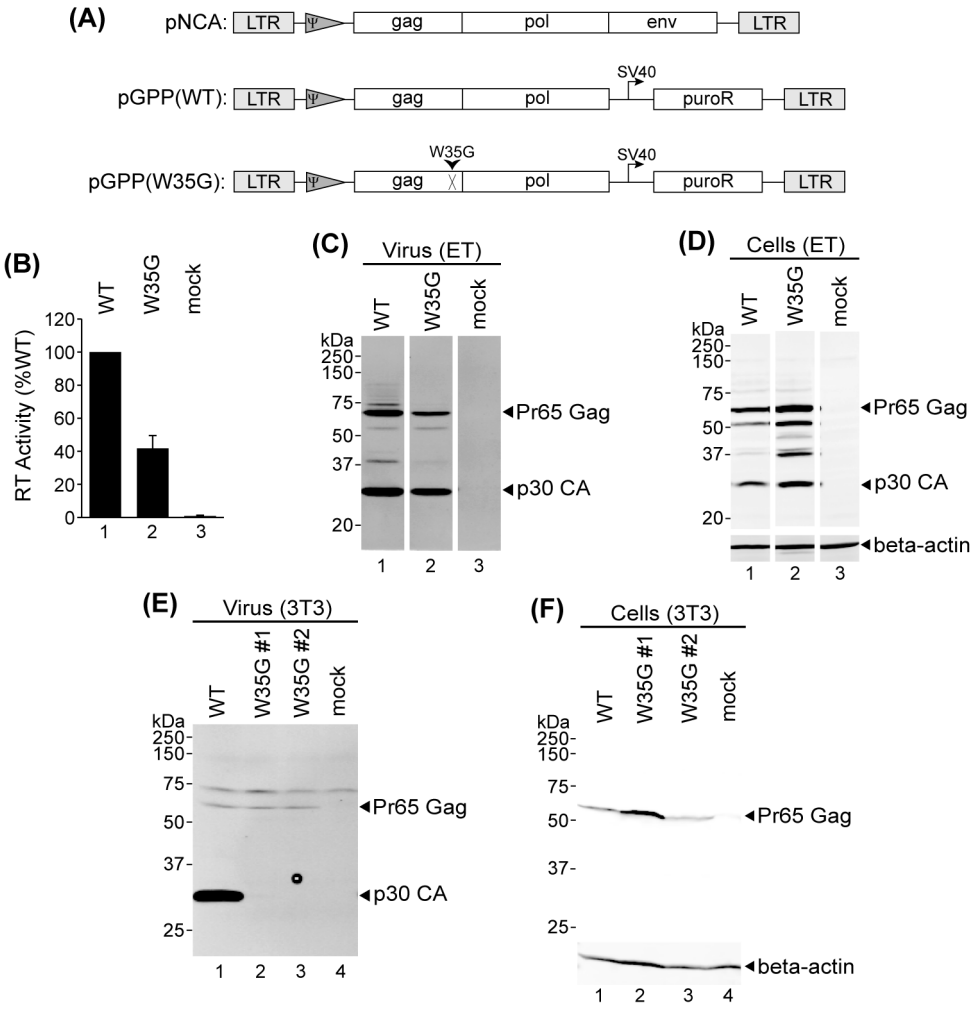

Figure II-2: Virus release of W35G NC mutant MoMLV. (A) Diagram of MoMLV *gag-pol-puro* (GPP) vectors. pNCA is the parental infectious MoMLV proviral clone from which pGPP(WT) and pGPP(W35G) were derived. pGPP(WT) contains an SV40 driven puroR cassette in the place of *env.* pGPP(W35G) contains a single amino acid substitution (W35G) in the NC of pGPP(WT). (B) RT activities of media from cells transfected with pGPP(WT) and pGPP(W35G). Quantification by phosphorimager analysis of RT activity upon endpoint dilution for the W35G mutant is shown relative to WT, which is set to 100%. Data represented are the mean of 6 independent experiments. Error bars indicate the standard error of the means. (C) Western blots of virus lysates and (D) lysates of ET cells transfected with pGPP(WT) and pGPP(W35G). (E) Western blots of virus lysates and (D) lysates of 3T3 cells stably transduced with pGPP(WT) and pGPP(W35G). W35G #1 and #2 represent two distinct clonal 3T3 cell lines stably transduced with pGPP(W35G).

by western blot analysis (Fig II-2C and D). Viral protein lysates revealed an approximate two-fold reduction in total Gag ($Pr65^{Gag}$ and p30 CA) released from cells for the W35G mutant relative to WT (Fig II-2C, lanes 1 and 2). Conversely, western blot analysis of cellular lysates revealed an approximate two-fold increase in total Gag retained in cells for the W35G mutant (Fig II-2D, lanes 1 and 2). This result suggests that introducing the W35G mutation into NC resulted in a modest (approximately two-fold) reduction in virus release from ET cells.

In contrast, although minor differences in $Pr65^{Gag}$ amounts were revealed by western blot analysis, no difference in the pattern of proteolytic processing was observed between WT and the W35G mutant (Fig II-2C and D). These results are consistent with previous studies (46, 83), and suggest that the W35G mutation does not alter Gag processing and has little effect on virus release in ET cells

Virus production of the W35G mutant was also examined in NIH 3T3 cells. 3T3 cells were stably transduced with pGPP(WT) and pGPP(W35G) and viral and cell-associated protein lysates were compared by western blot analysis (Fig II-2E and F). In contrast to virus production observed in ET cells, the W35G mutant exhibited a severe release defect relative to WT in 3T3 cells (Fig II-2E), despite similar protein expression levels in cells (Fig II-2F). These results suggest that there are cell type specific differences in the ability of W35G NC to support virus assembly. Transfected ET cells were used for virus production in subsequent experiments below.

W35G NC mutant virus gRNA packaging and dimerization

To determine the gRNA packaging phenotype of the W35G mutant, the amount of gRNA packaged in virions produced from ET cells transfected with WT and W35G proviral plasmids was determined by RNAse protection assay (RPA). Viral RNA samples were hybridized to a chimeric riboprobe containing sequences complementary to both MoMLV gRNA and 7SL, which is a host RNA packaged by MoMLV at levels proportional to virion proteins (99) (Fig II-3A). RNA from the same amount of virions, as quantified by RT activity, was loaded in each lane, with 7SL serving as an RNA internal control. Quantification of gRNA/7SL ratios revealed that gRNA packaging levels in the W35G mutant virions were approximately 5% of WT levels (Fig II-3B), in agreement with previous reports (46, 83).

Next, the impact of the W35G mutation on gRNA dimerization was examined by non-denaturing northern blotting (Fig II-3C). The results showed that nondenatured W35G mutant and WT virus gRNAs had indistinguishable gel mobilities (Fig II-3C, lanes 1 and 8), i.e., they migrated at the dimer position. Furthermore, the thermostability of the dimer linkage for W35G and WT gRNAs did not differ significantly (Fig II-3C, lanes 2 to 7 and 9 to 13). Additionally, the amount of RNA fragmentation, a characteristic typical of retroviral gRNAs (22, 60), was no greater for the W35G mutant than for the WT (Fig 3C).

WT and W35G NC incorporation into phenotypically mixed virions

The above studies demonstrated that the W35G mutation inhibits gRNA packaging without significantly affecting virus release from transfected human

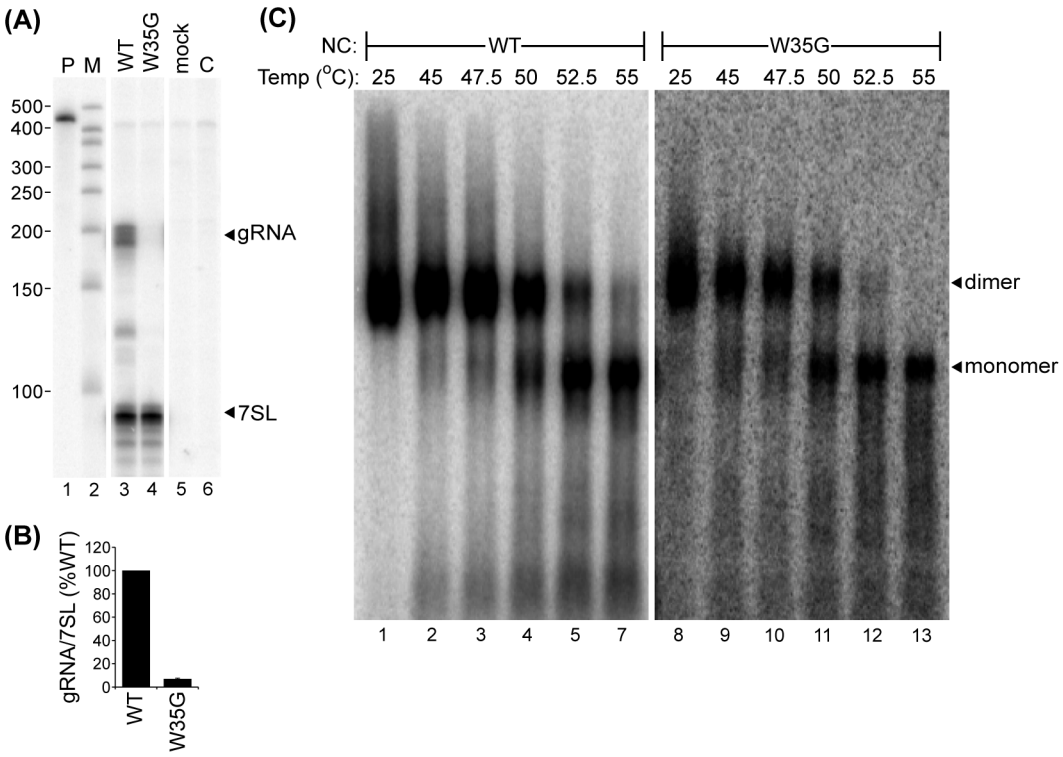

Figure II-3: W35G NC mutant gRNA. (A) RPA of viral RNA harvested from cells transfected with pGPP(WT) and pGPP(W35G). Mobilities of gRNA and 7SL products are indicated on the right. Lane markers include: undigested probe [P] (pAO993-11), RNA size markers [M], and digested probe-alone control [C]. Gel loading was normalized for virion content by RT activity. (B) Quantification of gRNA packaging shown in (A) by phosphorimager analysis is presented as ratios of gRNA/7SL, with the WT level set to 100%. Quantification represents the mean of four independent experiments and the error bars indicate the standard error of the means. (C) Non-denaturing northern blot of viral RNA harvested from cells transfected with pGPP(WT) and pGPP(W35G). RNAs were subjected to the indicated temperature for 10 min prior to electophoresis. Migrations of the gRNA dimer and denatured gRNA monomer are indicated. The sample lanes containing RNAs isolated from the W35G virus (lanes 8 to 13) were image-adjusted to WT-like intensities to compensate for reduced gRNA packaging levels.

cells, gRNA dimerization, gRNA integrity, or proteolytic processing of Gag. The mutation was therefore considered suitable for gRNA packaging studies using phenotypically mixed virions, which were prepared by co-expressing WT and W35G proviral expression plasmids at various input ratios.

As observed above, virion release for the W35G mutant alone was approximately two-fold lower then for WT (Fig II-4A, lanes 1 and 2). With virions produced from co-transfection of various input ratios of WT and W35G mutant plasmids, release recovered to near WT levels as the amount of input WT NC plasmid increased from 1% to 50% (Fig II-4A, lanes 3 to 10). Western blot analysis confirmed both the modest release defect of the W35G mutant alone (Fig II-4B, lanes 1 and 2) and the recovery to near WT levels of virus release as the amount of input WT NC plasmid increased from 1% to 50% (Fig II-4B, lanes 3 to 10).

Although these experiments examined virion production when W35G and wild type Gag were co-expressed, they did not directly address whether or not protein mixtures co-assembled to form individual virions. To determine if there was a bias in the incorporation of WT or W35G mutant NC into the phenotypically mixed virions, the assumption that virions contained ratios of WT and W35G NC that matched the stoichiometry of the input proviral expression plasmids was then tested. For this assay, packaging-defective MoMLV plasmids containing either WT or W35G NCs (called pΔΨMoMLV and pΔΨMoMLV(W35G) respectively) were transfected into ET cells in combination with a packaging-

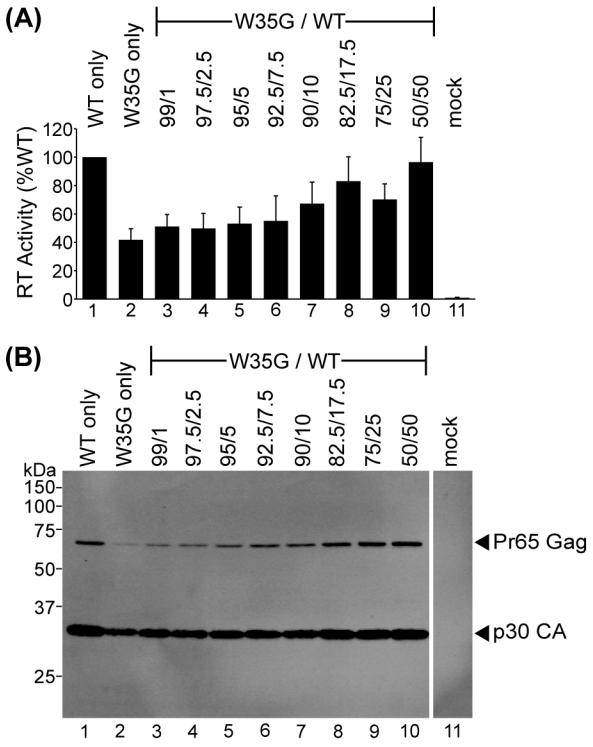

Figure II-4 : WT and W35G NC phenotypically mixed virion production. (A) Quantification of viral release into the culture media and (B) Western blot of lysates of virus harvested from media from cells transfected with the indicated ratios (W35G/WT) of pGPP(W35G) and pGPP(WT). Values for phenotypically mixed virions in (A) are normalized to WT levels, which are set to 100%. Data represent the means of at least 5 independent experiments. Error bars indicate the standard error of the means.

defective MoMLV plasmid containing a protease-inactivating aspartic acid-to-serine mutation at amino acid position 32 (pΔΨMoMLV(PR^-)) (Fig II-5A). This approach for testing co-assembly of co-expressed Gag proteins was designed to ensure that any proteolytic processing in newly formed virions was due to the incorporation of catalytically active protease associated with either a WT or W35G mutant NC-containing polyprotein.

Western blotting confirmed that virus harvested from ET cells transfected with pΔΨMoMLV(PR^-) was defective in the proteolytic processing of Gag (Fig II-5B, lane 1). Phenotypically mixed virions harvested from cells co-transfected with pΔΨMoMLV(PR^-) and increasing concentrations of the plasmids pΔΨMoMLV or pΔΨMoMLV(W35G) displayed increased Gag processing as the amount of protease competent MoMLV increased (Fig II-5B, lanes 2 to 4 and 5 to 7). Even at the highest level of WT PR examined here (30%; Fig II-5B lanes 4 and 7)), Gag processing was significantly lower than that observed for WT (Fig 2C) presumably because the PR point mutant used here associates at random with WT PR monomers in mixed virions to generate inactive PR^+: PR^- heterodimers. However, overall, the Gag processing profile at each concentration of protease-competent MoMLV was the same, regardless of whether the PR^+ plasmid contained WT or W35G mutant NC (Fig II-5B, lanes 2 to 4 and 5 to 7). These results suggest that there was no bias in virion incorporation of either WT or W35G NC and support the assumption that the ratios of WT and W35G NC in

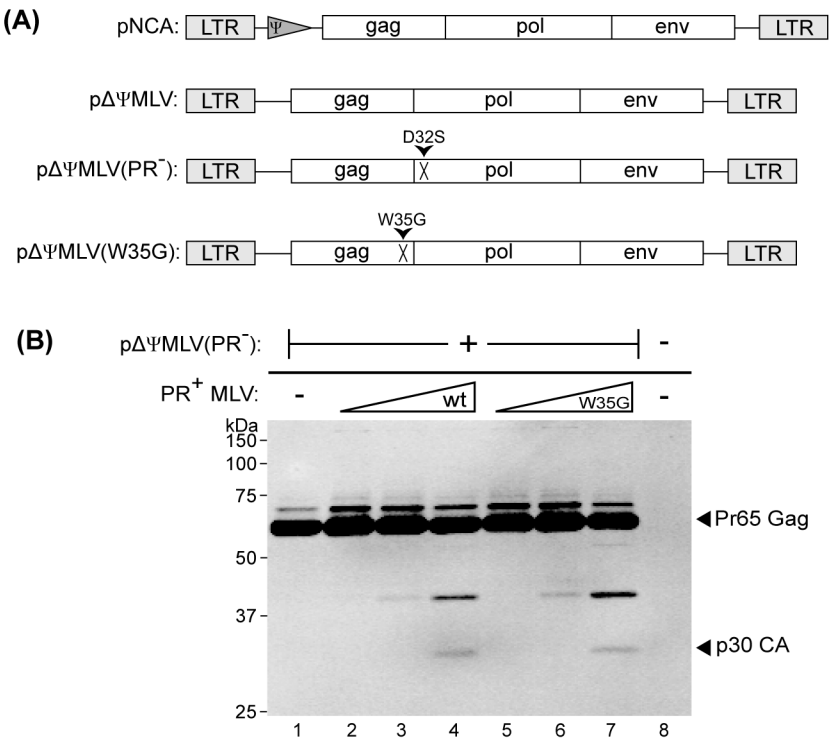

Figure II-5: WT and W35G NC incorporation into phenotypically mixed virions. (A) Diagram of ΔΨMoMLV vectors. pNCA is the parental infectious MoMLV proviral clone from which the following vectors were derived. pΔΨMoMLV contains a "classic Ψ" deletion (80). pΔΨMoMLV(PR$^-$) and pΔΨMoMLV(W35G) contain "classic Ψ" deletions and also contain single amino acid substitutions in protease (D32S) and NC (W35G) respectively. (B) Western blot of virus lysates of phenotypically mixed virions produced from cells transfected with pΔΨMoMLV(PR$^-$) and increasing concentrations of PR$^+$ MoMLV (pΔΨMoMLV or pΔΨMoMLV(W35G)). The following three PR$^-$/PR$^+$ ratios were utilized: 1/0.01, 1/0.10, and 1/0.30). The plasmid pMΨPuro was included in each transfection to serve as gRNA. Full length Pr65^{Gag} and processed p30 CA are indicated on the right.

individual phenotypically mixed virions matched the input proviral expression plasmid ratios.

gRNA packaging in phenotypically mixed virions

Having produced phenotypically mixed virions, and performed control experiments to examine biases in the co-assembly of WT and W35G mutant NCs, the gRNA packaging efficiency of these virions was determined by RPA. RNA harvested from phenotypically mixed virons was normalized to RT activity and probed with a chimeric riboprobe that recognized both gRNA and 7SL. As observed above, quantification of gRNA/7SL ratios showed that gRNA packaging levels for the W35G mutant were approximately 5% of WT levels (Fig II-6A and B, lanes 1 and 2). With phenotypically mixed virions, gRNA packaging recovered to near WT levels as the amount of WT NC increased from 1% to 50% of the total NC present (Fig II-6A and B, lanes 3 to 10). When the amount of WT NC was approximately 5-10% of the total, gRNA packaging recovered to within two-fold of WT levels (Fig II-6A and B, lanes 5 to 7).

Phenotypically mixed virus single-cycle infectivity

To determine whether packaging efficiency was the only replication defect of W35G NC containing virions, replication of phenotypically mixed virions was analyzed using a single-cycle infectivity assay. Virions produced from ET cells co-transfected with various ratios of pGPP(WT) and pGPP(W35G) mutant proviral plasmids were used to infect fresh target cells. Because pGPP derivatives contain a puromycin N-acetyltransferase (puroR) gene in place of the *env* open reading frame, provirus titer represented as puromycin-resistant colony

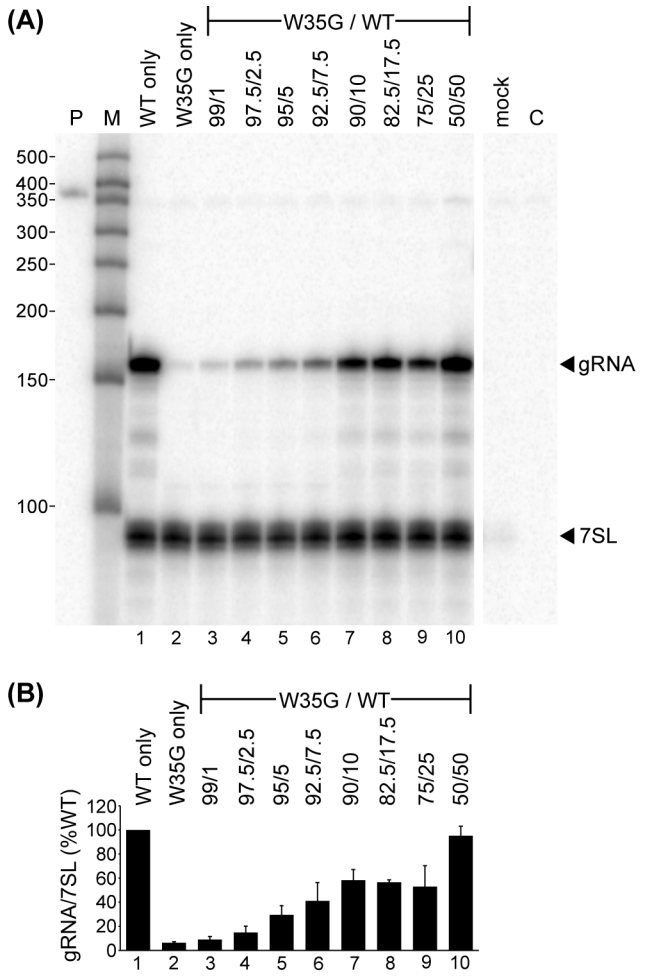

Figure II-6: gRNA packaging of WT and W35G NC phenotypically mixed virions. (A) RPA of viral RNA harvested from cells transfected with the indicated ratios (W35G/WT) of pGPP(W35G) and pGPP(WT). gRNA and 7SL bands are indicated on the right. Lane markers include: undigested probe [P] (pEG467-10), RNA size markers [M], and digested probe-alone control [C]. Gel loading was normalized for virion content by RT activity. (B) Quantification of gRNA packaging shown in (A) by phosphorimager analysis is presented as ratios of gRNA/7SL, with the WT level set to 100%. Quantification represents the mean of at least three independent experiments and the error bars indicate the standard error of the means.

forming units per milliliter (CFU/mL) could be determined (Fig II-7). The titer of the W35G mutant, when normalized for virion abundance, was decreased approximately 1000-fold relative to WT (Fig II-7A, lanes 1 and 2). For the phenotypically mixed virions, titer recovered as the amount of WT NC increased from 1% to 50% of the total NC and plateaued at approximately half of WT levels (Fig II-7A, lanes 3 to 10).

To determine what portion of the decrease in viral titer was due to gRNA packaging defects, the results were also normalized to input gRNA levels as measured by RPA (Fig II-6). In this case, the titer for virions containing 100% W35G mutant was approximately 100-fold lower than WT (Fig II-7B, lanes 1 and 2). Again, titer recovered to only half of WT levels as the amount of WT NC increased from 1% to 50% of the total NC (Fig II-7B, lanes 3 to 10).

Analysis of reverse transcription error rates of phenotypically mixed virus

The above results suggested that in addition to inhibiting gRNA packaging, the W35G mutation negatively impacted other NC functions early in the infection process. To test if errors in reverse transcription contributed to the decrease in proviral titer of the W35G mutant, a *lacZ* inactivation assay was performed (13, 105, 106). In these experiments, virions comprised of phenotypic mixtures of WT and W35G Gag, and which packaged a dual marker vector expressing both *lacZ* and puroR, were generated as described in Materials and Methods. These were used to infect fresh target cells, and provirus-containing puromycin resistant colonies were stained with X-Gal and counted (Fig II-8). Consistent with the results described above, colony forming unit titer decreased

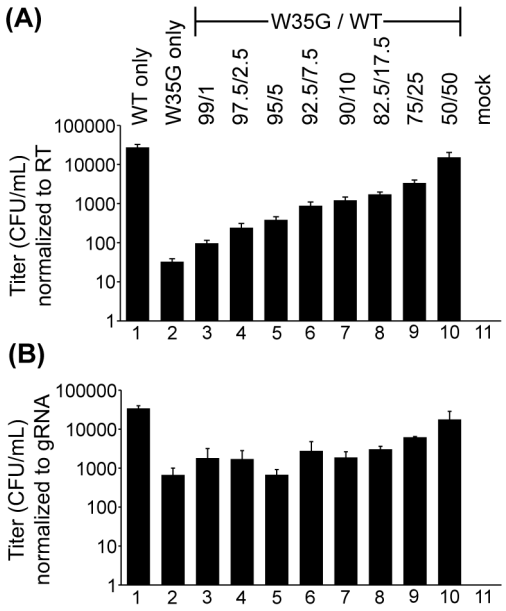

Figure II-7: Infectivity of WT and W35G NC pheotypically mixed virions. Titer of virus produced from cells transfected with the indicated ratios (W35G/WT) of pGPP(W35G) and pGPP(WT). Data was initially collected as puromycin-resistant colony forming units per mL (CFU/mL) and is presented in (A) normalized to virion RT activity (Fig 4) and (B) to virion gRNA packaging levels (Fig 6). Quantification represents the mean of at least three independent infections (of duplicate plates) with virons produced from at least three independent transfections. Error bars indicate the standard error of the means.

as the amount of WT NC decreased to 1% of the total NC (Fig II-8B, lanes 1 to 5). Additionally, the titer of the W35G mutant alone was decreased approximately 1000-fold relative to WT alone (Fig II-8B, lanes 1 and 7).

Consistent with previous studies (13, 105), the *lacZ* inactivation rate, represented as the percent of white colonies relative to the total number of colonies (% white colonies), for WT virus was approximately 10% (Fig II-8C, lane 1), and *lacZ* inactivation from control phenotypically mixed virions containing 95% RNAse H (RH) mutant and 5% WT RH increased approximately two-fold relative to WT only (Fig II-8C, lane 1 and 8).In the experimental samples, *lacZ* inactivation rates remained relatively unchanged for virions containing as little as 10% WT NC (Fig II-8C). However, with phenotypically mixed virions containing lower ratios of WT to W35G NC, the *lacZ* inactivation rates increased steeply (Fig II-8C, lanes 2 to 5). The *lacZ* inactivation rate of W35G mutant virus alone was 100%, as no blue colonies (out of 58 total colonies across five independent infections) were observed (Fig II-8C, lane 6). Taken together, these results suggest that in addition to decreases in gRNA packaging, errors in reverse transcription contributed to, but do not fully account for, decreases in provirus generation by W35G virus.

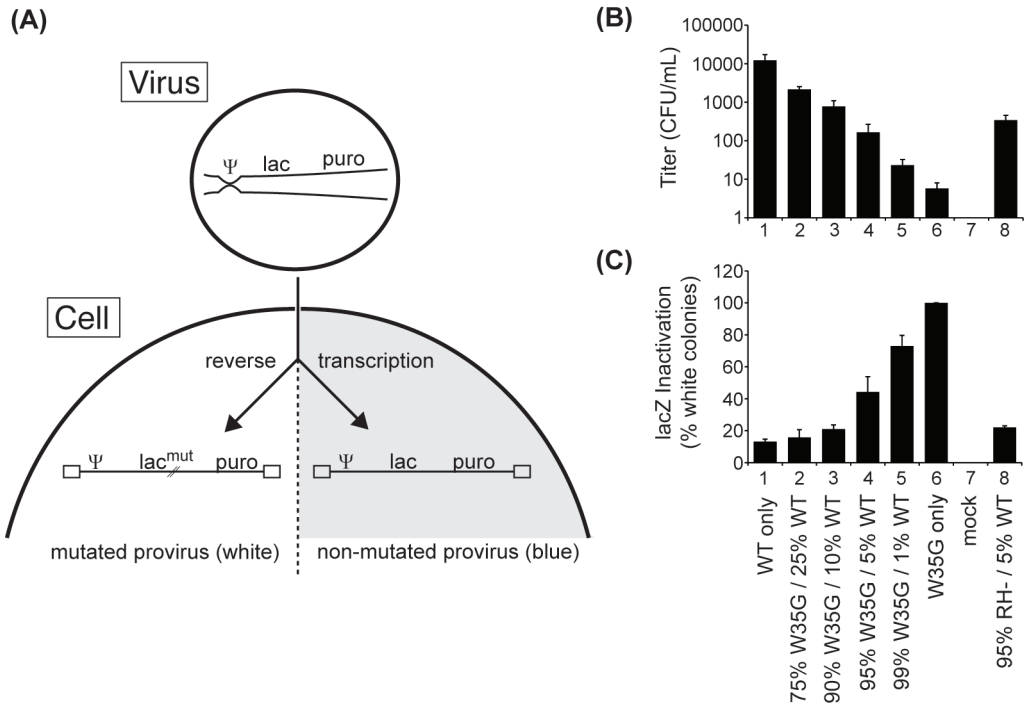

Figure II-8: Reverse transcription error rates of WT and W35G NC phenotypically mixed virions. (A) Schematic overview of the lacZ inactivation assay described in the text. (B) Titer of virus (CFU/mL) produced from cells transfected with the indicated ratios of pΔΨMoMLV, pΔΨMoMLV(W35G), or pMoMLVΨ^{-}DNAP^{+}RH^{-} (RH-). (C) lacZ inactivation (% white colonies) of virus produced from cells transfected with the indicated ratios of the above plasmids. Quantification in (B) and (C) represents the mean of at least four independent infections (of duplicate plates) with virus produced from three independent transfections. Error bars indicate the standard error of the means.

Discussion

The current model of gRNA packaging for MoMLV, based on *in vitro* binding studies, predicts that only a small number of functional Gag molecules (possibly only 12, or ≤1% of all Gag molecules) are required to engage in high-affinity interactions with gRNA to initiate retroviral assembly. This packaging model is consistent with fluorescence microscopy studies in cells, which indicate that the HIV dimeric RNA genome is trafficked to plasma membrane assembly sites by a small number (a dozen or fewer) of HIV-1 Gag proteins (61). The goal of the present study was to test predictions derived from the *in vitro* studies in a cell culture system and examine the threshold limits of MoMLV Gag required to package gRNA.

Phenotypically mixed virions containing WT and packaging deficient W35G mutant NCs were found to package near WT levels of gRNA when amounts of packaging-competent NC represented half of the total. When packaging-competent Gag was reduced to 5-10% of the total, virions showed a modest packaging defect (approximately two-fold). Similar results obtained for HIV-1 (120) suggest that this phenotype is conserved among retroviruses.

The results described here suggest that the threshold limits of MoMLV Gag required to packaged gRNA are greater than what the above packaging model predicts. A possible explanation for the modest defect observed at threshold levels of functional Gag is that the initially formed Gag NC-gRNA complex may be structurally compromised, to some extent, by the presence of mutant Gag proteins. In other words, proper gRNA packaging may require the

occupation of all high-affinity NC binding sites by WT NC, and the presence of even a small amount of mutant-NC containing Gag might be sufficient to disrupt proper packaging. Gag-Gag interactions mediated by the wild type CA domain could help recruit mutant Gag proteins to the packaging signal, thereby facilitating the incorporation of mutant Gag molecules despite the predicted reduction in NC:RNA affinity.

Additional work here demonstrated a genetic separation between gRNA packaging and other replication functions for the W35G mutant. For example, our results showed that the W35G mutation did not impair gRNA dimer formation or gRNA integrity. gRNA dimer formation is dependent on the ability of NC to lower the energy barrier required to disrupt and re-form favorable base pairing interactions within gRNA dimers (41, 108, 112). In addition, the coating of gRNA with one NC molecule every 5 to 8 nucleotides (71) is thought to be important to protect the gRNA from nuclease degradation both in cells (reviewed in (135)) and most relevant for our results, in virions (60, 64). In work describe here, the W35G mutant retained the ability to both protect the gRNA in virions from endoribonuclease digestion and promote the formation of gRNA dimers.

An additional phenotype of the W35G mutant described here was a modest but reproducible release defect in human 293T-derived ET cells. This corresponded to an increase in cell-associated viral protein, suggesting that Gag was retained in the cells. This phenotype has been observed in human cells with other NC mutants that have been shown to impair MoMLV assembly (92). Defects in virus release may be due to disruptions in NC-gRNA interactions in

higher order Gag oligomers that are responsible for forming the structure of newly forming virions (reviewed in (110)). Here, virus release from ET cells recovered when the amount of WT Gag in phenotypically mixed virions approached half of the total Gag, suggesting that the NC-gRNA interactions required to form higher order Gag oligomers do not require a full complement of packaging competent Gag.

Experiments described here were performed in human cells based on our observation that W35G virus release was severely attenuated in murine cells. This result correlates with previous studies where MoMLV NC Trp 35 mutants were shown to quickly revert to WT upon passaging in murine cells (46, 83).

Our results demonstrated that the W35G mutant was approximately 100-fold less infectious than WT in a single cycle infectivity assay, when normalized for packaged gRNA levels. Interestingly, in phenotypically mixed virions, infectivity did not recover to WT-like levels at the same W35G:WT NC ratio as virus release or gRNA packaging, suggesting that a full complement of WT NC may be required for productive early infection events.

NC is known to have many functions in the early steps of retroviral replication which are dependent on its nucleic acid chaperone activity (reviewed in (27, 71, 72, 135). For example, aberrant reverse transcription products result when NC's chaperone functions are impaired by mutating zinc-coordinating residues (44, 45), and Trp 35 mutant MoMLV NC has been shown to decrease reverse transcription through regions of RNA secondary structure (146). Consistent with the notion that disrupting NC's chaperones function results in

aberrant reverse transcription products, we observed defects in reverse transcription for the W35G mutant as measured by a genetic marker inactivation assay for phenotypiclally mixed virions containing ≥95% W35G. Although not tested explicitly, the observation of large decreases in titer at low W35G concentrations suggests that additional defects, such as in reverse transcription initiation, may have contributed to the defects in W35G virion infectivity. Published work showing that primer tRNA placement and annealing are dependent on retroviral NC's chaperone function are consistent with this notion (72).

In summary, the work presented here showed that MoMLV zinc knuckle mutant W35G and WT NC Gag molecules readily co-assembled, and that the resulting phenotypically mixed virions encapsidated roughly half as much gRNA as wild type particles when a 5-10% threshold of WT NC was reached. These studies also demonstrated that authentic dimerization of MoMLV gRNAs and the maintenance of gRNA integrity were independent of the chaperone functions provided by the MoMLV NC zinc knuckle. Nonetheless, replication defects for phenotypically mixed virions were greater than those predicted by gRNA packaging levels, further underscoring the myriad roles of NC in retroviral replication.

Materials and Methods

Cells and Transfectons

ET cells, which are 293T cells that constitutively expresses murine ecotropic envelope, and ET-pLacPuro cells, which are ET cells that constitutively

express an MoMLV vector containing both a LTR promoter driven *lacZ* gene and a simian virus 40 (SV40) promoter driven pruomycin N-acetltransferase (puroR) gene in place of the viral genes (106), were maintained in Dulbecco's modified Eagles's medium (DMEM; Invitrogen) supplemented with 10% fetal bovine serum (Gemini), 100 U/mL penicillin, and 100 μg/mL streptomycin (Invitrogen). D17/pJET cells, a canine osteosarcoma cell line that constitutively expresses murine ecotropic receptor (98), and NIH 3T3 cells were maintained in DMEM supplemented with 10% bovine serum (Invitrogen), 100U/mL penicillin, and 100 μg/mL streptomycin (Invitrogen). Both ET and D17/pJET cells were grown at 37°C with 5% CO_2 in a humidified incubator. Transfections were carried out using polyethlenimine (PEI) as described previously (64).

Plasmids

The MoMLV-based *gag-pol-puro* plasmid, pGPP(WT) (aka pSRK876-15), contains an intact provirus modified by the replacement of the *env* open reading frame with a puroR driven by a SV40 promoter (Fig II-2A) (106). The W35G NC mutation in pGPP(W35G) (aka pEG479-1) was generated by overlap extension PCR, sequenced, and used to replace the corresponding portion of pGPP(WT) (Fig II-2A).

The "classic Ψ" deletion (Δ215-568) (80) in pΔΨMoMLV (aka pAO147-2) was generated by overlap extension PCR, sequenced, and used to replace the corresponding portion of pNCA (24) (Fig 5A). A restriction fragment encompassing the W35G mutation in NC of pGPP(W35G) replaced the corresponding portion of pΔΨMoMLV to generate pΔΨMoMLV(W35G) (aka

pSFJ93-1) (Fig II-5A). For pΔΨMoMLV(PR$^-$) (aka pSFJ229-1), site directed mutagenesis was performed using the QuikChange II Site-Directed Mutagenesis Kit (Stratagene) to introduce an aspartic acid-to-serine mutation at amino acid position 32 of MoMLV protease (PR) in pΔΨMoMLV, which sequencing confirmed (Fig II-5A). Construction of the MoMLV packaging vector pMΨPuro (aka pAM86-5) and the RNAse H mutant (D524N) plasmid pMoMLVΨ$^-$DNAP$^+$RH$^-$ (aka pTW76-3) were described previously (13, 68).

The riboprobe templates were derivatives of pBSII SK(+) (Stratagene) that contained PCR fragments inserted into the EcoRV site. The PCR insert in pAO993-11 includes complementarity to portions of both MoMLV 5'-UTR (nucleotides(nt) 55-255) and 100 nt of 7SL RNA (99). The insert in pEG467-10, which was generated by PCR from pAO993-11, also included complementarity to portions of both MoMLV 5'-UTR (nt 55-214) and 100 nt of 7SL RNA (38).

Virus Isolation

Virus was isolated from tissue culture supernatants harvested at 48 h post transfection by centrifugation (64). For western blotting, the viral pellets were resuspended in RIPA lysis buffer (1% NP40, 0.1% sodium dodecyl sulfate, 0.5% sodium deoxycholate, 150 mM Nacl, 50 mM Tris [pH7.5]) supplemented with 1X protease inhibitor cocktail (PIC) tablet (Roche) and 1 mM phenylmethylsulfonyl fluoride (PMSF). Viral protein lysates were stored at -20°C. For RNAse protections assays, viral pellets were resuspended in TRIzol® reagent (Invitrogen) and stored at -80°C. For non-denaturing northern blots, RNA was isolated from viral pellets using proteinase K-based extraction (35). Virus was

quantified using an exogenous reverse transcriptase (RT) assay (38) based on a previously described protocol (134).

Western Blotting

Total cell protein was harvested in RIPA lysis buffer supplemented with 1X PIC tablet (Roche) and 1 mM PMSF. Cells were first lysed on ice for 30 min in RIPA buffer and then cleared by centrifugation at 13,000 rpm for 20 min at 4°C. Virus lysates were prepared as described above.

Cell and virus lysates were resolved by SDS-PAGE and transferred to polyvinylidene fluoride (PVDF; Bio-Rad) membranes overnight using a Mini-PROTEAN® 3 Cell transfer apparatus (Bio-Rad). Membranes were blocked in 1% nonfat dried milk in TBS (50 mM Tris [pH7.5], 150 mM NaCl) for 1 h at room temperature. After blocking, membranes were incubated with primary antibodies diluted in 1% nonfat dried milk in TBS containing 0.1% Tween-20 (TBS-T), for 1 h at room temperature. The rat mAb against MoMLV p30 CA was derived from hybridoma supernatants (from Bruce Chesebro: ATCC clone R187) and diluted 1:600. The beta-actin mAb (Ambion: AM4302) was diluted 1:5,000.

Secondary antibodies were diluted in 1% nonfat dried milk in TBS-T and incubated for 1 h at room temperature. The following dye-conjugated secondary antibodies were utilized at a 1:7,500 dilution: goat anti-rat IRDye® 800CW and goat anti-mouse IRDye® 680 (Li-Cor Biosciences). After incubation in both primary and secondary antibodies, the membranes were washed 3 times with TBS-T. A final wash in TBS was performed before proteins were detected and quantified using the Li-Cor Odyssey system (Li-Cor Biosciences).

RNAse Protection Assay (RPA)

To produce riboprobes, pAO993-11 and pEG467-10 (see above) were linearized with HindIII and *in vitro* transcribed using T3 RNA polymerase (Promega) and [α-^{32}P]-rCTP (Perkin-Elmer). pAO993-11 protects 200 nt of MoMLV gRNA and 100 nt of 7SL RNA while pEG467-10 protects 163 nt of MoMLV gRNA and 100 nt of 7SL RNA respectively. Hybridization of riboprobes with sample RNA, RNAse digestion, and resolution was carried out as described previously (86).

Non-Denaturing northern blot

Non-denaturing northern blot analysis of viral RNAs isolated by the proteinase-K-based extraction method (see above) was carried out as described previously (86).

Infections

D17/pJET cells were infected in 35 mm dishes for 4 h in the presence of hexadimethrine bromide (Polybrene; Sigma). Virus-containing media was then removed and cells were transferred to 10 cm dishes. 48 h post infection, media containing 2 μg/mL puromycin was added and after 12 days of selection, colonies were stained with crystal violet for counting. Infectious units are represented as colony forming units per milliliter (CFU/mL).

lacZ inactivation assay

Virions produced from ET-pLacPuro cells co-transfected with various ratios of p$\Delta\Psi$MoMLV and p$\Delta\Psi$MoMLV(W35G) or pMoMLVΨ^-DNAP$^+$RH$^-$ mutant proviral plasmids were used to infect D17/pJET cells as described above. After

selection, colonies were stained with 5-bromo-4-chloro-3-indolyl-β-D-galactopyranoside (X-Gal) and counted.

Chapter III

The molecular proportions of the Moloney murine leukemia virus Gag-Pol polyprotein and genomic RNA are determined by disparate mechanisms

Abstract

The Moloney murine leukemia virus ribonucleoprotein (RNP) complex is composed of a 20:1 mixture of the viral Gag and Gag-Pol polyproteins plus a single genomic RNA (gRNA) dimer. The mechanism that regulates the conserved proportions of RNP constituents is unknown. Here, I examined whether the proportions of Gag, Gag-Pol, and gRNA in virions are determined by sampling, that is, if they reflected expression ratios or intracellular concentrations, or more specific recruitment. To this end, I utilized an experimental system whereby MoMLV Gag, Gag-Pol, and gRNA, were expressed separately, thereby allowing manipulation of the ratios of the two polyproteins and gRNA. Upon varying the ratios of Gag and Gag-Pol in MoMLV particles, I observed that Gag-Pol incorporation was stochastic and that maintenance of the conserved 20:1 Gag:Gag-Pol ratio coincided with maximal particle production. An overabundance of Gag-Pol relative to Gag resulted in particles that maintained intracellular protein ratios but were defective in particle production. In addition, I obtained evidence that MoMLV Gag-Pol may be involved in regulating the amount of gRNA packaged into particles but that the NC domain of either Gag or Gag-Pol can provide the gRNA packaging function

during MoMLV assembly. By manipulating both the ratio of Gag to gRNA and that of Gag to Ψ/DLS's in MoMLV particles, I tested which of the above described mechanisms is responsible for determining the molecular proportion of Gag and gRNA. Unlike when Gag-Pol was overexpressed, I observed an upper limit of gRNA incorporation and no significant disruption of MoMLV particle production when the proportion of Gag to gRNA or Ψ/DLSs was altered.

Introduction

Retroviruses such as Moloney murine leukemia virus (MoMLV) can be considered RNP complexes, comprised of proteins and RNA, surrounded by a lipid envelope. Within the MoMLV RNP, the Gag and Gag-Pol polyproteins are the major and minor viral protein components respectively, whereas the viral gRNA is the major RNA component. Assuming that absolute numbers are analogous to those in HIV-1, the MoMLV RNP is composed of roughly 2,500 Gag molecules, 125 Gag-Pol meoecules, and precisely one gRNA dimer (16).

The MoMLV Gag precursor polyprotein is encoded by the *gag* gene. *gag* is located near the 5' end of the viral genome, immediately upstream of *pol*, which encodes the viral enzymes. MoMLV Pol is not expressed from its own mRNA, but is translated as a C-terminal extension of Gag when the *gag* stop codon is readthrough into the *pol* reading frame (reviewed in (50)). Therefore, the resulting Gag-Pol fusion is identical to Gag in its N-terminus.

The mechanism of MoMLV *gag* stop codon readthrough has been elucidated (54). Immediately downstream of the *gag* stop codon is an RNA

pseudoknot structure that is responsible for allowing readthrough via termination suppression (reviewed in (3)). Recent NMR-based structural studies have demonstrated that at physiological pH the pseudoknot adopts a conformation permissive for stop codon readthrough in approximately 5% of MoMLV RNAs, whereas a non-permissive conformation is observed in the remaining 95% (54). These ratios correlate well with the 20:1 Gag:Gag-Pol ratio observed for MoMLV (58).

The MoMLV Gag polyprotein directs virus assembly and gRNA packaging (reviewed in (110)). The nucleocapsid (NC) domain of MoMLV Gag mediates protein-RNA interactions that are important for these processes via its conserved "zinc knuckle" motif (51). Certain mutations within NC disrupt virus assembly, gRNA packaging, and infectivity (43, 46, 59, 83, 92, 111).

MoMLV gRNAs are packaged as dimers: they are linked near their 5' ends via a dimer linkage structure (DLS) that overlaps with a region known as Ψ (Psi) for "packaging signal". gRNA dimerization and packaging are physically and functionally linked (reviewed in (25)), and mutations or deletions of the Ψ/DLS region result in gRNA packaging defects (34, 80, 93). Like Gag, the MoMLV Gag-Pol polyprotein contains an NC domain. It is unknown if the RNA binding interactions of the NC protein in the context of Gag-Pol differ from those in Gag.

The MoMLV Gag-Pol polyprotein is thought to be incorporated into assembling virions via capsid (CA):CA interactions between the CA domains of Gag and of Gag-Pol respectively, in a manner similar to that observed for HIV-1

(56, 128). Retroviral Gag and Gag-Pol interactions, which are believed to occur subsequent to initial NC-RNA mediated Gag mulitmerization (66), are believed to take place within the cytoplasm (47, 70) and are followed by transport to sites of assembly at cell membranes (21, 104, 125).

The fact that an MoMLV RNP assembles from thousands of Gag molecules – each one containing a zinc knuckle-bearing NC domain with an intrinsic ability to form high affinity interactions with gRNA – and that not every NC forms high affinity interactions with a Ψ/DLS means that there is an asymmetry among Gag molecules within the RNP. Presumably, MoMLV Gag molecules are separated into two distinct pools: Gags that participate in high-affinity gRNA interactions and ones that do not (59, 86). Neither the "counting" mechanism that regulates the single-dimer packaging specificity of gRNA nor the mechanism that segregates the two pools of MoMLV Gag is known.

An additional asymmetry exists between Gag and Gag-Pol molecules within the RNP, since each of the thousands of Gag molecules contains a CA domain with an intrinsic ability to interact with Gag-Pol. That the "counting" mechanism that regulates the copy number of Gag-Pol packaged into RNPs is manifested by gene expression levels is suggested by the observation that the 20:1 Gag:Gag-Pol copy number in retroviral RNPs (16) matches the 20:1 Gag:Gag-Pol expression ratio in cells (54, 58). In other words, this correlation suggests that MoMLV Gag-Pol incorporation is stochastic and that incorporation

into virions is the result of “sampling” of intracellular population of Gag-Pol. This is in contrast to gRNA incorporation, which is highly specific.

The goal of the present study was to test the hypothesis that the ratio of Gag to Gag-Pol, and of Gag to gRNA in MoMLV particles is determined by intracellular expression ratios. In order to manipulate the ratios of Gag and Gag-Pol in the MoMLV RNP, an experimental complementation system was established whereby the intracellular expression of the two proteins was unlinked by placing each gene on a separate expression construct. Separating the expression of Gag and Gag-Pol allowed the ratio of the two proteins to be manipulated experimentally. Using this system, the stoichiometry of Gag-Pol in MoMLV particles could be determined. The impact of the manipulation of Gag:Gag-Pol ratios on MoMLV production, gRNA packaging, and infectivity was then examined. Furthermore, separating the expression of Gag and Gag-Pol provided a system to test whether or not the NC domain of Gag-Pol contributes to gRNA packaging.

Two strategies were employed to manipulate the copy number of gRNA within the MoMLV RNP. First, a gRNA overexpression system was used to manipulate the intracellular ratio of Gag and gRNA. Second, the ratio of Gag:Ψ/DLS was altered using MoMLV vectors that contained multiple Ψ/DLS regions.

Results

MoMLV particle production and incorporation of Gag-Pol

In order to test the hypothesis that the ratio of Gag and Gag-Pol in MoMLV particles is determined by intracellular expression ratios, an experimental system was designed that allowed Gag and Gag-Pol quantification. This system utilized MoMLV helper plasmids that contained protease (PR)-inactivating aspartic acid-to-serine (D32S) mutations (Fig III-1). Use of the PR^{D32S} helpers was designed to prevent the proteolytic processing of Gag and Gag-Pol in newly assembled particles, thereby allowing visualization of intact polyproteins by western blotting. The PR^{D32S} helper constructs provided all the MoMLV proteins *in trans* for the assembly of virus-like particles containing the MoMLV vector pMΨPuro (Fig III-1).

To confirm that PR was inactivated by this mutation, MoMLV particles were produced by co-transfection of 293T-derived ET cells (106) with $p\Psi^-$ MLV(PR^{D32S}) and pMΨPuro, and protein lysates of the resulting MoMLV particles were examined by western blot analysis (Fig III-2A). The results confirmed the absence of detectable proteolytic processing of Gag and Gag-Pol for the PR^{D32S} mutant, since no Pr65 Gag cleavage products were observed under these conditions (Fig III-2A). Furthermore, use of the PR^{D32S} mutant allowed resolution of full-length Pr180 Gag-Pol (Fig III-2A). Quantification of the amounts of protein shown in Fig III-2A revealed that ~6% of total Gag (Pr65 Gag + Pr180 Gag-Pol) was comprised of PR180 Gag-Pol. This result is consistent with reported MoMLV

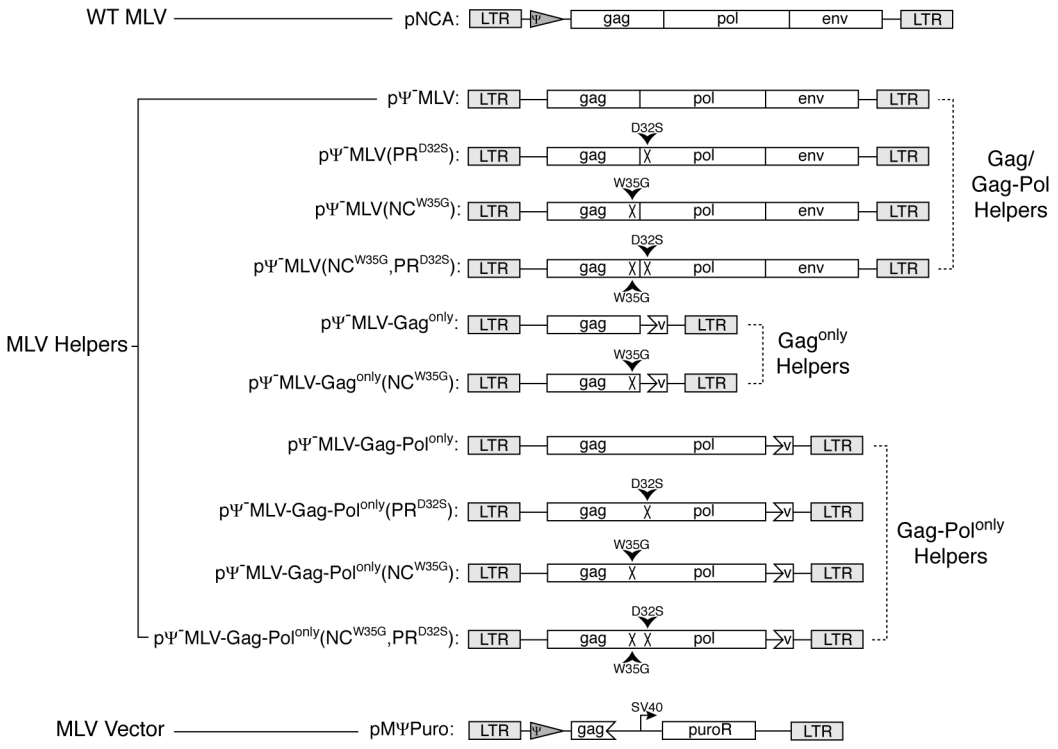

Figure III-1: Structure of MoMLV proviral clones. Diagram of MoMLV helper constructs used in the experiments described here. pNCA is the parental WT MoMLV clone from which all other constructs were derived. The MoMLV helpers contain a Ψ deletion from nucleotides 215-368. Gag/Gag-Pol helpers contain all the viral genes including *gag*, *pol*, and *env*. They include pΨ⁻MLV and pΨ⁻MLV-derived constructs that contain the indicated single amino acid substitutions in protease (D32S) and NC (W35G). The Gag^{only} helpers contain deletions of *pol* and *env* and include constructs containing both WT and W35G mutant NCs. Gag-Pol^{only} helpers are *env* deleted and contain a mutation that eliminates the Gag stop-codon. They include pΨ⁻MLV-Gag-Pol^{only} and pΨ⁻MLV-Gag-Pol^{only}-derived constructs that contain the indicated D32S and W35G point mutations. The MoMLV vector pMΨPuro contains an SV40 driven puromycin resistance (puroR) cassette in place of the viral genes.

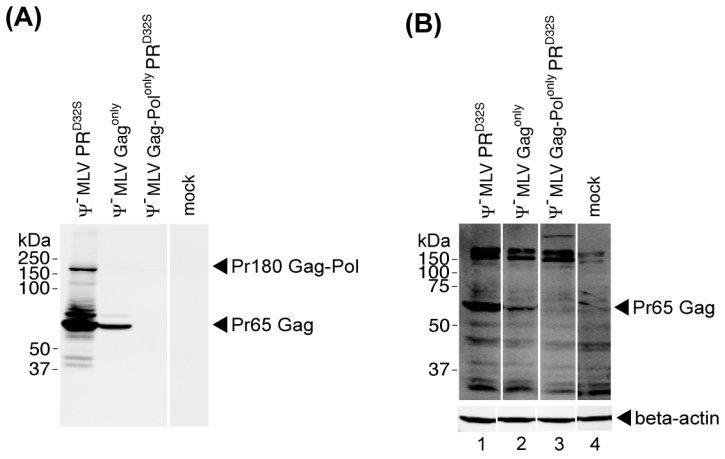

Figure III-2: MoMLV particle production. (A) Western blot of virus lysates and (B) cell lysates of ET cells transfected with the indicated MoMLV helpers. The MoMLV vector pMΨPuro was included in all transfections here to serve as gRNA.

gag stop codon readthrough frequencies that result in a 20:1 Gag:Gag-Pol expression ratio (54, 58).

Consistent with previous studies (122), transfection of ET cells with an MoMLV helper that produces only the Gag polyprotein, in this case pΨ⁻MLV-Gag^{only} (Fig III-1), resulted in efficient particle production (Fig III-2A, lane 2). Specifically, virus production remained approximately 20% as high for cells transfected with pΨ⁻MLV-Gag^{only} as with the helper pΨ⁻MLV(PR^{D32S}) (Fig III-2A, lanes 1 and 2). Cell-associated proteins of cells transfected with these helpers were also compared by western blot analysis (Fig III-2B), and reveal an approximately five-fold decrease in cell-associated Gag for pΨ⁻MLV-Gag^{only} relative to pΨ⁻MLV(PR^{D32S}) (Fig III-2B, lanes 1 and 2). These results suggest that differences in Gag expression between pΨ⁻MLV-Gag^{only} and pΨ⁻MLV(PR^{D32S}) helper constructs largely explain the observed decrease in virus production.

Also consistent with previous studies (33), transfection of ET cells with an MoMLV helper that produces only the Gag-Pol polyprotein, in this case pΨ⁻MLV-Gag-Pol^{only}(PR^{D32S}) (Fig III-1), resulted in drastic reductions in particle production, since only small amounts of Pr180 Gag-Pol (~1% relative to Pr65 Gag from pΨ⁻MLV-Gag^{only}) were observed in MoMLV protein lysates (Fig III-2A, lanes 2 and 3, and Fig III-3A, lanes 1 and 2).

To examine the impact of altered Gag:Gag-Pol polyprotein ratios on MoMLV production, pΨ⁻MLV-Gag^{only} and pΨ⁻MLV-Gag-Pol^{only}(PR^{D32S}) were transfected into ET cells, either alone or in combination with each other at various

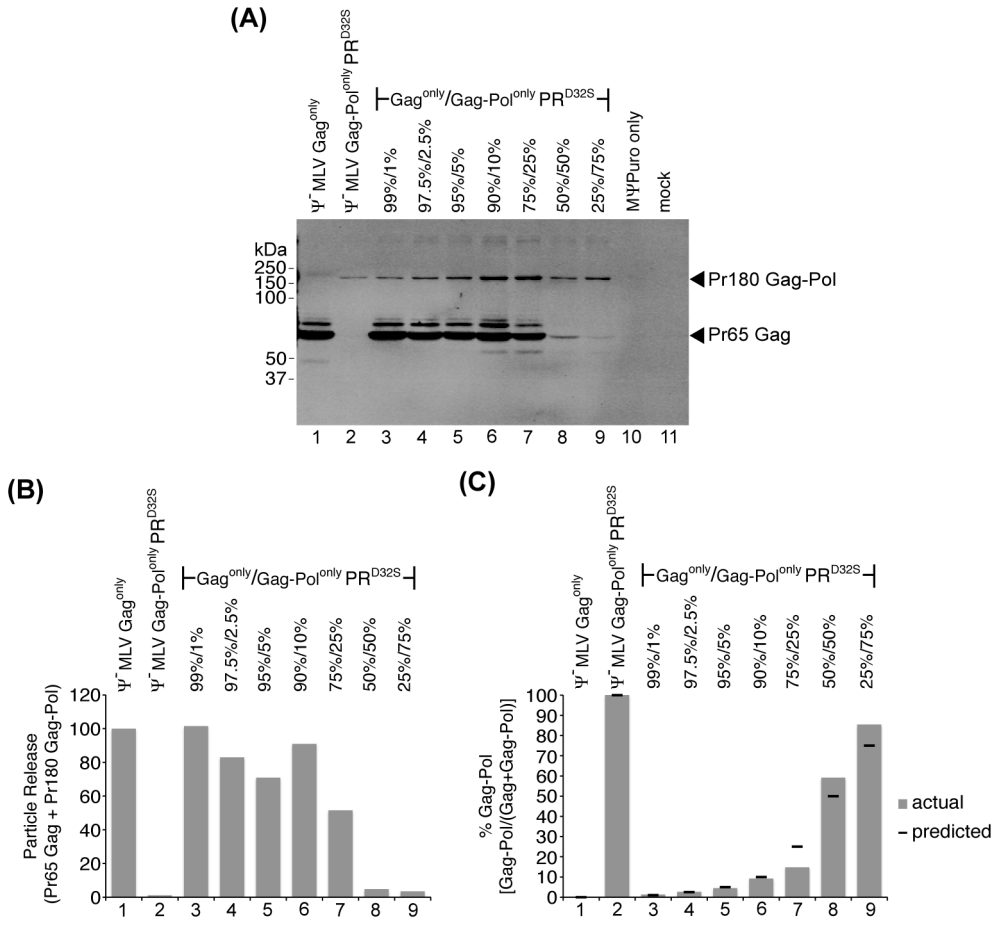

Figure III-3: Incorporation of Gag-Pol into MoMLV particles (A) Western blot of equal volumes of virus lysates of ET cells either transfected alone with the indicated Gag^{only} or Gag-Pol^{only} helpers (lanes 1 and 2) or co-transfected with the indicated ratio of Gag^{only}/Gag-Pol^{only} helpers (lanes 3 through 9). (B) Quantification of MoMLV particle production shown in (A) is presented as total Gag (Pr65 Gag + Pr180 Gag-Pol) released into the media and is shown relative to the Gag^{only} alone sample which is set to 100% (C) Quantification of the % Gag-Pol in MoMLV particles shown in (A) is presented as % Gag-Pol relative to total Gag (Pr65 Gag + Pr180 Gag-Pol). Grey columns represent quantification of WB bands and black bars represent the predicted % Gag-Pol based on input plasmid ratios. The MoMLV vector pMΨPuro was included in all transfections here to serve as gRNA.

molar ratios, in the presence the MoMLV vector pMΨPuro. MoMLV particle protein lysates were then examined by western blotting (Fig III-3A). Co-expression of Gag and Gag-Pol supported efficient particle production across a wide range of ratios (Fig III-3A, lanes 3 through 7). However, when Gag-Pol represented 50% or greater of the total viral polyproteins co-expressed in cells, particle production was attenuated, and particle release decreased approximately 100 fold or greater relative to particles containing 20:1 “wild-type like” Gag:Gag-Pol ratios (Fig III-3A and B, lanes 8 and 9).

Note that although particle yield decreased as the amount of input Gag-Pol expression plasmid increased from 1% to 75% of the total Gag expression plasmid, the amount of Gag-Pol in particles correspondingly increased (Fig III-3A, lanes 3 through 9). Quantification of Gag-Pol in these samples revealed that the amount of Gag-Pol observed in particles (actual) closely matched the input transfected plasmid amounts (predicted) (Fig III-3C). These results suggest that the incorporation of Gag-Pol into MoMLV virions is stochastic across a broad range of protein co-expression ratios.

Impact of MoMLV Gag:Gag-Pol ratio on single-cycle infectivity

Next, the impact of altered MoMLV Gag:Gag-Pol polyprotein ratios on virus infectivity was determined. Similar to the experiment above, Gag and Gag-Pol helpers were transfected into ET cells either alone or in combination with each other at various input ratios. However, for this assay the Gag-Pol helper pΨ^{-}

MLV-Gag-Pol^{only} (Fig III-1), which contains a functional PR, was utilized so that single-cycle infectivity could be measured. Virus produced in this manner was used to infect fresh target cells, and provirus titer, represented as puromycin-resistant colony forming units per milliliter (CFU/mL), was determined (Fig III-4A). The results indicated that titers remained relatively unchanged for virus containing 1% to 25% Gag-Pol (Fig III-4A, lanes 3 through 7). In contrast, the titers of virus containing 50% Gag-Pol or greater (Fig III-4A, lanes 8 and 9) was decreased approximately 100-fold or more relative to the titers of virus with 25% or less Gag-Pol. These approximate 100-fold decreases in titer match the approximate 100-fold decrease in virus production shown in Fig III-2, thereby suggesting that defects in titer reflected defects in virus production and that infectivity per virion remained largely unchanged by excess Gag-Pol.

Unexpectedly, virus produced from the Gag helper constructs alone (Fig III-4A, lane 1) yielded low but reproducible proviral titers that were greater than those observed when cells were infected with media from mock transfected cells (Fig III-4A, lane 10). This result was unexpected, since virus that lacks Pol should not produce titer in the single-cycle infectivity assay. To determine if the titer observed for these MoMLV particles resulted from reverse transcription products, a single-cycle infectivity assay was performed in the presence of the reverse transcriptase inhibitor 3'-azido-3'-deoxythimidine (AZT) (Fig III-4B). Whereas in the absence of AZT a small but reproducible titer (23±6 CFU/mL) was observed with virus produced from the helper pΨ^{-}MLV-Gag^{only}, titer was below the limit of

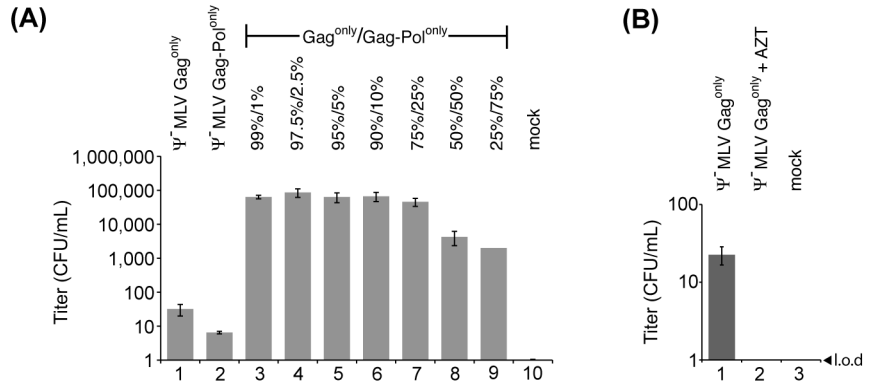

Figure III-4: Impact of MoMLV Gag:Gag-Pol ratio on single-cycle infectivity (A) Titer of virus produced from ET cells transfected with the indicated Gag^{only} or $Gag\text{-}Pol^{only}$ helpers (lanes 1 and 2) or co-transfected with the indicated ratio of Gag^{only}/$Gag\text{-}Pol^{only}$ helpers (lanes 3 thru 9). (B) Titer of virus produced from ET cells transfected with the indicated Gag^{only} helper either in the absence or presence of 200 μM AZT. The limit of detection (l.o.d.) for this assay is indicated. Quantification is presented as puromycin-resistant colony forming units per mL (CFU/mL). Error bars indicate the standard error of the means. The MoMLV vector pMΨPuro was included in each transfection to serve as gRNA.

detection (<1 CFU/mL) in the presence of AZT (Figure III-4B). This suggests that the proviral titer observed for pΨ⁻MLV-Gag^{only} virus in Fig III-4A and B was the result of some form of reverse transcription.

Impact of MoMLV Gag:Gag-Pol ratio on gRNA packaging

One way of quantifying gRNA packaging is determining the ratio of gRNA/7SL. 7SL is a host RNA packaged by MoMLV at levels proportional to virion proteins (99) and therefore serves as an internal standard for normalizing MoMLV particle numbers. To compare the ratio of gRNA/7SL for the Gag and Gag-Pol complementation system to WT MoMLV, a plasmid containing a WT proviral MoMLV clone (pNCA) was transfected into ET cells, then virion RNA was harvested from the media and gRNA packaging was examined by RNAse protection assay (RPA) using a chimeric riboprobe containing sequences complementary to gRNA and 7SL (Fig III-5A). The results established a baseline for packaging that was consistent with values previously reported for MLV (99).

Next, the impact of altered MoMLV Gag:Gag-Pol polyprotein ratios on gRNA packaging was determined. As above, pΨ⁻MLV-Gag^{only} and pΨ⁻MLV-Gag-Pol^{only}(PR^{D32S}) were transfected into ET cells either alone or in combination with each other at various molar ratios along with the MoMLV vector pMΨPuro. MoMLV particle RNA was then harvested and gRNA packaging was examined by RPA using the same riboprobe as above (Fig III-5C).

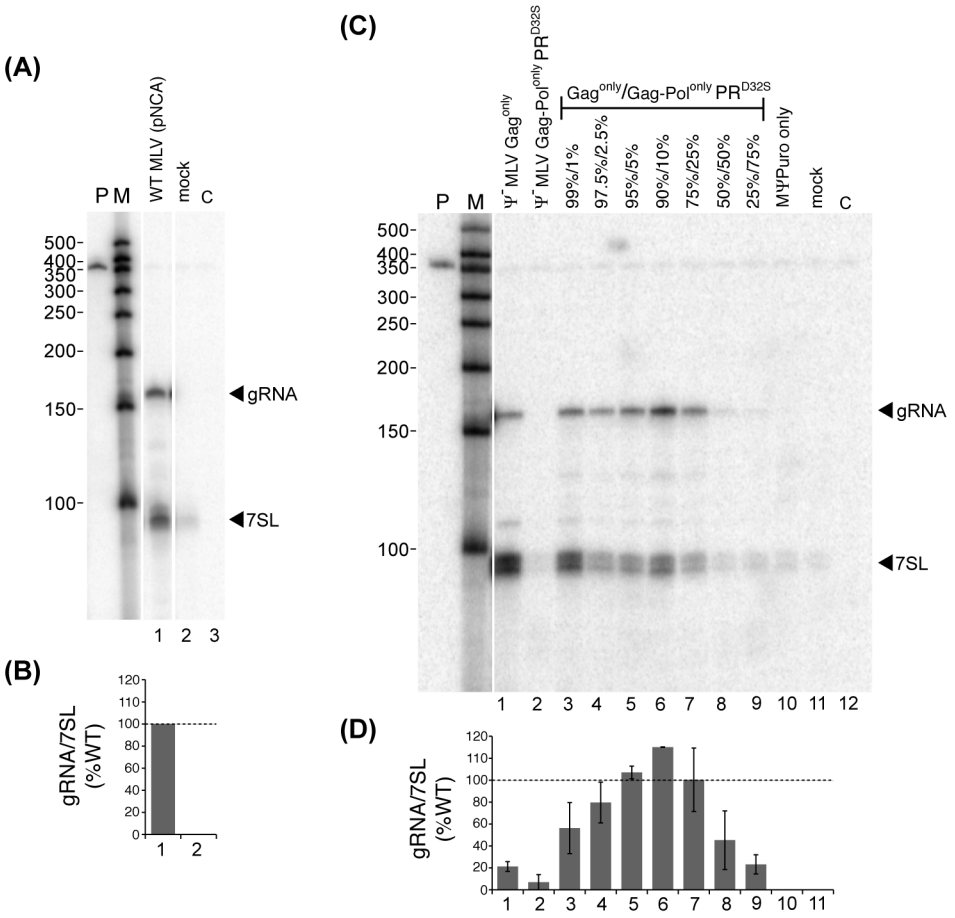

Figure III-5: Impact of MoMLV Gag:Gag-Pol ratio on gRNA packaging. (A) RPA of particle RNA harvested from ET cells transfected with WT MoMLV (pNCA). (B) Quantification of gRNA packaging is presented as a ratio of gRNA/7SL (with WT set to 100%) and represents a single experiment. (C) RPA of particle RNA harvested from ET cells transfected with the indicated Gag^{only}, and $Gag\text{-}Pol^{only}$ helpers (lanes 1 and 2) or co-transfected with the indicated ratio of Gag^{only}/$Gag\text{-}Pol^{only}$ helpers (lanes 3 through 9). The plasmid pMΨPuro was included in each transfection to serve as gRNA. (D) Quantification of gRNA packaging in (C) is presented as ratios of gRNA/7SL (normalized to 100% WT in (A) and (B)) and represents the results of two experiments. Error bars indicate the standard error of the means. Lane markers for RPAs include: undigested probe [P] (pEG467-10), RNA size markers [M], and digested probe-alone control [C]. gRNA and 7SL bands are indicated on the right.

Consistent with the results described above, co-expression of excess Gag and lower levels of Gag-Pol across a wide range of ratios resulted in efficient particle production (Fig III-5C, lanes 3 through 7), and particle production was attenuated (reflected by decreases in 7SL signal) when Gag-Pol represented 50% or greater of the total protein (Fig III-5C, lanes 8 and 9). Packaged gRNA (Fig III-5B) had a ratio of gRNA/7SL for WT MoMLV similar to the gRNA/7SL ratio when pΨ⁻MLV-Gag^{only} and pΨ⁻MLV-Gag-Pol^{only}(PR^{D32S}) were transfected into ET cells at a 95%:5% ratio (Fig III-4D, lane 5). This result is consistent with the presumed 95%:5% Gag:Gag-Pol expression ratio in cells for WT MoMLV.

Additional quantification of gRNA/7SL revealed increasing amounts of gRNA packaged as the amount of Gag-Pol in particles increased from 1% to 10% of total viral polyproteins (Fig III-5D, lanes 3 through 7). Specifically, gRNA/7SL increased approximately 5 fold for particles containing 10% Gag-Pol compared to virions containing 100% Gag only (Fig III-5D). These results suggest that the Gag-Pol polyprotein may play a role in regulating the amount of gRNA packaged in virions.

gRNA packaging function of the Gag-Pol polyprotein

My previous work showed that packaging of a full complement of gRNA requires that only a small fraction of the total MoMLV Gag molecules provide packaging competent NC (59). The experimental system used here allowed the question of whether either Gag or Gag-Pol could serve as this source of packaging-competent NC. To this end, a single mutation of Trp 35 within the

zinc-knuckle of NC was introduced into the Gag^{only} and $Gag\text{-}Pol^{only}$ expression constructs to produce $p\Psi^{-}$MLV-Gag^{only}(NC^{W35G}) and $p\Psi^{-}$MLV-$Gag\text{-}Pol^{only}$(NC^{W35G}) respectively (Fig III-1). The Trp 35 mutation was selected based on previous studies showing that mutations of this residue lead to significant reductions in MoMLV gRNA packaging, but only nominally affected other assembly functions of NC (46, 59, 83) when virus was produced by transient transfection in human cells.

To determine if NC's packaging function could be provided in the context of the Gag-Pol polyprotein, combinations of Gag and Gag-Pol expression constructs containing WT or Trp 35 mutant NCs (NC^{W35G}) were co-transfected into ET cells at 20:1 "WT-like" Gag:Gag-Pol ratios along with the MoMLV vector pMΨPuro. Under these conditions, particle production was low and background levels were too high to permit accurate gRNA quantification by RPA. Therefore a single-cycle infectivity assay was utilized to examine gRNA packaging indirectly.

For this assay, MoMLV particles were used to infect fresh target cells and provirus titer was determined (Fig III-6). Titer of virus containing NC^{WT} Gag and NC^{WT} Gag-Pol (Fig III-6, lane 5) was infectious whereas titer of virus containing W35G mutant NC in Gag and Gag-Pol was reduced to background levels (Fig III-6, lane 8). The titer of virus containing NC^{WT} Gag and NC^{W35G} Gag-Pol was similar to that containing NC^{WT} Gag and NC^{WT} Gag-Pol (Fig III-6, lanes 5 and 6), suggesting that this NC mutation does not impact the function of Gag-Pol in this assay and confirming that the W35G NC mutation may be utilized to compare

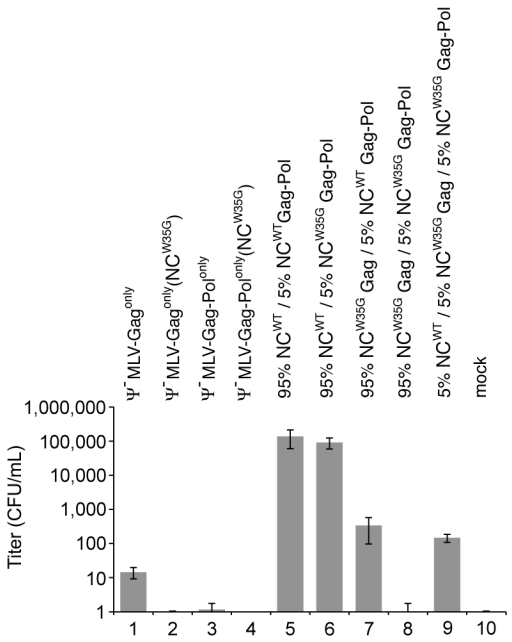

Figure III-6: gRNA packaging function of the MoMLV Gag-Pol polyprotein. Titer of virus produced from ET cells transfected with the indicated Gag^{only} or $Gag\text{-}Pol^{only}$ helpers (lanes 1 thru 4) or co-transfected with a 95%/5% ratio of the indicated WT or NC^{W35G} Gag^{only}/$Gag\text{-}Pol^{only}$ helpers (lanes 5 through 9). Titer is presented as CFU/mL and represents the mean of at least three independent infections. Error bars indicate the standard error of the means.

packaging functions of Gag and Gag-Pol despite previously shown defects in reverse transcription (59).

For virus containing NC^{W35G} Gag and NC^{WT} Gag-Pol, where the packaging competent NC was present only within the Gag-Pol polyprotein, the titer was ~2.5 log units lower than thiters for NC^{WT} Gag and NC^{WT} Gag-Pol virus (Fig III-6, lanes 7 and 5). However, when compared to virus where the packaging competent NC was present only within the Gag polyprotein, and represented 5% of the total protein, the titer was only approximately two-fold lower than that of NC^{W35G} Gag/ NC^{WT} Gag-Pol virus (Fig III-6, compare lanes 7 and 9). These results demonstrate that a packaging-competent NC can support virus replication when provided in the context of either the Gag or Gag-Pol polyprotein and suggest that NC in the context of either Gag or Gag-Pol may provide the gRNA packaging function for MoMLV.

Limits of MoMLV gRNA packaging

The experiments described above demonstrated that alterations in the conserved Gag:Gag-Pol ratios and overexpression of Gag-Pol resulted in defects in MoMLV particle production. In order to test if alterations in Gag:gRNA ratios also resulted in defects in particle production, MoMLV particles were produced by co-transfecting ET cells with the helper pMΨ^-MLV and increasing amounts of the

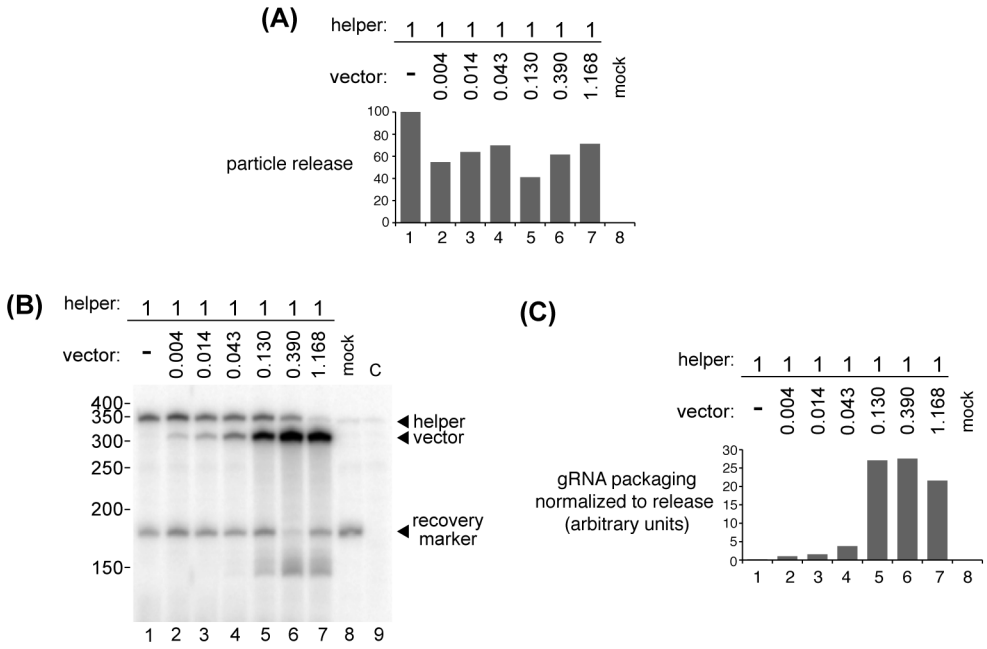

Figure III-7: Limits of MoMLV gRNA packaging. (A) MoMLV particle release from cells co-transfected with the MoMLV helper pMΨ⁻MLV and increasing concentrations of the MoMLV vector pMΨPuro was determined by RT activity of media harvested from cells and normalized to helper RNA amounts in cells as determined by RPA. Quantification by phosphoimager analysis is shown relative to the helper alone control (lane 1) which is set to 100%. (B) RPA of RNA harvested from media, from cells transfected as above probed with the riboprobe pD1040-2. (C) Quantification MoMLV vector RNA packaging shown in (B) normalized to particle release shown in (A). The input molar ratio of helper and vector are indicated above each panel, with the amount of helper set to 1. The following concentrations of pMΨPuro were used in the experiments here: 0.02, 0.06, 0.18, 0.56, 1.67, and 5 μg. The total amount of input DNA in each transfection was kept constant by the inclusion of molecular biology grade (fish sperm) carrier DNA (Roche).

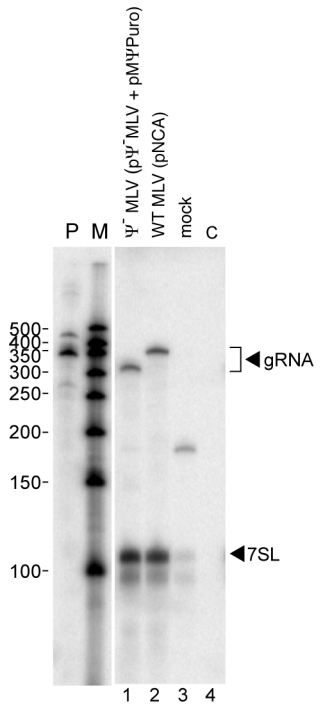

Figure III-8: gRNA packaging in Ψ⁻ MoMLV particles. RPA of RNA harvested from media from cells co-transfected with the MoMLV helper pMΨ⁻MLV and the MoMLV vector pMΨPuro (lane 1) or WT MoMLV (pNCA, lane 2). The RPA was co-probed with the riboprobe pD1040-2 (to detect gRNA) and pBRU-7SL (to detect 7SL).

MoMLV vector pMΨPuro. Particle production was then quantified by a reverse transcriptase (RT) assay (Fig III-7A). Minor reductions in particle production relative to the Ψ^- helper alone (approximately two-fold or less) were observed across all concentrations of co-expressed input MoMLV vector plasmid (Fig III-7A, lanes 1 through 7).

Next, gRNA packaging in MoMLV particles, produced as described above, was examined by RPA (Fig III-7B). Consistent with previous studies that demonstrated that the Ψ/DLS deletion (residues 215 to 368) in pMΨ^-MLV results in gRNA packaging at ~1% of WT (86), MoMLV helper RNA derived from pMΨ^-MLV was efficiently packaged in the absence of the MoMLV vector pMΨPuro (Fig III-7B, lane 1). As the amount of Ψ^+ gRNA (derived from the MoMLV vector pMΨPuro) co-expression increased, the amount of pMΨ^-MLV helper RNA in particles correspondingly decreased (Fig III-7B and C, lanes 2 through 7).

Quantification of gRNA packaging (Fig III-7C), when normalized for particle production (Fig III-7A), showed that as the amount of co-transfected vector plasmid increased approximately 80-fold, the amount of gRNA packaged per particle increased approximately 25-fold (Fig III-7C, compare lanes 2 and 5). Increasing the amount of vector included in the transfection 250-fold did not further increase the amount of gRNA packaged per particle, suggesting the amount of gRNA packaged in this case represents the upper limit of gRNA packaging by MoMLV under these conditions (Fig III-7C, compare lanes 5 and 7), and that gRNA packaging is saturable.

To compare the upper limit of gRNA packaging observed here to packaging by WT MoMLV, MoMLV particles were produced by co-transfecting ET cells with the helper pMΨ⁻MLV and 5 μg pMΨPuro (same condition as Fig III-7B, lane 7) or with pNCA alone (WT MoMLV). Next, gRNA packaging was determined by RPA utilizing two riboprobes, one complementary to MoMLV gRNA and one to 7SL (Fig III-8). The observation that similar amounts (less than 2-fold difference) of gRNA are packaged for WT MoMLV, compared to when a MoMLV vector is overexpressed (Fig III-8, lanes 1 and 2), suggests that the upper limit of gRNA packaging obverved in Fig III-7 is the amount of gRNA packaged by WT MoMLV.

Impact of Ψ/DLS multiplication on MoMLV particle production and gRNA packaging

The above experiments demonstrated that alterations in Gag:gRNA expression ratios did not impact particle production, but the plateau in packaging levels suggested a maximal RNA packaging capacity. To address if the maximum was reached by RNA mass or by Ψ recognition, I tested if alterations in the Gag:Ψ/DLS ratio affected RNA packaging saturation levels. To this end, several MoMLV vectors containing additional copies of the native Ψ/DLS were constructed (Fig III-9). These vectors contained one, two, three, or four additional Ψ/DLS sites in addition to the native Ψ/DLS (Fig III-9).

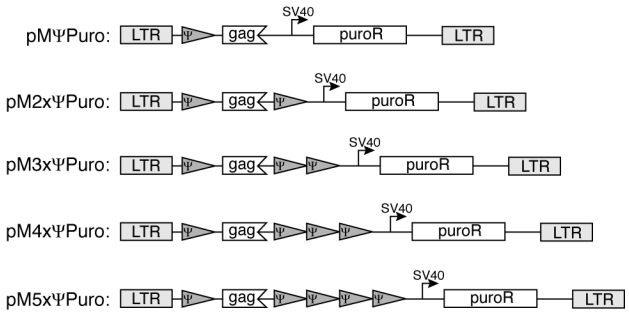

Figure III-9: Structure of MoMLV vectors containing multiple Ψ/DLS's. Diagram of MoMLV vectors used in the experiments described here. pMΨPuro is the parental MoMLV vector clone from which all other vectors were derived. pMΨPuro contains an SV40 driven puroR cassette in place of the viral genes. The vectors pM2xΨPuro, pM3xΨPuro, pM4xΨPuro, pM5xΨPuro contain two, three, four, and five Ψ/DLS regions (including the native Ψ/DLS), respectively in the same orientation.

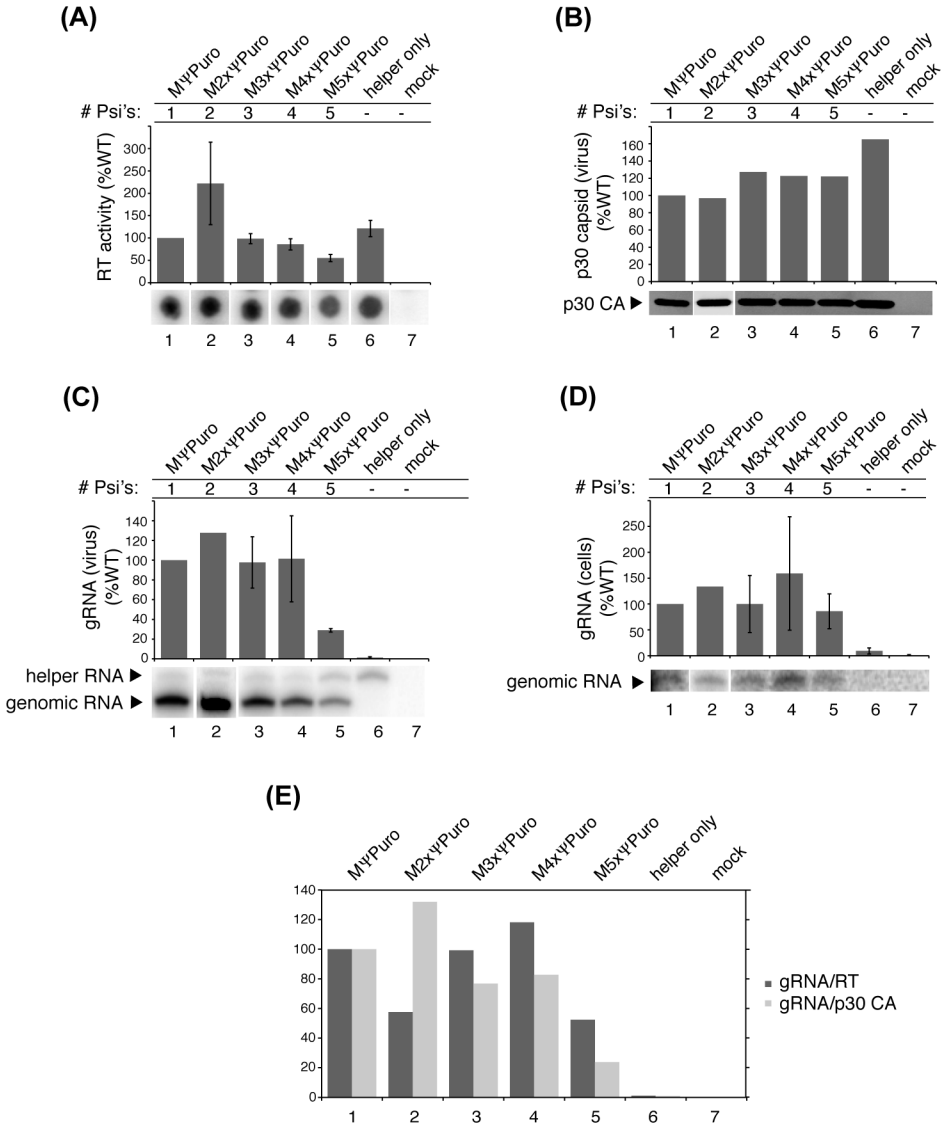
(A)
MψPuro
M2xψPuro
M3xψPuro
M4xψPuro
M5xψPuro
helper only
mock
Psi's:
1 2 3 4 5 - -
RT activity (%WT)
300
250
200
150
100
50
0
1 2 3 4 5 6 7
(B)
MψPuro
M2xψPuro
M3xψPuro
M4xψPuro
M5xψPuro
helper only
mock
Psi's:
1 2 3 4 5 - -
p30 capsid (virus) (%WT)
160
140
120
100
80
60
40
20
0
p30 CA ▶
1 2 3 4 5 6 7
(C)
MψPuro
M2xψPuro
M3xψPuro
M4xψPuro
M5xψPuro
helper only
mock
Psi's:
1 2 3 4 5 - -
gRNA (virus) (%WT)
140
120
100
80
60
40
20
0
helper RNA ▶
genomic RNA ▶
1 2 3 4 5 6 7
(D)
MψPuro
M2xψPuro
M3xψPuro
M4xψPuro
M5xψPuro
helper only
mock
Psi's:
1 2 3 4 5 - -
gRNA (cells) (%WT)
250
200
150
100
50
0
genomic RNA ▶
1 2 3 4 5 6 7
(E)
MψPuro
M2xψPuro
M3xψPuro
M4xψPuro
M5xψPuro
helper only
mock
140
120
100
80
60
40
20
0
1 2 3 4 5 6 7
gRNA/RT
gRNA/p30 CA

Figure III-10: Impact of Ψ/DLS multiplication on MoMLV particle production and gRNA packaging. (A) RT activities of media and (B) western blot of virus lysates produced from from cells co-transfected with the indicated MoMLV vector and the MoMLV helper pMΨ⁻MLV. (C) RPA of RNA harvested from pelleted virions harvested from cells co-transfected with the indicated MoMLV vector and the MoMLV helper pMΨ⁻MLV. (D) RPA of RNA harvested from from cells co-transfected with the indicated MoMLV vector and the MoMLV helper pMΨ⁻MLV. (E) gRNA packaging data normalized to virion production by either RT activity or p30 CA. Quantification by phosphorimager analysis of RT activity, densitometry of WB band intensities, and phosphorimager analysis of gRNA packaging by RPA are all shown relative to the pMΨPuro vector which is set to 100%. Where present, error bars indicate that quantification represents the mean of at least two experiments and represent the standard error of the means.

MoMLV particles were produced by co-transfecting ET cells with the MoMLV helper pMΨ⁻MLV and each of the MoMLV vectors. Particle production from these cells was then examined by both RT assay (Fig III-10A) and western blot analysis (Fig III-10B). Only modest differences (approximately two-fold or less) in particle production were observed, as measured by both RT and western blot, for co-expression with all multiple Ψ/DLS containing MoMLV vectors (Fig III-10A and B).

Next, the impact to MoMLV Ψ/DLS multiplication on gRNA packaging was examined. RNA for analysis by RPA was isolated from MoMLV particles that were produced as described above (Fig III-10C). gRNA packaging observed for the MoMLV vectors containing two, three, and four Ψ/DLS's was indistinguishable (Fig III-10C). In contrast, approximately five-fold reductions in gRNA packaging were observed for the vector pM5xΨPuro (Fig III-10C, lane 5).

Normalized for particle production relative to the WT vector pMΨPuro, 50-80% reductions were observed (Fig III-10E). Taken together, these results suggest that the multiplications of MoMLV Ψ/DLS's on the gRNAs tested here did not significantly alter particle production or gRNA packaging until there were five Ψ/DLS's on a single gRNA.

Discussion

The MoMLV RNP is composed of roughly 2,500 Gag molecules, 125 Gag-Pol molecules, and one gRNA dimer (16). The counting mechanism that accounts for the asymmetry between the Gag-Pol molecules and Gag as well as the gRNA dimer and Gag is unknown. The goal of the present study was to test the hypothesis that the copy number of Gag-Pol and the gRNA in the MoMLV were determined by dissimilar mechanisms. Specifically, I predicted that Gag-Pol is incorporated randomly and the ratio of Gag:Gag-Pol in MoMLV is due to intracellular expression ratios. However, gRNA incorporation is highly specific, and thus I predicted that RNA packaging is not strictly dependent on intracellular Gag:gRNA expression ratios.

The Gag:Gag-Pol co-expression system described here allowed an examination of the stoichiometry and incorporation of Gag-Pol in MoMLV virions. Using the pΨ$^-$MLV(PR^{D32S}) helper revealed that Gag-Pol was present in virions at ~6% the total Gag under native Gag:Gag-Pol expression conditions. This matches the reported readthrough rate of the MoMLV *gag* stop-codon that is required to produce Gag-Pol (54, 58). When the Gag:Gag-Pol ratios were

manipulated, the numerical proportion of Gag-Pol in virions relative to Gag matched the input, thereby suggesting that the incorporation of Gag-Pol into virions is principally a stochastic process. This result supports the hypothesis that the conserved copy number of Gag-Pol in MoMLV particles is due to random incorporation of the polyproteins.

In contrast to the results observed for Gag-Pol, when MoMLV gRNAs were overexpressed relative to Gag, gRNA incorporation was not recruited in proportion to expression levels, since saturable limits of gRNA packaging were observed. These results support the hypothesis that the conserved copy number of gRNAs within MoMLV particles is due to specific incorporation of the gRNA dimer that results from specific Gag:Ψ/DLS interactions. As gRNA expression in cells increased, the amount of gRNA per particle increased to a saturable upper limit. Although the results did not resolve the question of whether or not more empty particles were produced when gRNAs are expressed at low levels, the finding that RNA packaging plateaued at a level similar to that observed for WT MLV suggests that packaging is limited to a single RNA dimer for MLV.

The gRNA overexpression experiments described here also provide a numerical prediction of the ratio of MoMLV gRNA and mRNA within the host cell. Previous studies have suggested that MLV gRNAs and mRNAs exist in two distinct non-equilibrating pools (84). However, the molar proportion of these two pools is unknown. The experiments here suggest that saturable packaging levels are achieved when the gRNA (vector) pool represents 10-15% of the mRNA

(helper) pool (Fig III-7). If MoMLV replication has evolved to ensure replication occurs naturally under conditions of optimal gRNA/mRNA ratios, these findings suggest that ~15% of the total unspliced MoMLV RNA resides in the gRNA pool.

The precise molecular mechanism that regulates the single gRNA dimer packaging specificity is unknown. An additional novel gRNA packaging phenotype observed here may shed light on this mechanism. As the amount of MoMLV Gag-Pol present in virions increased, the amount of gRNA per virion correspondingly increased. These results suggest that maintenance of the conserved 20:1 Gag:Gag-Pol ratio may be critical to regulate the amount of gRNA packaged into virions. The results suggest that the Gag-Pol polyprotein and the ratio of Gag to Gag-Pol may be involved in regulating this packaging specificity.

If the single dimer packaging specificity is dependent on specific interactions between Gag and the Ψ/DLS of the gRNA dimer, then duplication of the Ψ/DLS may negatively impact MoMLV production or gRNA packaging. My results showed that multiplication of the MoMLV Ψ/DLS did not impact either MoMLV particle production or gRNA packaging, except in a single case: when five Ψ/DLS sites were present on a single MoMLV gRNA. This suggests that even in the presence of additional Ψ/DLS sites, MoMLV Gag was able to maintain gRNA packaging specificity. One caveat of these experiments is that it is unknown whether or not the non-native Ψ/DLS sites on the multiple Ψ/DLS vectors form additional intra- or inter-molecular dimer linkages.

When MoMLV Gag and Gag-Pol were produced from two distinct expression constructs, marked defects in virus particle production and infectivity were observed at equimolar ratios of the two polyproteins and when Gag-Pol represented the majority polyprotein. These results are consistent with previous studies with HIV-1 (49, 121). When Gag-Pol is overrepresented in cells, newly assembling virions may be disrupted due to improper membrane curvature at sites of assembly or to the inability of assembled virions to accommodate the larger (relative to Gag) Gag-Pol molecule. The aberrant virion morphology observed for HIV-1 when Gag-Pol is overrepresented in cells is consistent with this notion (49).

Two interesting phenotypes were observed here when MoMLV Gag was expressed from the pΨ⁻MLV-Gag^{only} helper construct. First, an approximately five-fold decrease in cell associated Gag was observed in cells for pΨ⁻MLV-Gag^{only} relative to pΨ⁻MLV. The decrease in cell associated Gag could potentially result from differences in nuclear export of the MoMLV RNAs produced from pΨ⁻MLV-Gag^{only} and pΨ⁻MLV. Previous studies have suggested that sequences within the 5'-UTR may function in nuclear export (4), however, other sequences within the MoMLV RNA (that have been removed in the pΨ⁻MLV-Gag^{only} helper) may also be important for efficient nuclear export.

Second, MoMLV particles produced from pΨ⁻MLV-Gag^{only} yielded low but reproducible proviral titers that were abolished in the presense of AZT. These results suggest that reverse transcription products were actively produced after

infection with MoMLV particles presumably lacking Pol. One explanation for this phenotype is that MoMLV particles produced by pΨ⁻MLV-Gag^{only} contained functional Pol derived from an endogenous retrovirus (ERV) source. The human genome contains substantial ERV sequences (estimated to represent ~8% of the total genome), many of which retain protein coding capacity (reviewed in (137)). Moreover, retroviral infection has been shown to upregulate ERV RNA and protein expression (136) thereby suggesting that the conditions described here may be condusive for the incorporation of ERV derived Pol into MoMLV particles.

Additional experiments here revealed that the Gag-Pol polyprotein may interact directly with the gRNA, since viral titers were indistinguishable when a packaging competent NC was provided either in the context of Gag or Gag-Pol polyproteins. Previous studies with HIV-1 have suggested that HIV-1 Gag-Pol may not interact directly with RNA (66) and that Gag-Pol is recruited into assembling virions via CA:CA interactions (reviewed in (53)). However, work with the yeast retrotransposon Ty3 showed that the “zinc-knuckle” motif of NC could support retrotransposition when provided either in the context of Gag or Gag-Pol (102). My work here provides evidence that at least for MoMLV, Gag-Pol may interact with gRNA, since a functional NC could support single-cycle infectivity in the context of either Gag or Gag-Pol.

In summary, my experiments showed that the stoichiometry of Gag-Pol in MoMLV virions matches the conserved readthrough rate in cells and that the incorporation of Gag-Pol into virions is principally stochastic. Furthermore, my

studies confirmed the importance to virion production of maintaining the conserved 20:1 Gag:Gag-Pol ratio and suggest that Gag-Pol plays a direct role in regulating the amount of gRNA packaged, possibly through a direct interaction with gRNA itself. These findings underscore the importance of Gag-Pol in MoMLV assembly and suggest that pharmacologic skewing of protein ratios could inhibit virus replication. Furthermore, I contrasted the mechanism of incorporation of MoMLV Gag-Pol with that of gRNAs, since gRNA incorporation was specific as opposed to stochastic. Finally, my findings showed that MoMLV particle production was not significantly altered when the proportion of Gag to gRNA or Ψ/DLSs was changed.

Materials and Methods

Cells and Transfectons.

ET cells are 293T cells that constitutively express murine ecotropic envelope (106). D17/pJET cells are canine osteosarcoma cells that constitutively express murine ecotropic receptor. Cells were maintained in Dulbecco's modified Eagle's medium (DMEM; Invitrogen) supplemented with 10% fetal bovine serum (Gemini) (for ETs) or 10% bovine serum (Invitrogen) (for D17/pJETs), 100U/mL penicillin, and 100 μg/mL streptomycin (Invitrogen). Cells were grown at 37°C with 5% CO_2 in a humidified incubator. Transfections were carried out using polyethlenimine (PEI) or calcium phosphate precipitation as described previously (64, 106).

Plasmids.

The MoMLV helper pΨ⁻MLV (aka pAM37-9) was derived from pNCA (Colicelli and Goff 1988) and contains a deletion in the packaging signal region from nucleotides 215-368 (106). All other MoMLV helpers described here were derived from pΨ⁻MLV. pΨ⁻MLV-Gag^{only} (aka pSD50-1) contains a deletion that removes the *pol* and all but the last 100 nucleotides of the *env* reading frames. In addition, it contains a four-nucleotide substitution (GGAG to ACGC) immediately downstream of the Gag stop-codon to prevent read-through via termination suppression. pΨ⁻MLV-Gag-Pol^{only} (aka pSD45-1) contains a deletion that removes all but the last 100 nucleotides of the *env* reading frame and a mutation that eliminates the Gag stop-codon.

A restriction fragment encompassing the W35G NC mutation of pGPP(W35G) (aka pEG479-1) (59) was used to introduce the W35G mutation into the following MoMLV helpers: pΨ⁻MLV(NC^{W35G}) (aka pSFJ346-1), pΨ⁻MLV-Gag^{only}(NC^{W35G}) (aka pSFJ22-1), and pΨ⁻MLV-Gag-Pol^{only}(NC^{W35G}) (aka pSFJ23-1). A similar strategy was employed to introduce the W35G NC mutation into pΨ⁻MLV(NC^{W35G},PR^{D32S}) (aka pSFJ370-1) and pΨ⁻MLV-Gag-Pol^{only}(NC^{W35G},PR^{D32S}) (aka pSFJ230-7). This was followed QuickChange II (Stratagene) site-directed mutagenesis to introduce the D32S mutation into PR. The PR mutations in pΨ⁻MLV(PR^{D32S}) (aka pSFJ369-1) and pΨ⁻MLV-Gag-Pol^{only}(PR^{D32S}) (aka pSFJ229-7) were also introduced by site-directed mutagenesis. Sequencing confirmed the products of site-directed mutagenesis.

The MoMLV vector pMΨPuro (aka pAM86-5) contains an SV40 driven puromycin resistance cassette in the place of the viral genes and has been described previously (68).

The MoMLV vectors pM2xΨPuro (aka pSFJ98-3), pM3xΨPuro (aka pSFJ295-1), pM4xΨPuro (aka pSFJ298-3), and pM5xΨPuro (aka pSFJ299-5) contain one, two, three, and four Ψ/DLS regions (in addition to the native Ψ/DLS) respectively. To produce these vectors, a PCR fragment encompassing the Ψ/DLS region of pNCA (from nucleotides 199-621) was generated that contained built-on BglII and BamHI ends. The PCR fragment was subcloned into pUC19 and verified by sequencing. The Ψ/DLS region was then removed by BglII/BamHI digestion and concatamerized. Ψ/DLS concatamers containing two, three, and four Ψ/DLS regions in the same orientation were then selected and inserted into the BamHI site of pMΨPuro.

The riboprobes pEG467-10 and pD1040-2 are derivatives of pBSII SK(+) (Stratagene) and contain PCR or restriction fragments inserts respectively (38, 123). The PCR fragment insert in pEG467-10 includes complementarity to portions of both MoMLV 5'-UTR (nt 55-214) and 100nt of 7SL RNA (38). The restriction fragment insert in pD1040-2 is complementary to 330bp (MscI to BsrBI) of MoMLV Gag MA (123).

Virus and Cell Isolation.

Tissue culture supernatents were harvested at 48 h post transfection for isolation of virus by sucrose-cushion centrifugation (64). Viral pellets were either

resuspended in TRIzol® reagent (Invitrogen) for RNA isolation and subsequent RNAse protection assays (RPA) or resuspended in RIPA lysis buffer (1% NP40, 0.1% sodium dodecyl sulfate, 0.5% sodium deoxycholate, 150mM Nacl, 50mM Tris [pH7.5]) supplemented with 1X protease inhibitor cocktail tablet (Roche) and 1 mM phenylmethylsulfonyl fluoride for western blotting. Cells were harvested 48 h post transfection in either RIPA lysis buffer as described previously (59) to produce cell protein lysates for western blotting or in TRIzol® reagent (Invitrogen) for RNA isolation and subsequent analysis by RPA. Where applicable, virus was quantified in tissue culture supernatents using an exogenous reverse transcriptase (RT) assay (38) based on a previously described protocol (134).

Western Blotting.

Cell and virus lysates were resolved by SDS-PAGE, transferred to polyvinylidene fluoride (PVDF; Bio-Rad) membranes, blocked, blotted, and detected using the Licor Odyssey system (Li-Cor Biosciences), as previously described (59). The following primary antibodies were used: (1) rat mAb against MoMLV p30 CA, which was derived from hybridoma supernatants (from Bruce Chesebro: ATCC clone R187), and (2) mouse beta-actin mAb (Ambion: AM4302). Secondary antibodies included (1) goat anti-rat IRDye® 800CW and (2) goat anti-mouse IRDye® 680 (Li-Cor Biosciences).

RNAse Protection Assay (RPA).

Riboprobes were produced by first linearizing the plasmid pEG467-10 (see above) with HindIII and then *in vitro* transcribing them using T3 RNA polymerase

(Promega) and [α-^{32}P]-rCTP (Perkin-Elmer). The riboprobe pEG467-10 protects 163 nt of MoMLV gRNA and 100 nt of 7SL RNA. Hybridization of riboprobes with sample RNA, RNAse digestion, and resolution was carried out as described previously (86).

Infections.

For the single cycle infectivity assay, virus produced in ET cells was used to infect D17/pJET target cells. Infection and puromycin selection conditions have been described previously (59). Infectious units are represented as colony forming units per milliliter (CFU/mL).

Chapter IV

Concusions and Future Directions

Dissertation Overview

The Moloney murine leukemia virus RNP is composed of a 20:1 mixture of Gag and Gag-Pol polyproteins plus a dimeric RNA genome. The putative copy numbers of these RNP constituents are ~2,500 Gag molecules, ~125 Gag-Pol molecules (16, 132), and precisely one gRNA dimer (19). Presumably, each of the ~2,500 Gag molecules possesses intrinsic potential for high-affinity interactions required to package gRNA, due to the presence of an RNA binding motif within NC, as well as potential to recruit Gag-Pol into assembling virions, due the presence of Gag-Pol interacting motifs within CA. The mechanisms that account for the drastic asymmetry in the proportions of Gag, Gag-Pol and gRNA within the RNP are unknown. The overall goal of this dissertation was to define parameters that are responsible for these molecular proportions in MoMLV.

Studies with MoMLV and HIV-1 suggest that only a very small fraction of the ~2,500 Gag molecules in a virion engage the gRNA dimer with high affinity during virus assembly (61, 86). These studies support a model whereby the retroviral Gag molecules may be separated into two distinct pools: one that participates in high-affinity gRNA interactions and one that does not. The goal of the work described in Chapter II (59) was to manipulate the molecular proportions of Gag molecules, in the context of the two-pool model described

above, and examine the effects on gRNA packaging. Specifically, I tested the hypothesis that specific RNA binding capability is required in only a small fraction of the ~2,500 Gag molecules to package gRNA.

To that end, I developed an experimental system that allowed two pools of Gag molecules to be co-expressed in cells: one that was able to participate in high-affinity gRNA interactions and one that was not. By manipulating the molecular proportions of the two pools of Gag molecules experimentally, I showed that a full complement of packaging-competent Gag was not required to package gRNA, but the required size of the pool was greater than predicted by previous studies (61, 86).

I hypothesized that regulation of the copy number of MoMLV Gag-Pol molecules and of the gRNA dimer in the RNP occur via two different mechanisms. First, the ratio of Gag and Gag-Pol in newly forming RNPs is dependent on the conserved expression ratios of Gag and Gag-Pol in cells. Second, the highly specific selection of a single gRNA dimer into the MoMLV RNP is not strictly dependent of the expression ratios of Gag and gRNA in cells, and instead relies on the specific high-affinity interactions between a small pool of Gag molecules (Chapter II) and the Ψ/DLS of the gRNA dimer.

The goal of the work described in Chapter III was to manipulate the molecular proportions of (1) Gag and Gag-Pol, (2) Gag and gRNA, and (3) Gag and Ψ/DLS, examine the incorporation of each of these molecules into the MoMLV RNP, and determine the impact of alterations of these ratios on MoMLV particle production, gRNA packaging, and infectivity. Specifically, experiments

were designed to test the hypothesis that Gag-Pol and gRNA are incorporated by two disparate mechanisms.

To that end, I developed an experimental system to allow manipulation of the molecular proportions of Gag, Gag-Pol, gRNA, and the Ψ/DLS in MoMLV RNPs. My results showed that the incorporation of Gag-Pol into the MoMLV RNP did indeed represent a stochastic sampling from the cell, since the ratio of Gag and Gag-Pol in RNPs matched the intracellular expression ratios. Additionally, I showed that when Gag-Pol was overrepresented relative to Gag in the MoMLV RNP, particle production was impaired. This observation was in contrast to when the ratio of Gag to gRNA or Gag to Ψ/DLS was altered in the RNP. In these cases, upper limits of gRNA packaging were observed and no defects in particle production were observed.

The major findings highlighted in this dissertation, including and in addition to those described above, are presented as follows:

Chapter II

• MoMLV gRNA packaging-competent Gag and mutant gRNA packaging-incompetent Gag co-assemble to form particles.

• Mutations that render MoMLV Gag packaging-incompetent do not affect gRNA dimer formation or gRNA stability.

• A full complement of packaging-competent MoMLV Gag is not required to package gRNA.

• MoMLV gRNA packaging requires 5-10 fold more packaging-competent Gag in cultured cells than predicted by *in vitro* binding studies.

Chapter III

• Separate expression of MoMLV Gag and Gag-Pol supports particle production, gRNA packaging, and virus infectivity.

• Incorporation of Gag-Pol into MoMLV virions is stochastic over a broad range of Gag and Gag-Pol coexpression ratios.

• Inversion of the conserved molecular proportions of MoMLV Gag and Gag-Pol results in reductions in particle production and infectivity.

• Alterations in the molecular proportion of MoMLV Gag-Pol relative to Gag results in molar alterations in gRNA packaging.

• The RNA binding motif of NC supports MoMLV replication in the context of either Gag or Gag-Pol, suggesting that the NC of Gag-Pol may serve to package gRNA.

• Incorporation of gRNAs into MoMLV particles is not stochastic, since packaging plateaued at an upper limit similar to that observed for WT MLV.

• Overexpression of MoMLV gRNAs or multiple copies of the Ψ/DLS on the gRNA do not impair particle production.

Conclusions

Chapter II

As described above, the goal of the work presented in Chapter II was to test the hypothesis that only a small fraction of the ~2,500 Gag molecules in an MoMLV RNP are required to package gRNA. In order to test this hypothesis, I developed an experimental system whereby MoMLV virions could be produced that contained phenotypic mixtures of two types of Gags: packaging-competent and packaging-incompetent. By manipulating the ratios of the two types of Gags in MoMLV virions, the threshold limit of packaging-competent Gag required for gRNA packaging could be determined. My results support the hypothesis; MoMLV gRNA is packaged even when most of the Gag is not packaging-competent.

I first generated a packaging-incompetent Gag molecule by introducing a single amino-acid mutation (W35G) within the zinc-knuckle of NC (Fig II-1). Introducing this mutation into Gag resulted in virus that was defective in gRNA packaging (Fig II-3A). However, this mutation did not significantly alter virus production (FigII-2B,C, and D) or gRNA dimerization and stability (Fig II-3B) when expressed by transient transfection in human cells. Next, packaging-competent WT NC Gag and packaging-incompetent W35G NC Gag were co-expressed to produce virions that contained phenotypic mixtures of WT and W35G NC Gag (Fig II-5B) and that were infectious (Fig II-4A and B and Fig II-7A and B). Finally, utilizing phenotypically mixed MoMLV, I determined that a full complement of WT NC was not required to package gRNA, however, the amount

of WT NC required to package gRNA was greater than predicted (Fig II-6A and B).

Future Directions

In vitro binding studies suggested that ≤1% of Gag molecules may be required to bind the gRNA dimer with high-affinity for gRNA packaging during MoMLV assembly (86). My virus results suggested that the minimum Gag required was ≥5-10%. There are two potential explanations for this discrepancy. First, more high-affinity Gag-gRNA interactions may be required to package gRNA during virus replication. Second, the presence of mutant Gag may result in a defect whereby the number of functional Gag molecules required for gRNA packaging is increased.

In order to differentiate between these two possibilities, additional experiments could be performed to estimate the number of Gag molecules required to package gRNA in cultured cells. Using methods similar to those employed for HIV-1 by Jouvenet et al. (61), MoMLV gRNAs could be constructed that contain stem loops that bind the bacteriophage MS2 protein. These RNAs could then be visualized by fluorescence microscopy in cells that express MS2-GFP and their localization relative to Gag molecules in cells could be determined. The sensitivity of this assay allowed for estimation of the amounts of HIV-1 Gag (one dozen Gag molecules or fewer) required to recruit gRNA for packaging during assembly (61) and could potentially enable the same determination for MLV.

My results are consistent with a model where two pools of Gag are present within cells: one that participates in high-affinity gRNA interactions and one that does not. However, the mechanism that causes the separation of a single population of Gag into these pools is unknown. It is possible that the pool of Gag that participates in high-affinity gRNA interactions is not different from the pool of Gag that does not, and is defined simply upon binding to the gRNA high-affinity binding sites. An alternate explanation is that the pool of Gag that participates in high-affinity gRNA interactions is preexisting and requires an active mechanistic separation. Evidence and future experiments to explore the latter explanation is provided in the Future Directions section of Chapter III below.

Although not directly related to the specific goals of this dissertation, two additional phenotypes were observed in the work described in Chapter II. First, the W35G NC mutation resulted in defects in reverse transcription (Fig II-8). My hypothesis is that the W35G NC mutation impairs the chaperone function of NC during reverse transcription. Investigating this error in reverse transcription could reveal novel information about NC's chaperone function.

Second, a major difference in virus production for the W35G NC Gag was observed in human cells versus murine cells (Fig II-2). Many cellular factors regulate the trafficking of Gag to sites of retrovirus assembly and support retrovirus budding (reviewed in (30, 101)). The phenotype observed for W35G NC Gag in murine cells may result from the improper recruitment of specific cellular factors required for viral protein trafficking or budding due to the mutation

in NC. Further flouresence microscopy studies examining WT and W35G NC Gag trafficking in human and murine cell types could reveal differences in protein trafficking to sites of assembly. Furthermore, electron microscopy could be used to examine budding defects of WT and W35G Gag MoMLV in human and murine cells.

Chapter III

The goal of the work presented in Chapter III was to test the hypothesis that Gag-Pol and gRNA are incorporated by two disparate mechanisms. I tested this hypothesis by developing an experimental system to manipulate the molecular proportions of (1) Gag and Gag-Pol, (2) Gag and gRNA, and (3) Gag and Ψ/DLS in MoMLV. By manipulating the proportions of these molecules in MoMLV particles, the mechanism of incorporation was examined and the resulting affects of altering these ratios on MoMLV production, gRNA packaging, and infectivity were determined. The results supported the hypothesis that MoMLV Gag-Pol and gRNA are incorporated by disparate mechanisms.

I first developed an experimental system whereby the Gag and Gag-Pol polyproteins were coexpressed using two separate constructs (Fig III-1 and Fig III-2). This allowed me to manipulate the molecular proportions of the two molecules and examine the impacts on gRNA packaging. I showed that co-expression of Gag and Gag-Pol from two separate constructs could support virus production (Fig III-3) and that this virus was capable of supporting a single round of replication (Fig III-4). Furthermore, when the ratio of Gag and Gag-Pol was manipulated, the incorporation of Gag-Pol into virions was stochastic (Fig III-3).

Moreover, when the amount of Gag-Pol outnumbered Gag, virion production decreased (Fig III-3).

In addition, I provided indirect evidence that either Gag or Gag-Pol could serve to bind gRNA for packaging by showing that single cycle infectivity of MoMLV could be supported by a RNA binding competent NC provided on either Gag or Gag-Pol (Fig III-6). Finally, I showed that when the ratio of Gag and Gag-Pol is altered, the amount of gRNA packaged in virions is changed (Fig III-5). Specifically when the amount of Gag-Pol in virions increased, gRNA amounts in virions also increased (Fig III-5).

Next, I developed an experimental system to manipulate the ratio of Gag to gRNA and Gag to Ψ/DLS. First, gRNAs were overexpressed in cells to alter their proportion in MoMLV particles (Fig III-7). When gRNAs were overexpressed, particle production was not affected (Fig III-7), however, gRNA packaging per particle increased to an upper threshold limit (Fig III-7). Second, MoMLV vectors were constructed to contain various multiples of the Ψ/DLS site (Fig III-9) in order to manipulate the ratio of Gag to Ψ/DLS's on gRNAs (Fig III-10). Multiple copies of the MoMLV Ψ/DLS on a single gRNA did not impact particle production or gRNA packaging (Fig III-10) except when five Ψ/DLSs were present on a single MoMLV gRNA.

Future Directions

The Gag^{only} and $Gag\text{-}Pol^{only}$ expression system described above is an artificial system in the sense that Gag and Gag-Pol are normally expressed in *cis* from a single viral RNA. Studies where mutations were introduced in the RNA

pseudoknot regulating MoMLV *gag* stop codon readthrough resulted in altered Gag/Gag-Pol ratios (54). The gRNA packaging phenotype of MoMLV containing these mutations could be determined as described in Chapter III. If the readthrough mechanism that regulates the molecular proportions of Gag and Gag-Pol also lead to altered Gag/gRNA proportions, then the prediction is that pseudoknot mutations that alter Gag/Gag-Pol proportions would also alter Gag/gRNA proportions.

The results described in Chapter II are consistent with a model where two pools of Gag are present within cells: one that participates in high-affinity gRNA interactions and one that does not. Results in Chapter III provide a potential mechanistic explanation for the separation of the two pools of Gag. In Chapter III, I observed that when the amount of MoMLV Gag-Pol present in virions increased, the amount of gRNA per virion correspondingly increased. It's possible that Gag:Gag-Pol interactions may drive Gag molecules towards a gRNA high-affinity binding fate and having the appropriate ratio of Gag:Gag-Pol results in an appropriate number of Gag molecules binding the MoMLV Ψ/DLS with high affinity. The flouescence microscopy experiments designed to examine Gag:gRNA interactions described above could be expanded to test whether or not Gag-Pol is present within these initial Gag:gRNA complexes.

Results described in Chapter III also showed that gRNA packaging in MoMLV reached a saturable upper limit (when gRNAs were expressed *in trans*) similar to that observed for WT MoMLV (when gRNAs were expressed *in cis*). Future experiments could be designed to determine whether the intracellular

ratios of Gag to gRNA are similar in each case. This would reveal whether the selectivity of gRNA incorporation is different for the co-expression system versus WT MoMLV.

Previous studies have shown that when a HIV-1 Ψ/DLS site was inserted into a gRNA in addition to the native Ψ/DLS gRNA, monomers appeared within newly formed virions as determined by non-denaturing northern blotting (117). In that case, ~30-40% of the gRNA within the virions was monomeric, while the remaining gRNA was dimeric (117). Furthermore, the total gRNA packaged (normalized to virion amounts) remained relatively unchanged relative to WT gRNA (117). Additional experiments showed that when two non-native HIV-1 Ψ/DLS sites were inserted into a gRNA that had its native Ψ/DLS removed, gRNA monomers appeared exclusively in newly formed virions (116). Moreover, the amount of gRNA packaged (normalized to virion amounts) was cut roughly in half relative to WT gRNA in this case (116).

These results suggest that when a native HIV-1 Ψ/DLS is present on the gRNA in addition to a non-native Ψ/DLS, some intra-molecular Ψ/DLS interactions may occur in addition to inter-molecular Ψ/DLS interactions, resulting in the packaging of gRNA monomers. In addition, they suggest that when two non-native Ψ/DLSs are present on the gRNA in the absence of a native Ψ/DLS, only intra molecular Ψ/DLS interactions occur, resulting in the exclusive packaging of monomers (114). These presumably are present in each virion as a single gRNA species, since the quantity of gRNA in virions is cut roughly in half in this case (however the copy number of gRNAs was not specifically determined

in these studies) (116).Taken together, these studies point to a model whereby one dimer linkage consisting of two joined Ψ/DLS sites is necessary to specify single-dimer packaging specificity. This is in contrast to a model whereby recognition of two HIV-1 gRNAs is necessary to specify single-dimer packaging specificity.

Future experiments could be performed to determine if the MoMLV vectors containing multiple Ψ/DLS sites (Chapter III) are packaged as monomers, similar to HIV-1. MoMLV vectors could also be constructed to contain a deletion of the native Ψ/DLS site and the addition of two non-native Ψ/DLS sites. If MoMLV is similar to HIV-1, I would predict that MoMLV would package exclusively monomers in this case. These experiments would help to refine the model that describes the "counting" mechanism that regulates the single-dimer packaging specificity for retroviruses.

Impact of Ψ/DLS duplication in the reverse orientation from the native Ψ/DLS on MoMLV particle production and gRNA packaging.

Work described in Chapter III examined the impact of MoMLV Ψ/DLS multiplication on particle production and gRNA packaging. The MoMLV vectors used in Chapter III contained additional Ψ/DLS sites in tandem, in the same orientation as the native Ψ/DLS site. I also tested whether the orientation of the non-native Ψ/DLS site in the vector containing two Ψ/DLS's altered the phenotype observed in Chapter III. Preliminary experimental results reported in the following subsection revealed that insertion of a second Ψ/DLS in the reverse

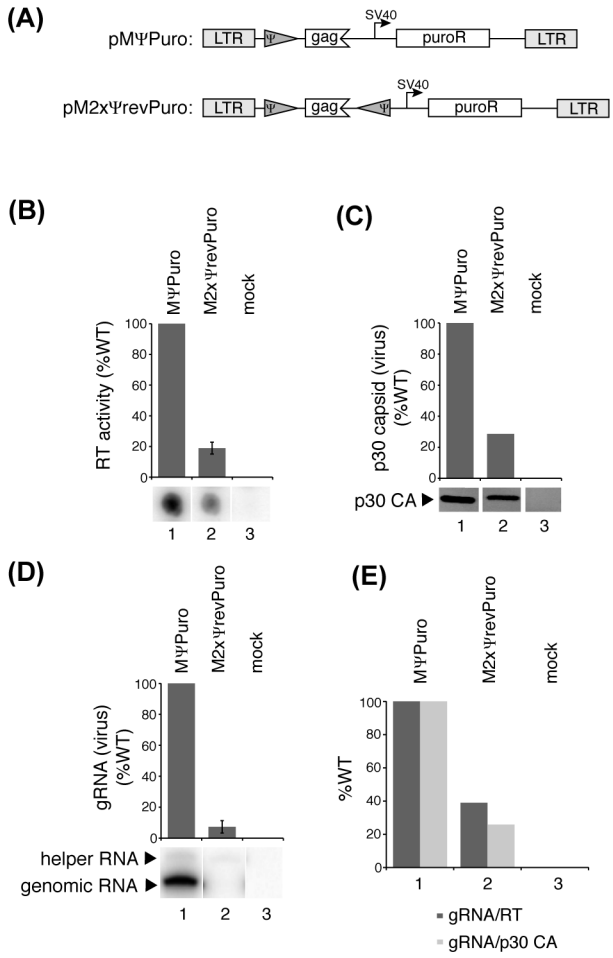

Figure IV-1: Impact of Ψ/DLS duplication in the reverse orientation from the native Ψ/DLS on MoMLV particle production and gRNA packaging. (A) Structure of MoMLV duplicate psi vector used here. (B) RT activities of media and (C) western blot of virus lysates produced from from cells co-transfected with the indicated MLV vector and the MLV helper pMΨ⁻MLV. (D) RPA of RNA harvested from pelleted virions harvested from cells co-transfected with the indicated MLV vector and the MLV helper pMΨ⁻MLV. (E) gRNA packaging data represented normalized to virion production by either RT activity or p30 CA. Quantification by phosphorimager analysis of RT activity, densitometry of WB band intensities, and phosphorimager analysis of gRNA packaging by RPA are all shown relative to the pMΨPuro vector, which is set to 100%. Where present, error bars indicate that quantification represents the mean of at least two experiments and represent the standard error of the means.

orientation from the native Ψ/DLS resulted in defects in particle production and gRNA packaging.

First, I constructed a MoMLV vector called pM2xΨrevPuro (derived from pMΨPuro) that contains one additional non-native Ψ/DLS site in the opposite orientation as the native Ψ/DLS site (Fig IV-1A). MoMLV particles were produced by co-transfecting ET cells with the MoMLV helper pΨ⁻MLV and the MoMLV vector pMΨPuro or pM2xΨrevPuro. Virion production from these cells was examined by both RT assay (Fig IV-1B) and western blot analysis (Fig IV-1C). The MoMLV vector pM2xΨrevPuro yielded an ~4-5 fold defect in virion production relative to the WT MoMLV vector (Fig IV-1A and B, lane 3).

Next, the impact of MoMLV Ψ/DLS duplication (for pM2xΨrevPuro) on gRNA packaging was examined. RNA was isolated from virions that were produced as described above for analysis by RPA (Fig IV-1D). An approximately 5-10 fold reduction in gRNA packaging was observed for pM2xΨrevPuro relative to pMΨPuro (Fig IV-1D). gRNA packaging decreased approximately three fold when normalized for particle production by RT activity or western blot (Fig IV-1E).

To determine whether the defect in particle production for pM2xΨrevPuro virus was due to decreased expression of the vector in cells, an RPA was performed on RNA harvested from cells transfected as described above. Only modest differences (approximately two-fold or less) in vector RNA expression levels were observed in cells by RPA for all MoMLV helpers (data not shown), suggesting that differences in particle production were not due to defects in vector expression. To determine if the defect in particle production for

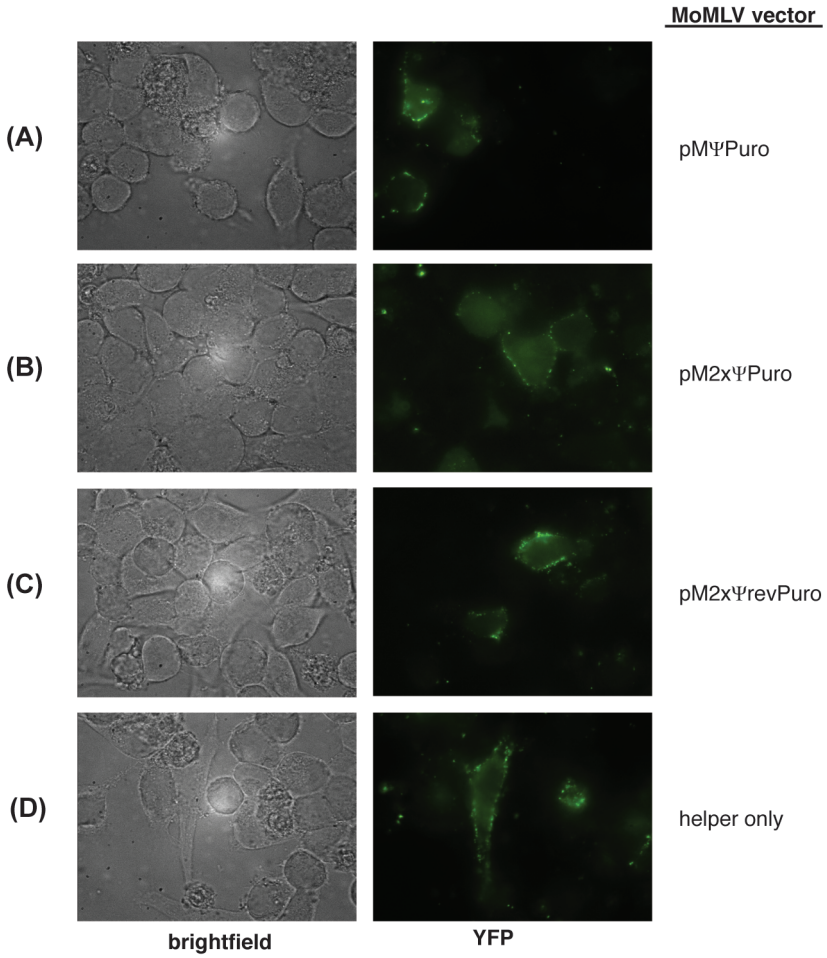

Figure IV-2: Impact of Ψ/DLS duplication in the reverse orientation from the native Ψ/DLS on MoMLV Gag localization. HeLa cells expressing MoMLV Gag-YFP, the MoMLV helper pΨMLV, and the following MoMLV vectors: (A) pMΨPuro, (B) pM2xΨPuro, or (C) pM2xrevΨPuro.

pM2xΨrevPuro was due to mis-localization of Gag during particle assembly, we used fluorescence microscopy and determined Gag localization in HeLa cells transfected with the MoMLV helper pΨ⁻ MLV, a yellow fluorescent protein-tagged MoMLV Gag construct (Gag-YFP), and either of the following three MoMLV vectors: pMΨPuro, pM2xΨPuro, and pM2xΨrevPuro. We saw no differences in Gag-YFP localization in cells transfected with either of the three constructs (Fig IV-2), suggesting that Gag mis-localization was not the cause of the defect in particle production for pM2xΨrevPuro.

The defect in MoMLV particle production observed here may potentially be explained by innate immune sensing in cells transfected with pM2xΨrevPuro. The inclusion of two Ψ/DLS sites in opposite orientation may result in the formation of extensive double stranded RNA (dsRNA) secondary structures that may be recognized as pathogen-associated molecular patterns (PAMPs) (reviewed in (82)). In host cells, dsRNA PAMPs may be detected in the cytoplasm as foreign (since host cells do not produce dsRNA) by cellular recognition proteins, including for example RIG-I and MDA5 (reviewed in (133)). PAMP detection triggers signaling cascades that activate type I interferon (IFN) genes and pro-inflammatory cytokine genes that result in antiviral effects (133). Upregulation of type I IFN in host cells blocks MoMLV infection at late stages (18, 119). Follow-up studies can be designed to test the hypothesis that the defects in particle production for cells transfected with pM2xΨrevPuro are due to innate immune signaling.

Implications

Understanding the mechanisms by which retroviruses regulate the incorporation of particle components and maintain the conserved copy numbers of these components is important as a possible target for antiviral therapy. Currently, no clinically approved antiretroviral therapies have been developed that target the Gag protein (reviewed in (139)). Therapeutic interventions that target Gag's critical role in molecular counting during retroviral assembly represent a novel approach for antiretroviral drug development.

For example, studies with MoMLV described in this dissertation, along with previous studies with HIV-1 (49, 121), showed that alterations of the conserved Gag:Gag-Pol ratios in retroviral particles result in defects in particle production and infectivity. RNA aptamers represent one potential tool to disrupt the conserved Gag:Gag-Pol ratios. RNA aptamers are short synthetic oligonucleotides designed to bind specific molecular targets and represent a promising new class of drugs (reviewed in (96)). An RNA aptamer that bound and locked the RNA pseudoknot responsible for Gag stop-codon readthrough in the readthrough permissive conformation could potentially alter the Gag:Gag-Pol ratios resulting in defects in particle production.

References

1. **Albritton, L. M., L. Tseng, D. Scadden, and J. M. Cunningham.** 1989. A putative murine ecotropic retrovirus receptor gene encodes a multiple membrane-spanning protein and confers susceptibility to virus infection. Cell **57:**659-666.
2. **Arhel, N.** 2010. Revisiting HIV-1 uncoating. Retrovirology **7:**96.
3. **Balvay, L., M. L. Lastra, B. Sargueil, J.-L. Darlix, and T. Ohlmann.** 2007. Translational control of retroviruses. Nat Rev Microbiol **5:**128-140.
4. **Basyuk, E., S. Boulon, F. Skou Pedersen, E. Bertrand, and S. Vestergaard Rasmussen.** 2005. The packaging signal of MLV is an integrated module that mediates intracellular transport of genomic RNAs. J Mol Biol **354:**330-339.
5. **Bender, M. A., T. D. Palmer, R. E. Gelinas, and A. D. Miller.** 1987. Evidence that the packaging signal of Moloney murine leukemia virus extends into the gag region. J Virol **61:**1639-1646.
6. **Berkowitz, R. D., A. Ohagen, S. Höglund, and S. P. Goff.** 1995. Retroviral nucleocapsid domains mediate the specific recognition of genomic viral RNAs by chimeric Gag polyproteins during RNA packaging in vivo. J Virol **69:**6445-6456.
7. **Berlioz, C., and J.-L. Darlix.** 1995. An internal ribosomal entry mechanism promotes translation of murine leukemia virus gag polyprotein precursors. J Virol **69:**2214-2222.
8. **Bowerman, B., P. O. Brown, J. M. Bishop, and H. E. Varmus.** 1989. A nucleoprotein complex mediates the integration of retroviral DNA. Genes & development **3:**469-478.
9. **Brierley, I., S. Pennell, and R. J. C. Gilbert.** 2007. Viral RNA pseudoknots: versatile motifs in gene expression and replication. Nat Rev Microbiol **5:**598-610.
10. **Briggs, J. A. G., and H. G. Kräusslich.** 2011. The molecular architecture of HIV. J Mol Biol **410:**491-500.
11. **Briggs, J. A. G., J. D. Riches, B. Glass, V. Bartonova, G. Zanetti, and H. G. Kräusslich.** 2009. Structure and assembly of immature HIV. PNAS **106:**11090-11095.
12. **Briggs, J. A. G., M. N. Simon, I. Gross, H. G. Kräusslich, S. D. Fuller, V. M. Vogt, and M. C. Johnson.** 2004. The stoichiometry of Gag protein in HIV-1. Nat Struct Mol Biol **11:**672-675.
13. **Brincat, J. L., J. K. Pfeiffer, and A. Telesnitsky.** 2002. RNase H activity is required for high-frequency repeat deletion during Moloney murine leukemia virus replication. J Virol **76:**88-95.

14. **Buchschacher, G. L., L. Yu, F. Murai, T. Friedmann, and A. Miyanohara.** 1999. Association of murine leukemia virus pol with virions, independent of Gag-Pol expression. J Virol **73:**9632-9637.
15. **Campbell, S. M., and V. M. Vogt.** 1995. Self-assembly in vitro of purified CA-NC proteins from Rous sarcoma virus and human immunodeficiency virus type 1. J Virol **69:**6487-6497.
16. **Carlson, L.-A., J. A. G. Briggs, B. Glass, J. D. Riches, M. N. Simon, M. C. Johnson, B. Müller, K. Grünewald, and H. G. Kräusslich.** 2008. Three-dimensional analysis of budding sites and released virus suggests a revised model for HIV-1 morphogenesis. Cell Host Microbe **4:**592-599.
17. **Cen, S., M. Niu, J. Saadatmand, F. Guo, Y. Huang, G. J. Nabel, and L. Kleiman.** 2004. Incorporation of pol into human immunodeficiency virus type 1 Gag virus-like particles occurs independently of the upstream Gag domain in Gag-pol. J Virol **78:**1042-1049.
18. **Chang, E. H., S. J. Mims, T. J. Triche, and R. M. Friedman.** 1977. Interferon inhibits mouse leukaemia virus release: an electron microscope study. J Gen Virol **34:**363-7.
19. **Chen, J., O. A. Nikolaitchik, J. Singh, A. Wright, C. E. Bencsics, J. M. Coffin, N. Ni, S. Lockett, V. K. Pathak, and W.-S. Hu.** 2009. High efficiency of HIV-1 genomic RNA packaging and heterozygote formation revealed by single virion analysis. PNAS **106:**13535-13540.
20. **Chen, X., and S. L. Wolin.** 2004. The Ro 60 kDa autoantigen: insights into cellular function and role in autoimmunity. J Mol Med **82:**232-239.
21. **Chen, Y. L., P. W. T'ai, C. C. Yang, and C. T. Wang.** 1997. Generation of infectious virus particles by transient co-expression of human immunodeficiency virus type 1 gag mutants. J Gen Virol **78:**2497-2501.
22. **Coffin, J. M.** 1979. Structure, replication, and recombination of retrovirus genomes: some unifying hypotheses. J Gen Virol **42:**1-26.
23. **Coffin, J. M., S. H. Hughes, and H. E. Varmus (ed.).** 1997. Retroviruses. Cold Spring Harbor Laboratory Press. Plainview, NY.
24. **Colicelli, J., and S. P. Goff.** 1988. Sequence and spacing requirements of a retrovirus integration site. J Mol Biol **199:**47-59.
25. **D'Souza, V., and M. F. Summers.** 2005. How retroviruses select their genomes. Nat Rev Microbiol **3:**643-655.
26. **D'Souza, V., and M. F. Summers.** 2004. Structural basis for packaging the dimeric genome of Moloney murine leukaemia virus. Nature **431:**586-590.
27. **Darlix, J.-L., J. Godet, R. Ivanyi-Nagy, P. Fossé, O. Mauffret, and Y. Mély.** 2011. Flexible Nature and Specific Functions of the HIV-1 Nucleocapsid Protein. J Mol Biol **410:**565-581.
28. **Déjardin, J., G. Bompard-Maréchal, M. Audit, T. J. Hope, M. Sitbon, and M. Mougel.** 2000. A novel subgenomic murine leukemia virus RNA transcript results from alternative splicing. J Virol **74:**3709-3714.
29. **Dey, A., D. York, A. Smalls-Mantey, and M. F. Summers.** 2005. Composition and sequence-dependent binding of RNA to the

nucleocapsid protein of Moloney murine leukemia virus. Biochemistry **44:**3735-3744.
30. **Dordor, A., E. Poudevigne, H. Göttlinger, and W. Weissenhorn.** 2011. Essential and supporting host cell factors for HIV-1 budding. Future Microbiol **6:**1159-1170.
31. **Dulude, D., Y. A. Berchiche, K. Gendron, L. Brakier-Gingras, and N. Heveker.** 2006. Decreasing the frameshift efficiency translates into an equivalent reduction of the replication of the human immunodeficiency virus type 1. Virology **345:**127-136.
32. **Fan, H.** 1997. Leukemogenesis by Moloney murine leukemia virus: a multistep process. Trends Microbiol **5:**74-82.
33. **Felsenstein, K. M., and S. P. Goff.** 1988. Expression of the gag-pol fusion protein of Moloney murine leukemia virus without gag protein does not induce virion formation or proteolytic processing. J Virol **62:**2179-2182.
34. **Fisher, J., and S. P. Goff.** 1998. Mutational Analysis of Stem-Loops in the RNA Packaging Signal of the Moloney Murine Leukemia Virus. Virology **244:**133-145.
35. **Flynn, J. A., W. An, S. R. King, and A. Telesnitsky.** 2004. Nonrandom dimerization of murine leukemia virus genomic RNAs. J Virol **78:**12129-12139.
36. **Ganser, B. K., A. Cheng, W. I. Sundquist, and M. Yeager.** 2003. Three-dimensional structure of the M-MuLV CA protein on a lipid monolayer: a general model for retroviral capsid assembly. EMBO J **22:**2886-2892.
37. **Ganser-Pornillos, B. K., M. Yeager, and W. I. Sundquist.** 2008. The structural biology of HIV assembly. Curr Opin Struct Biol **18:**203-217.
38. **Garcia, E. L., A. A. Onafuwa-Nuga, S. Sim, S. R. King, S. L. Wolin, and A. Telesnitsky.** 2009. Packaging of host mY RNAs by murine leukemia virus may occur early in Y RNA biogenesis. J Virol **83:**12526-12534.
39. **Gareiss, P. C., and B. L. Miller.** 2009. Ribosomal frameshifting: an emerging drug target for HIV. Curr Opin Investig Drug **10:**121-128.
40. **Gherghe, C., T. Lombo, C. W. Leonard, S. A. K. Datta, J. W. Bess, R. J. Gorelick, A. R. Rein, and K. M. Weeks.** 2010. Definition of a high-affinity Gag recognition structure mediating packaging of a retroviral RNA genome. PNAS **107:**19248-19253.
41. **Girard, P.-M., H. de Rocquigny, B. P. Roques, and J. Paoletti.** 1996. A Model of PSI Dimerization: Destabilization of the C278−G303 Stem−Loop by the Nucleocapsid Protein (NCp10) of MoMuLV. Biochem **35:**8705-8714.
42. **Goff, S. P.** 2007. Retroviridae: The retroviruses and their replication. In Knipe DM, Howley PM, Eds., 5 ed, vol. II. Lippincott Williams & Wilkins, Philidelphia.
43. **Gonsky, J., E. Bacharach, and S. P. Goff.** 2001. Identification of residues of the Moloney murine leukemia virus nucleocapsid critical for viral DNA synthesis in vivo. J Virol **75:**2616-2626.
44. **Gorelick, R. J., D. J. Chabot, D. E. Ott, T. D. Gagliardi, A. R. Rein, L. E. Henderson, and L. O. Arthur.** 1996. Genetic analysis of the zinc finger in

the Moloney murine leukemia virus nucleocapsid domain: replacement of zinc-coordinating residues with other zinc-coordinating residues yields noninfectious particles containing genomic RNA. J Virol **70:**2593-2597.

45. **Gorelick, R. J., W. Fu, T. D. Gagliardi, W. J. Bosche, A. R. Rein, L. E. Henderson, and L. O. Arthur.** 1999. Characterization of the block in replication of nucleocapsid protein zinc finger mutants from moloney murine leukemia virus. J Virol **73:**8185-8195.
46. **Gorelick, R. J., L. E. Henderson, J. P. Hanser, and A. R. Rein.** 1988. Point mutants of Moloney murine leukemia virus that fail to package viral RNA: evidence for specific RNA recognition by a "zinc finger-like" protein sequence. PNAS **85:**8420-8424.
47. **Halwani, R., A. Khorchid, S. Cen, and L. Kleiman.** 2003. Rapid localization of Gag/GagPol complexes to detergent-resistant membrane during the assembly of human immunodeficiency virus type 1. J Virol **77:**3973-3984.
48. **Hamard-Peron, E., and D. Muriaux.** 2011. Retroviral matrix and lipids, the intimate interaction. Retrovirology **8:**15.
49. **Haraguchi, H., S. Sudo, T. Noda, F. Momose, Y. Kawaoka, and Y. Morikawa.** 2010. Intracellular localization of human immunodeficiency virus type 1 Gag and GagPol products and virus particle release: relationship with the Gag-to-GagPol ratio. Microbiol Immunol **54:**734-746.
50. **Hatfield, D. L., J. G. Levin, A. R. Rein, and S. Oroszlan.** 1992. Translational suppression in retroviral gene expression. Adv Virus Res **41**:193-239.
51. **Henderson, L. E., T. D. Copeland, R. C. Sowder, G. W. Smythers, and S. Oroszlan.** 1981. Primary structure of the low molecular weight nucleic acid-binding proteins of murine leukemia viruses. J Biol Chem **256:**8400-8406.
52. **Henderson, L. E., H. C. Krutzsch, and S. Oroszlan.** 1983. Myristyl amino-terminal acylation of murine retrovirus proteins: an unusual post-translational proteins modification. PNAS **80:**339-343.
53. **Hill, M. K., G. Tachedjian, and J. Mak.** 2005. The packaging and maturation of the HIV-1 Pol proteins. Curr HIV Res **3:**73-85.
54. **Houck-Loomis, B., M. A. Durney, C. Salguero, N. Shankar, J. M. Nagle, S. P. Goff, and V. M. D'Souza.** 2011. An equilibrium-dependent retroviral mRNA switch regulates translational recoding. Nature **480:**561-564.
55. **Houzet, L., J. L. Battini, E. Bernard, V. Thibert, and M. Mougel.** 2003. A new retroelement constituted by a natural alternatively spliced RNA of murine replication-competent retroviruses. EMBO J **22:**4866-4875.
56. **Huang, M., and M. A. Martin.** 1997. Incorporation of Pr160(gag-pol) into virus particles requires the presence of both the major homology region and adjacent C-terminal capsid sequences within the Gag-Pol polyprotein. J Virol **71:**4472-4478.

57. **Jacks, T., M. D. Power, F. R. Masiarz, P. A. Luciw, P. J. Barr, and H. E. Varmus.** 1988. Characterization of ribosomal frameshifting in HIV-1 gag-pol expression. Nature **331:**280-283.
58. **Jamjoom, G. A., R. B. Naso, and R. B. Arlinghaus.** 1977. Further characterization of intracellular precursor polyproteins of Rauscher leukemia virus. Virology **78:**11-34.
59. **Johnson, S. F., E. L. Garcia, M. F. Summers, and A. Telesnitsky.** 2012. Moloney murine leukemia virus genomic RNA packaged in the absence of a full complement of wild type nucleocapsid protein. Virology **430:**100-109.
60. **Johnson, S. F., and A. Telesnitsky.** 2010. Retroviral RNA dimerization and packaging: the what, how, when, where, and why. PLoS Pathogens **6(10):**e1001007.
61. **Jouvenet, N., S. Simon, and P. D. Bieniasz.** 2009. Imaging the interaction of HIV-1 genomes and Gag during assembly of individual viral particles. PNAS **106:**19114-19119.
62. **Karacostas, V., E. J. Wolffe, K. Nagashima, M. A. Gonda, and B. Moss.** 1993. Overexpression of the HIV-1 gag-pol polyprotein results in intracellular activation of HIV-1 protease and inhibition of assembly and budding of virus-like particles. Virology **193:**661-671.
63. **Keenan, R. J., D. M. Freymann, R. M. Stroud, and P. Walter.** 2001. The signal recognition particle. Annual review of biochemistry **70:**755-775.
64. **Keene, S. E., S. R. King, and A. Telesnitsky.** 2010. 7SL RNA is retained in HIV-1 minimal virus-like particles as an S-domain fragment. J Virol **84:**9070-9077.
65. **Kelly, S. M., and A. H. Corbett.** 2009. Messenger RNA Export from the Nucleus: A Series of Molecular Wardrobe Changes. Traffic **10:**1199-1208.
66. **Khorchid, A., R. Halwani, M. A. Wainberg, and L. Kleiman.** 2002. Role of RNA in facilitating Gag/Gag-Pol interaction. J Virol **76:**4131-4137.
67. **Kim, J. W., E. I. Closs, L. M. Albritton, and J. M. Cunningham.** 1991. Transport of cationic amino acids by the mouse ecotropic retrovirus receptor. Nature **352:**725-728.
68. **Kulpa, D., R. S. Topping, and A. Telesnitsky.** 1997. Determination of the site of first strand transfer during Moloney murine leukemia virus reverse transcription and identification of strand transfer-associated reverse transcriptase errors. EMBO J **16:**856-865.
69. **Kutluay, S. B., and P. D. Bieniasz.** 2010. Analysis of the Initiating Events in HIV-1 Particle Assembly and Genome Packaging. PLoS Pathogens **6:**e1001200.
70. **Lee, Y. M., and X. F. Yu.** 1998. Identification and characterization of virus assembly intermediate complexes in HIV-1-infected CD4+ T cells. Virology **243:**78-93.
71. **Levin, J. G., J. Guo, I. Rouzina, and K. Musier-Forsyth.** 2005. Nucleic Acid Chaperone Activity of HIV-1 Nucleocapsid Protein: Critical Role in Reverse Transcription and Molecular Mechanism. Prog Nuc Acid Res Mol Biol **80**:217-286.

72. **Levin, J. G., M. Mitra, A. P. Mascarenhas, and K. Musier-Forsyth.** 2010. Role of HIV-1 nucleocapsid protein in HIV-1 reverse transcription. RNA Biol **7:**754-774.
73. **Lewinski, M. K., and F. D. Bushman.** 2005. Retroviral DNA integration--mechanism and consequences. Adv Gen **55:**147-181.
74. **Lewis, P. F., and M. Emerman.** 1994. Passage through mitosis is required for oncoretroviruses but not for the human immunodeficiency virus. J Virol **68:**510-516.
75. **Lu, K., X. Heng, and M. F. Summers.** 2011. Structural determinants and mechanism of HIV-1 genome packaging. J Mol Biol **410:**609-633.
76. **Ly, H., and T. G. Parslow.** 2002. Bipartite signal for genomic RNA dimerization in Moloney murine leukemia virus. J Virol **76:**3135-3144.
77. **Maeda, N., and H. Fan.** 2008. Oncogenesis by retroviruses: old and new paradigms. Rev Med Vriol **18**:387-405.
78. **Mak, J., and L. Kleiman.** 1997. Primer tRNAs for reverse transcription. J Virol **71:**8087-8095.
79. **Mann, R., and D. Baltimore.** 1985. Varying the position of a retrovirus packaging sequence results in the encapsidation of both unspliced and spliced RNAs. J Virol **54:**401-407.
80. **Mann, R., R. C. Mulligan, and D. Baltimore.** 1983. Construction of a retrovirus packaging mutant and its use to produce helper-free defective retrovirus. Cell **33:**153-159.
81. **Maurel, S., L. Houzet, E. L. Garcia, A. Telesnitsky, and M. Mougel.** 2007. Characterization of a natural heterodimer between MLV genomic RNA and the SD' retroelement generated by alternative splicing. RNA **13:**2266-2276.
82. **Medzhitov, R.** 2007. Recognition of microorganisms and activation of the immune response. Nature **449:**819-826.
83. **Méric, C., and S. P. Goff.** 1989. Characterization of Moloney murine leukemia virus mutants with single-amino-acid substitutions in the Cys-His box of the nucleocapsid protein. J Virol **63:**1558-1568.
84. **Messer, L. I., J. G. Levin, and S. K. Chattopadhyay.** 1981. Metabolism of viral RNA in murine leukemia virus-infected cells; evidence for differential stability of viral message and virion precursor RNA. J Virol **40:**683-90.
85. **Mitchell, R. S., B. F. Beitzel, A. R. W. Schroder, P. Shinn, H. Chen, C. C. Berry, J. R. Ecker, and F. D. Bushman.** 2004. Retroviral DNA integration: ASLV, HIV, and MLV show distinct target site preferences. PLoS Biol **2:**E234.
86. **Miyazaki, Y., E. L. Garcia, S. R. King, K. Iyalla, K. Loeliger, P. Starck, S. Syed, A. Telesnitsky, and M. F. Summers.** 2010. An RNA structural switch regulates diploid genome packaging by Moloney murine leukemia virus. J Mol Biol **396:**141-152.
87. **Miyazaki, Y., R. N. Irobalieva, B. S. Tolbert, A. Smalls-Mantey, K. Iyalla, K. Loeliger, V. D'Souza, H. Khant, M. F. Schmid, E. L. Garcia, A. Telesnitsky, W. Chiu, and M. F. Summers.** 2010. Structure of a

conserved retroviral RNA packaging element by NMR spectroscopy and cryo-electron tomography. J Mol Biol **404:**751-772.

88. **Moloney, J.** 1960. Biological studies on a lymphoid-leukemia virus extracted from sarcoma 37. I. Origin and introductory investigations. J Nat Cancer Inst **24:**933-951.
89. **Morellet, N., N. Jullian, H. de Rocquigny, B. Maigret, J.-L. Darlix, and B. P. Roques.** 1992. Determination of the structure of the nucleocapsid protein NCp7 from the human immunodeficiency virus type 1 by 1H NMR. EMBO J **11:**3059-3065.
90. **Mortuza, G. B., L. F. Haire, A. Stevens, S. J. Smerdon, J. P. Stoye, and I. A. Taylor.** 2004. High-resolution structure of a retroviral capsid hexameric amino-terminal domain. Nature **431:**481-485.
91. **Mougel, M., and E. Barklis.** 1997. A role for two hairpin structures as a core RNA encapsidation signal in murine leukemia virus virions. J Virol **71:**8061-8065.
92. **Muriaux, D., S. Costes, K. Nagashima, J. Mirro, E. Cho, S. Lockett, and A. R. Rein.** 2004. Role of murine leukemia virus nucleocapsid protein in virus assembly. J Virol **78:**12378-12385.
93. **Muriaux, D., J. Mirro, D. P. Harvin, and A. R. Rein.** 2001. RNA is a structural element in retrovirus particles. PNAS **98:**5246-5251.
94. **Murray, P. S., Z. Li, J. Wang, C. L. Tang, B. Honig, and D. Murray.** 2005. Retroviral matrix domains share electrostatic homology: models for membrane binding function throughout the viral life cycle. Structure **13:**1521-1531.
95. **Murti, K. G., M. Bondurant, and A. Tereba.** 1981. Secondary structural features in the 70S RNAs of Moloney murine leukemia and Rous sarcoma viruses as observed by electron microscopy. J Virol **37:**411-419.
96. **Ni, X., M. Castanares, A. Mukherjee, and S. E. Lupold.** Nucleic acid aptamers: clinical applications and promising new horizons. Curr Med Chem **18:**4206-14.
97. **Nitta, T., Y. Kuznetsov, A. McPherson, and H. Fan.** 2010. Murine leukemia virus glycosylated Gag (gPr80gag) facilitates interferon-sensitive virus release through lipid rafts. PNAS **107:**1190-1195.
98. **O'Reilly, L., and M. J. Roth.** 2000. Second-site changes affect viability of amphotropic/ecotropic chimeric enveloped murine leukemia viruses. J Virol **74:**899-913.
99. **Onafuwa-Nuga, A. A., S. R. King, and A. Telesnitsky.** 2005. Nonrandom packaging of host RNAs in moloney murine leukemia virus. J Virol **79:**13528-13537.
100. **Onafuwa-Nuga, A. A., and A. Telesnitsky.** 2009. The remarkable frequency of human immunodeficiency virus type 1 genetic recombination. Microbiol Mol Biol Rev **73:**451-80.
101. **Ono, A.** 2009. HIV-1 Assembly at the Plasma Membrane: Gag Trafficking and Localization. Future Virol **4:**241-257.

102. **Orlinsky, K. J., and S. B. Sandmeyer.** 1994. The Cys-His motif of Ty3 NC can be contributed by Gag3 or Gag3-Pol3 polyproteins. J Virol **68:**4152-4166.
103. **Park, J., and C. D. Morrow.** 1991. Overexpression of the gag-pol precursor from human immunodeficiency virus type 1 proviral genomes results in efficient proteolytic processing in the absence of virion production. J Virol **65:**5111-5117.
104. **Park, J., and C. D. Morrow.** 1992. The nonmyristylated Pr160gag-pol polyprotein of human immunodeficiency virus type 1 interacts with Pr55gag and is incorporated into viruslike particles. J Virol **66:**6304-6313.
105. **Pfeiffer, J. K., M. M. Georgiadis, and A. Telesnitsky.** 2000. Structure-based moloney murine leukemia virus reverse transcriptase mutants with altered intracellular direct-repeat deletion frequencies. J Virol **74:**9629-9636.
106. **Pfeiffer, J. K., R. S. Topping, N. H. Shin, and A. Telesnitsky.** 1999. Altering the intracellular environment increases the frequency of tandem repeat deletion during Moloney murine leukemia virus reverse transcription. J Virol **73:**8441-8447.
107. **Pornillos, O., J. E. Garrus, and W. I. Sundquist.** 2002. Mechanisms of enveloped RNA virus budding. Trends Cell Biol **12:**569-579.
108. **Prats, A. C., C. Roy, P. Wang, and M. Erard.** 1990. cis elements and trans-acting factors involved in dimer formation of murine leukemia virus RNA. J Virol **64:**774-783.
109. **Prizan-Ravid, A., E. Elis, N. Laham-Karam, S. Selig, M. Ehrlich, and E. Bacharach.** 2010. The Gag Cleavage Product, p12, is a Functional Constituent of the Murine Leukemia Virus Pre-Integration Complex. PLoS Pathogens **6:**e1001183.
110. **Rein, A. R., S. A. K. Datta, C. P. Jones, and K. Musier-Forsyth.** 2011. Diverse interactions of retroviral Gag proteins with RNAs. Trends Biochem Sci **36:**373-380.
111. **Rein, A. R., D. P. Harvin, J. Mirro, S. M. Ernst, and R. J. Gorelick.** 1994. Evidence that a central domain of nucleocapsid protein is required for RNA packaging in murine leukemia virus. J Virol **68:**6124-6129.
112. **Rein, A. R., L. E. Henderson, and J. G. Levin.** 1998. Nucleic-acid-chaperone activity of retroviral nucleocapsid proteins: significance for viral replication. Trends in biochemical sciences **23:**297-301.
113. **Rein, A. R., M. R. McClure, N. R. Rice, R. B. Luftig, and A. M. Schultz.** 1986. Myristylation site in Pr65gag is essential for virus particle formation by Moloney murine leukemia virus. PNAS **83:**7246-7250.
114. **Rice, W. G., C. A. Schaeffer, B. Harten, F. Villinger, T. L. South, M. F. Summers, L. E. Henderson, J. W. Bess, L. O. Arthur, and J. S. McDougal.** 1993. Inhibition of HIV-1 infectivity by zinc-ejecting aromatic C-nitroso compounds. Nature **361:**473-475.
115. **Roe, T., T. C. Reynolds, G. Yu, and P. O. Brown.** 1993. Integration of murine leukemia virus DNA depends on mitosis. EMBO J **12:**2099-2108.

116. **Sakuragi, J.-i., A. Iwamoto, and T. Shioda.** 2002. Dissociation of genome dimerization from packaging functions and virion maturation of human immunodeficiency virus type 1. J Virol **76:**959-967.
117. **Sakuragi, J.-i., T. Shioda, and A. T. Panganiban.** 2001. Duplication of the primary encapsidation and dimer linkage region of human immunodeficiency virus type 1 RNA results in the appearance of monomeric RNA in virions. J Virol **75:**2557-2565.
118. **Sakuragi, J.-i., S. Ueda, A. Iwamoto, and T. Shioda.** 2003. Possible role of dimerization in human immunodeficiency virus type 1 genome RNA packaging. J Virol **77:**4060-4069.
119. **Salzberg, S., M. Bakhanashvili, and M. Aboud.** 1978. Effect of interferon on mouse cells chronically infected with murine leukaemia virus: kinetic studies on virus production and virus RNA synthesis. J Gen Virol **40:**121-30.
120. **Schwartz, M. D., D. Fiore, and A. T. Panganiban.** 1997. Distinct functions and requirements for the Cys-His boxes of the human immunodeficiency virus type 1 nucleocapsid protein during RNA encapsidation and replication. J Virol **71:**9295-9305.
121. **Shehu-Xhilaga, M., S. M. Crowe, and J. Mak.** 2001. Maintenance of the Gag/Gag-Pol ratio is important for human immunodeficiency virus type 1 RNA dimerization and viral infectivity. J Virol **75:**1834-1841.
122. **Shields, A., W. N. Witte, E. Rothenberg, and D. Baltimore.** 1978. High frequency of aberrant expression of Moloney murine leukemia virus in clonal infections. Cell **14:**601-609.
123. **Shin, N. H., D. Hartigan-O'Connor, J. K. Pfeiffer, and A. Telesnitsky.** 2000. Replication of lengthened Moloney murine leukemia virus genomes is impaired at multiple stages. J Virol **74:**2694-2702.
124. **Shinnick, T. M., R. A. Lerner, and J. G. Sutcliffe.** 1981. Nucleotide sequence of Moloney murine leukaemia virus. Nature **293:**543-548.
125. **Smith, A. J., N. Srinivasakumar, M. L. Hammarskjöld, and D. Rekosh.** 1993. Requirements for incorporation of Pr160gag-pol from human immunodeficiency virus type 1 into virus-like particles. J Virol **67:**2266-2275.
126. **South, T. L., P. R. Blake, D. R. Hare, and M. F. Summers.** 1991. C-Terminal retroviral-type zinc finger domain from the HIV-1 nucleocapsid protein is structurally similar to the N-terminal zinc finger domain. Biochem **30:**6342-6349.
127. **South, T. L., and M. F. Summers.** 1993. Zinc- and sequence-dependent binding to nucleic acids by the N-terminal zinc finger of the HIV-1 nucleocapsid protein: NMR structure of the complex with the Psi-site analog, dACGCC. Protein Sci **2:**3-19.
128. **Srinivasakumar, N., M. L. Hammarskjöld, and D. Rekosh.** 1995. Characterization of deletion mutations in the capsid region of human immunodeficiency virus type 1 that affect particle formation and Gag-Pol precursor incorporation. J Virol **69:**6106-6114.

129. **Stoye, J. P., J. Bloomberg, J. M. Coffin, H. Fan, B. Hahn, J. Neil, S. Quakenbush, A. Rethwiln, and M. Trisen.** 2012. Retroviridae. In virus taxonomy: ninth report of the International Committee on Taxonomy of Viruses. Elsevier/Academic Press, London. 477-495.
130. **Summers, M. F., L. E. Henderson, M. R. Chance, J. W. Bess, T. L. South, P. R. Blake, I. Sagi, G. Perez-Alvarado, R. C. Sowder, and D. R. Hare.** 1992. Nucleocapsid zinc fingers detected in retroviruses: EXAFS studies of intact viruses and the solution-state structure of the nucleocapsid protein from HIV-1. Protein Sci **1:**563-574.
131. **Summers, M. F., T. South, and B. Kim.** 1990. High-resolution structure of an HIV zinc fingerlike domain via a new NMR-based distance geometry approach. Biochem **29:**340-346.
132. **Swanson, C. M., and M. H. Malim.** 2008. SnapShot: HIV-1 Proteins. Cell **133:**742-742.e1.
133. **Takeuchi, O., and S. Akira.** 2009. Innate immunity to virus infection. Immunological Rev **227:**75-86.
134. **Telesnitsky, A., S. Blain, and S. P. Goff.** 1995. Assays for retroviral reverse transcriptase. Methods Enzymol **262:**347-362.
135. **Thomas, J. A., and R. J. Gorelick.** 2008. Nucleocapsid protein function in early infection processes. Virus Res **134:**39-63.
136. **Valadkhan, S.** 2005. snRNAs as the catalysts of pre-mRNA splicing. Curr Opin Chem Biol **9:**603-608.
137. **van der Kuyl, A. C.** HIV infection and HERV expression: a review. Retrovirology **9:**6.
138. **Vogt, P. K., and S. S. Hu.** 1977. The genetic structure of RNA tumor viruses. Ann Rev Gen **11:**203-238.
139. **Waheed, A. A., and E. O. Freed.** 2012. HIV type 1 Gag as a target for antiviral therapy. AIDS Res Human Retroviruses **28:**54-75.
140. **Wang, M. Q., and S. P. Goff.** 2003. Defects in virion production caused by mutations affecting the C-terminal portion of the Moloney murine leukemia virus capsid protein. J Virol **77:**3339-3344.
141. **Welker, R., H. Kottler, H. R. Kalbitzer, and H. G. Kräusslich.** 1996. Human immunodeficiency virus type 1 Nef protein is incorporated into virus particles and specifically cleaved by the viral proteinase. Virology **219:**228-236.
142. **Wright, E. R., J. B. Schooler, H. J. Ding, C. Kieffer, C. Fillmore, W. I. Sundquist, and G. J. Jensen.** 2007. Electron cryotomography of immature HIV-1 virions reveals the structure of the CA and SP1 Gag shells. EMBO J **26:**2218-2226.
143. **Wu, X., Y. Li, and B. Crise.** 2003. Transcription Start Regions in the Human Genome Are Favored Targets for MLV Integration. Science **300**:1749-1751.
144. **Yeager, M., E. M. Wilson-Kubalek, S. G. Weiner, P. O. Brown, and A. R. Rein.** 1998. Supramolecular organization of immature and mature murine leukemia virus revealed by electron cryo-microscopy: implications for retroviral assembly mechanisms. PNAS **95:**7299-7304.

145. **Yu, S. S., J. M. Kim, and S. Kim.** 2000. The 17 nucleotides downstream from the env gene stop codon are important for murine leukemia virus packaging. J Virol **74:**8775-8780.
146. **Zhang, W., C. Hwang, W. Hu, and R. J. Gorelick.** 2002. Zinc Finger Domain of Murine Leukemia Virus Nucleocapsid Protein Enhances the Rate of Viral DNA Synthesis in Vivo. J Virol **76:**7473-7484.